The effect of BX795 on type I, II, III interferons and interleukin-4 mediated JAK/STAT signaling pathways

Kunning Li

A thesis submitted to McGill University in partial fulfillment of the requirements of the degree of Master of Science

December 2019

Division of Experimental Medicine,

Department of Medicine,

McGill University

Montreal, Quebec, Canada

©Kunning Li 2019

ABSTRACT

The Janus kinase (JAK)/ signal transducers and activators of transcription (STAT) signaling pathway is a critical pathway involved in the control of immune responses. A variety of cytokines and growth factors use this pathway for signal transduction, including interferons (IFNs) and interleukins (ILs). Deregulation of this pathway has been associated with numerous immunodeficiency syndromes and hematologic malignancies. BX795, the compound of our interest, is a synthetic TBK1 inhibitor. Recent studies have shown that BX795 inhibits a number of distinct pathways, including PDK1 and JNK/p38 pathways. Hence, we reasoned that BX795 also has a direct inhibitory effect on the JAK/STAT pathway. Our results demonstrated that BX795 strongly suppresses STAT phosphorylation in IFNα, IFNγ, IFNλ, and IL-4-mediated JAK/STAT pathways. Particularly for IFNα signaling pathway, BX795 inhibited STAT1 phosphorylation under both direct cytokine induction and viral infection. VSVΔ51 replications and virus-mediated apoptosis were enhanced by BX795 in TBK1-/- and glioma cells. However, the effect of the combined oncolytic virotherapy requires further validation via *in vitro* models. Blockade of p-JAK1 and STAT1 interaction is suggested to be the potential mechanism of inhibition. In contrast, BX795 was only able to suppress STAT6 phosphorylation under direct IL-4 stimulation *in vitro* and *in vivo*, but not in ovalbumin-induced asthma model. In fact, other Th2 response biomarkers, such as OVA-specific IgE in serum and IL-4 in lung homogenate, were upregulated under BX795 treatment after OVA challenge. This finding suggests that BX795 may have a higher selectivity towards inhibition of STAT1 and Th1 response. Altogether, this study reveals a novel inhibitory effect of BX795 on the JAK/STAT signalling pathway. By unfolding its effect and mechanism of action, BX795 can provide insights on the development of next-generation JAK inhibitors with higher selectivity. This study also highlights the therapeutic potential of BX795 in combined therapy with VSV to mediate oncolysis against OV-resistant cancers.

RÉSUMÉ

La voie de signalisation de la kinase Janus (JAK) / transducteur de signal et activateur de la transcription (STAT) est une voie critique impliquée dans le contrôle des réponses immunitaires. Divers cytokines et facteurs de croissance utilisent cette voie pour la transduction du signal, notamment les interférons (IFN) et les interleukines (IL). La dérégulation de cette voie a été associée à de nombreux syndromes d'immunodéficience et de malignités hématologiques. Le BX795, le composé qui nous intéresse, est un inhibiteur synthétique de la TBK1. Des études récentes ont montré que le BX795 inhibe un certain nombre de voies distinctes, notamment les voies PDK1 et JNK / p38. Par conséquent, nous avons estimé que BX795 avait également un effet inhibiteur direct sur la voie JAK / STAT. Nos résultats ont démontré que le BX795 inhibe fortement la phosphorylation de STAT dans les voies IFNα, IFNγ, IFNλ et JAK / STAT induites par IL-4. En particulier pour la voie de signalisation de l'IFNα, BX795 a inhibé la phosphorylation de STAT1 à la fois par induction directe de cytokines et par infection virale. Les réplications de VSVΔ51 et l'apoptose induite par le virus ont été renforcées par BX795 dans les cellules TBK1 -/- et les cellules de gliome. Cependant, l'effet de la virothérapie oncolytique combinée nécessite une validation supplémentaire dans des modèles *in vitro*. Le blocage de l'interaction p-JAK1 et STAT1 est suggéré comme étant le mécanisme potentiel de l'inhibition. En revanche, le BX795 n'a pu supprimer la phosphorylation de STAT6 que sous stimulation directe de l'IL-4 *in vitro* et *in vivo*, mais pas dans le modèle de l'asthme induit par l'ovalbumine. En fait, d'autres biomarqueurs de la réponse Th2, tels que les IgE spécifiques d'ovules dans le sérum et l'IL-4 dans l'homogénat de poumon, ont été régulés positivement sous traitement BX795 après une provocation par OVA. Cette découverte suggère que BX795 pourrait avoir une sélectivité plus élevée vis-à-vis de l'inhibition de la réponse de STAT1 et de Th1. Au total, cette étude révèle un nouvel effet inhibiteur du BX795 sur la voie de signalisation JAK / STAT. En

développant son effet et son mécanisme d'action, le BX795 peut fournir des informations sur le développement d'inhibiteurs de JAK de nouvelle génération offrant une sélectivité plus élevée. Cette étude souligne également le potentiel thérapeutique du BX795 dans le traitement combiné du VSV pour la médiation de l'oncolyse dans les cancers résistants au VO.

ACKNOWLEDGEMENTS

In completing my Master's thesis project, I would first like to thank my supervisor, Rongtuan Lin, for guiding me through my research project and providing me the resources and opportunity to learn different techniques to complete my project in this wonderful laboratory. I am grateful for having him as my supervisor. His encouragement and guidance have been greatly appreciated throughout my research experience.

I would like to thank all members of my thesis committee, Dr. Koren Mann, Dr. Anne Gatignol, and Dr. Kostas Pantopoulos for their time and valuable advices on my project.

Furthermore, I would like to thank all members of the lab for their support and advices through my study. In particular, I would like to thank Dr. Zhenlong Liu for teaching me all the laboratory and data analysis techniques used in this project. Thank you for your patience and guidance with organizing experiments and revising the manuscript. I would also like to acknowledge Samar Bel Hadj for training me when I first arrived in the lab and helping me to translate the abstract into French. She worked countless hours to assist me with ordering materials, monitoring tissue cultures, and providing moral support. A special thank to Marie-Line Goulet for teaching me and offering precious advices on how to perform *in vivo* experiments on mice. I'd also like to thank Jingyu Huang, Chen Wang, Dr. Yuan Jiang, and Dr. Chenhe Su for their helps with the experiments and being an indispensable source of moral support.

Last but not least, I would like to thank my lovely family and friends for their unconditional love, full support, and patience throughout my graduate studies. Their reassurance and guidance has been a crucial source of my motivation.

CONTRIBUTION OF THE AUTHORS

Kunning Li

- Designed and performed all experiments in this study.
- Composed the thesis.

Mr. Jingyu Huang

- Contributed in collecting cell lysates for Figure 4B and 4C.

Ms. Samar Bel Hadj

- Collected serum and contributed in collecting the lung from mice in the OVA-induced asthma model study for Figure 9.
- Revised the abstract.

Dr. Zhenlong Liu

- Provided guidance on co-immunoprecipitation for Figure 3.
- Collected serum from mice in the OVA-induced asthma model study for Figure 9.
- Performed ELISA on OVA-specific IgE for Figure 9F.

Dr. Huiqing Lv

- Performed ELISA on OVA-specific IgE for Figure 9F.

Ms. Marie-Line Goulet

- Assisted in the design of *in vivo* experiments for Figure 7, 8, and 9.
- Collected organs and assisted in performing flow cytometry analysis for Figure 8.
- Performed IV tail-injection for Figure 9B and 9C.

Dr. Rongtuan Lin

- Supervised the study.
- Revised the thesis.

Table of Contents

LIST OF ABBREVIATIONS

AHR	Airway hyperresponsiveness
Akt	Protein kinase B
ATP	Adenosine triphosphate
CD	Cluster of differentiation
cGAMP	Cyclic GMP-AMP
cGAS	Cyclic GMP-AMP synthase
CML	Chronic myeloid leukemia
DNA	Deoxyribonucleic acid
ERK	Extracellular signal-regulated kinase
FERM	Band 4.1, ezrin, radixin, moesin
GAS	Gamma-activated sequence
GM-CSF	Granulocyte macrophage-colony stimulating factor
GOF	Gain of function
HDI	Histone deacetylase inhibitors
HDM	House dust mite
HSV	Herpes simplex virus
IFN	Interferon
IFNAR	IFNα receptor
IFNGR	IFNγ receptor
IKK	IκB kinase
Ig	Immunoglobulin
IL	Interleukin
IL-4Rα	IL-4 receptor alpha chain
IRAK	Interleukin-1 receptor-associated kinase

IRF	Interferon regulatory factor
ISG	Interferon-stimulated gene
ISGF3	Interferon stimulated gene factor 3
ISRE	Interferon-stimulated response elements
JAK	Janus Kinase
JH	Jack Homology
JNK	c-Jun N-terminal kinase
KD	Kinase domain
LNK	Night light-inducible and clock-regulated gene
LOF	Loss of function
MAPK	Mitogen-activated protein kinase
MAVS	Mitochondrial antiviral-signaling protein
MDA5	Melanoma differentiation-associated protein 5
MEF	Mouse embryonic fibroblast
MHC	Major histocompatibility complex
MOI	Multiplicity of infection
mRNA	Messenger RNA
mTOR	Mammalian target of rapamycin
MyD88	Myeloid differentiation factor 88
NK	Natural killer cell
OV	Oncolytic virus
OVA	Ovalbumin
PDK1	3-phosphoinositide-dependent kinase-1
PRR	Pathogen recognition receptor
PTK	Protein tyrosine kinase

RdRp	RNA-dependent-RNA-polymerase
RIG-I	Retinoic acid-inducible gene I
RLR	RIG-I-like receptor
RNA	Ribonucleic acid
RNP	Ribonucleoprotein
RSV	Respiratory syncytial virus
SCID	Severe combined immunodeficiency
SeV	Sendai virus
SH2	Src homology 2
SNP	Single nucleotide polymorphism
SOCS	Suppressor of cytokine signaling
STAT	Signal Transducer and Activator of Transcription
STING	Stimulator of interferon genes
TAD	Transcriptional activation domain
TANK	TRAF Family Member Associated NFκB Activator
TBK1	TANK-binding kinase 1
Th	T helper
TLR	Toll-like receptor
VCAM-1	Vascular cell adhesion molecules-1
VSV	Vesicular stomatitis virus

CHAPTER 1. INTRODUCTION

1.1. Rationale and objectives

The Janus kinase (JAK)/ signal transducers and activators of transcription (STAT) signaling pathway is critical in the control of immune responses and hematopoiesis. Mutations in this pathway are associated with various immunodeficiency syndromes and hematologic malignancies. JAK inhibitors thus become a major interest for therapeutic treatments. BX795, a synthetic TBK1 inhibitor, has shown to exhibit off-target effects on numerous pathways involved in cancer. In this study, we propose to examine the effect and mechanism of BX795 in the JAK/STAT signaling pathway.

The primary objectives of the study were as follows:

1) Characterize the effect of BX795 on the JAK/STAT signaling pathway in response to type I, type II, type III interferons (IFNs) and interleukin-4. In particular, IFNα from type I IFN, IFNγ from type II IFN, and IFNλ from type III IFN were examined as a representative of each type of IFNs.
2) Determine the mechanism of action employed by BX795 on the JAK/STAT pathway. Co-immunoprecipitation was performed to examine the role of BX795 on the interaction between JAK and STAT proteins.
3) Investigate the therapeutic potential of BX795 in disease models associated with the JAK/STAT pathway. The effect of BX795 in combined oncolytic virotherapy with VSV under IFNα induction and OVA-induced allergic asthmatic model were evaluated to determine if inhibition observed in *in vitro* studies translate to preclinical successes.

1.2. JAK and STAT structure and signaling

The Janus kinase (JAK)/ signal transducers and activators of transcription (STAT) signaling pathway plays a crucial role in the control of immune responses, hematopoiesis, mammary gland development, and other processes (1). In mammals, there are four known JAKs (JAK1, JAK2, JAK3, TYK2) and seven STATs (STAT1, STAT2, STAT3, STAT4, STAT5a, STAT5b, STAT6) (2).

The JAKs are a family of tyrosine kinases. All members of the JAK family possess the following distinct domains: N-terminal FERM (band 4.1, ezrin, radixin, moesin) domain, SH2 (Src homology 2) domain, pseudokinase domain, and C-terminal protein tyrosine kinase (PTK) domain (Figure 1) (3). FERM domain acts as an adaptor and scaffolding unit to interact with membrane-associated proteins (4). SH2 domain binds to phosphotyrosine residues and is responsible for the activation and dimerization of STATs. Negative regulators of the pathway, including suppressor of cytokine signaling (SOCS) and Night light-inducible and clock-regulated gene (LNK) proteins, also contain a SH2 domain to target JAK phosphotyrosines for inhibition or dephosphorylation (5, 6). Pseudokinase domain, also called Jak Homology 2 domain (JH2), is required for modulating the PTK domain activity, including ligand-induced JAK activation and suppression of ligand-independent kinase activities (7). The PTK domain (JH1 domain) is the catalytic phosphotransferase domain that is highly homologous among the JAKs and other tyrosine kinases (8). It contains an adenosine triphosphate (ATP)-binding site adjacent to the catalytic site, and phosphorylates tyrosine residues on substrates (9).

On the other hand, STAT proteins are transcription factors downstream of JAKs. STAT consists of a N-domain, coiled-coil domain, DNA-binding domain, SH2 domain, and a

transcriptional activation domain (TAD) (10) (Figure 1). N-domain, coiled-coil domain, and TAD domain are involved in protein-protein interaction with STAT cofactors (11). In addition, N-domain also modulates receptor recognition, phosphatase recruitment, and formation of STAT tetramers and dimers between non-phosphorylated STAT monomers (12). Similar to JAKs, STATs contain a SH2 domain that is targeted by most STAT inhibitors (13). The DNA binding domain allows STAT to bind to promoters of target genes, and the TAD recruits transcriptional activators to enhance transcription (13).

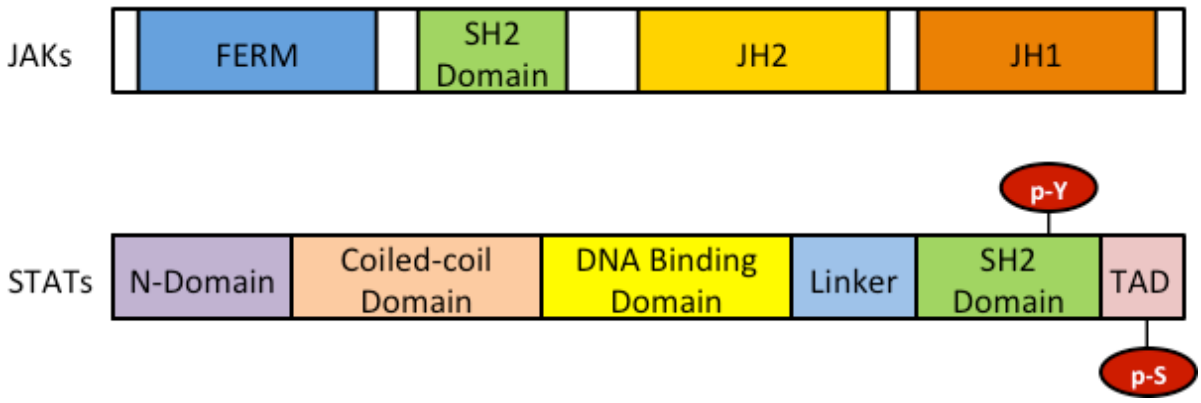

Figure 1. Structure of JAKs and STATs protein.

JAKs contain 4 functional domains: the FERM domain, SH2 domain, pseudokinase (JH2) domain, and tyrosine kinase (JH1) domain. STATs contain 6 major domains: N-domain, coiled-coil domain, DNA binding domain, linker, SH2 domain, and transactivation domain (TAD). Phosphotyrosine (p-Y) and phosphoserine (p-S) residues are also shown.

The JAK/STAT signaling pathway can be activated by a wide array of cytokines, including different types of interferons (e.g. IFNα/β, IFNγ, and IFNλ) (Figure 2) and interleukins (e.g. IL-4) (Figure 3). Signaling begins as extracellular cytokines or growth factors bind to their corresponding receptors. The receptors undergo conformational changes to bring receptor-associated JAKs in proximity (14). JAKs then activate themselves via auto-phosphorylation or transphosphorylation on tyrosine residues (15). Activated JAKs phosphorylate the tyrosine

residues on cognate receptors, which serve as a docking site for STAT transcription factors (15). Subsequently, STAT monomers are phosphorylated by JAKs, leading to dimerization (either homodimers, heterodimers, or tetramers), followed by translocation into the nucleus where they bind to specific DNA binding sites to regulate gene expression. The detailed mechanisms for IFNα, IFNγ, IFNλ, and IL-4-mediated JAK/STAT signaling pathways are described in the following sections 1.1.1 – 1.1.4.

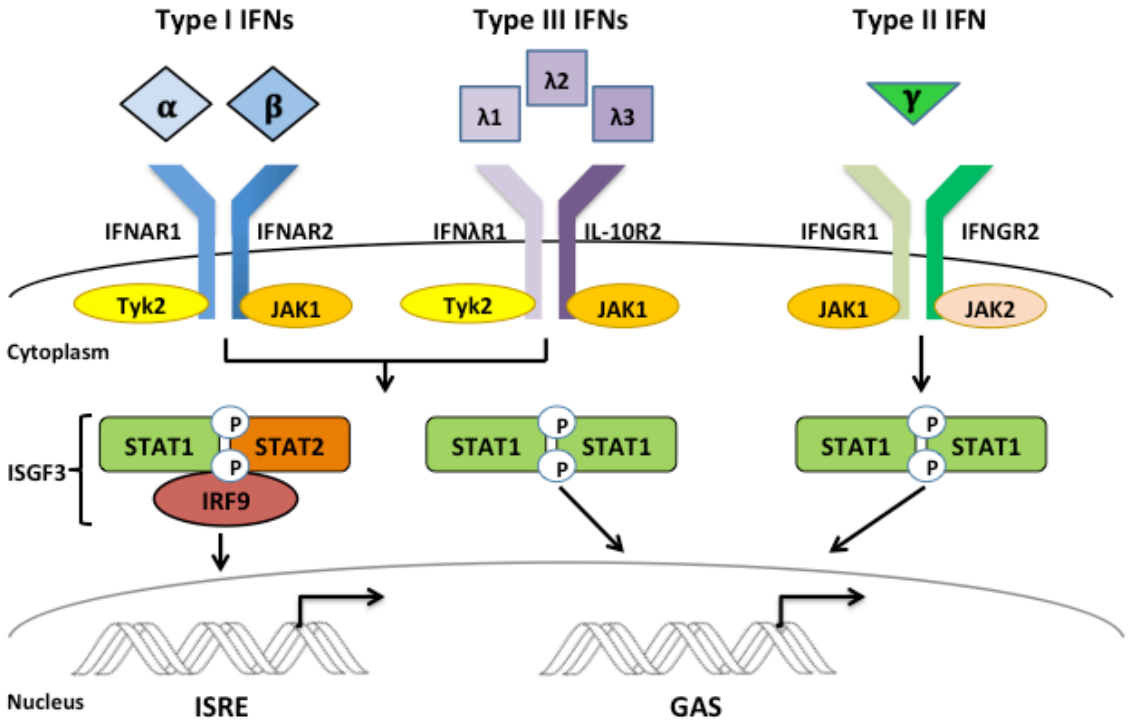

Figure 2. Type I, II, and III IFNs signaling through the JAK/STAT pathway.

Type I IFNs (including IFNα and IFNβ) and type III IFNs (IFNλs) bind to distinct receptors (IFNAR1/IFNAR2 or IFNλ1/IL-10R2, respectively), but activate the same downstream signaling cascade through ISGF3 complex and STAT1 homodimers. In contrast, IFNγ signals through IFNGR1 and IFNGR2 and activates STAT1 to form homodimers. ISGF3 complex binds to ISRE promoters to activate the transcription of IFN-stimulated genes, whereas STAT1 homodimers bind to GAS promoters to initiate the transcription of other genes.

1.2.1. IFNα-mediated JAK/STAT signaling pathway

IFNα is a type I IFN secreted by almost all cell types, although predominantly hematopoietic cells, to induce antiviral response and tumor cell apoptosis (16). It modulates antiviral responses by promoting antigen presentation, restraining pro-inflammatory pathways, and activating the adaptive immune system via inducing the development of T and B cell responses (4). IFNα promotes the survival of natural killer (NK) cells and their IFNγ production through IL-15 induction (17). In addition, IFNα regulates the production of various cytokines in macrophages, including IL-6 and IL-12, and induces their antibody-dependent cytotoxicity (18). IFNα also plays a role in the differentiation of dendritic cells (DCs) from monocytes (19). IFNα skews the differentiation of naïve T cells into IFNγ-producing T helper (Th) 1 cells, and enhances the production of immunoglobulin (Ig) G and immunologic memory (20). Overexpression of IFN α has been associated with the pathogenesis of systemic lupus erythematosus, an autoimmune disease causing symptoms such as arthritis, rash and photosensitivity (5).

IFNα-mediated JAK/STAT pathway involves the activation of heterodimeric receptor IFNα receptor 1 (IFNAR1) and IFNAR2 (21) (Figure 2). JAK1 and Tyk2 associated with the receptor subsequently leads to the phosphorylation and formation of STAT1/2 heterodimer and STAT1 homodimer primarily (22). STAT1/2 heterodimer, in conjunction with interferon regulatory factor 9 (IRF9), forms the interferon stimulated gene factor 3 (ISGF3) complex to bind to interferon-stimulated response elements (ISRE) and induce the expression of hundreds of IFN-stimulated genes (ISGs), including *IFIT1* and *DDX588* (22). STAT1 homodimers and other STATs, such as STAT3 and STAT4, can also initiate the transcription of various ISGs (23, 24).

1.2.2. IFNγ-mediated JAK/STAT signaling pathway

IFNγ is a type II IFN that activates immune responses against intracellular pathogens, tumor surveillance, and immunoediting. IFNγ is produced by professional antigen-presenting cells, including monocytes, DCs, NK cells, and T cells (25). These cells can secrete IL-12 to promote IFNγ synthesis, or secrete IL-4, IL-10, and other negative regulators to restrict IFNγ production (26, 27). IFNγ mediates the innate immunity through NK cell and macrophage activation (28). It also promotes specific cytotoxic immunity by skewing the adaptive immune response towards Th1 phenotype and upregulating proteins involved in antigen processing, presentation, and costimulation on antigen-presenting cells (29).

IFNγ signaling initiates as IFNγ binds to IFNγ receptor 1 (IFNGR1) and IFNγ receptor 2 (IFNGR2), which are responsible for ligand binding and signal transduction, respectively (30) (Figure 2). STAT1 is preferentially phosphorylated by JAK1 and JAK2 kinases, followed by dimerization and binding to gamma-activated sequence (GAS) to stimulate STAT1 target genes (30).

1.2.3. IFNλ-mediated JAK/STAT signaling pathway

IFNλ1, IFNλ2, and IFNλ3 are type III IFNs involved in the regulation of innate and adaptive immune response in response to viral infection. IFNλ can elicit antiviral activity directly or indirectly via IFNα signaling through the suppressor of cytokine signaling-1 (SOCS1) and the ubiquitin-specific peptidase 18 inhibitory feedback loops (31). IFNλ can also induce macrophage and DC polarization and the subsequent priming and activation of pathogen-specific T and B cells (31). In particular, IFNλ has been shown to shift the T helper cell balance towards Th1 (32, 33). Single nucleotide polymorphism (SNPs) of IFNλ genes have

been associated with reduced effectiveness in Hepatitis C virus treatment and higher inflammation and liver fibrosis in chronic hepatitis B patients (34, 35).

Mechanistically, IFNλ signalling initiates as IFNλ binds to IFNλR1 to trigger the recruitment of a second receptor chain, IL-10R2 (36, 37) (Figure 2). This ternary receptor complex allows JAK1 and Tyk2 to transphosphorylate the receptor chains and STAT proteins, including STAT1 and STAT2 (38). Similar to type I IFN signalling cascade, IFNλ also results in the formation of ISGF3 and activation of ISRE for ISGs induction (38).

1.2.4. IL-4-mediated JAK/STAT signaling pathway

IL-4 is a key modulator of immune response. It regulates proliferation and apoptosis in cells from hematopoietic and non-hematopoietic origin, including mast cells, eosinophils, basophils, DCs, myeloid cells, muscular cells, and neural cells (39, 40). It drives Th2 cell differentiation, IgE class switching, and tissue repair and homeostasis (41-43). Th2 response is essential for defense against parasitic infections (44). In addition, IL-4 induces the expression of vascular cell adhesion molecules-1 (VCAM-1) and secretion of Th2 cytokines, such as IL-5, IL-6, and IL-9 (45, 46). High levels of Th2 cytokines and IL-4 have been associated with the development of allergic asthma (47).

IL-4 signaling transits signals through IL-4 receptor alpha chain (IL-4Rα) (Figure 3). Upon binding, IL-4Rα dimerizes with either the common γ chain (γc) to form type-1 signaling complex, or with IL-13 receptor alpha 1 (IL-13Rα1) to form type-2 signaling complex (48). Type-1 signaling complex is mainly expressed on hematopoietic cells, which facilitates Th2 response and alternatively activated macrophages development (48). Type-2 signaling complex is expressed on non-hematopoietic cells to mediate responses upon IL-4 and IL-13

induction, such as mucus production and airway hyperactivity (49). IL-13 shares the same type-2 receptors for signaling (50). Type-1 complex activates JAK1 and JAK3, whereas type-2 complex signals through JAK1 and Tyk2. Both complexes lead to the phosphorylation of STAT6, which then dimerizes and translocate to the nucleus to induce the transcription of target genes, including *SOCS1* and *GATA3* (51, 52).

Figure 3. IL-4 signaling via JAK/STAT pathway.

IL-4 can signal through both type 1 (IL-4Rα and γc) and type 2 (IL-4Rα and IL-13α1) receptor complexes. IL-4Rα activates JAK1, γc activates JAK3, and IL-13α1 activates Tyk2. Activated JAKs then phosphorylate STAT6, lead to STAT6 dimerization and induce the transcription of IL-4 and STAT6 responsive genes, including *GATA3* and *SOCS1*.

1.3. Diseases associated with JAK/STAT pathway mutations

Mutations and polymorphisms in *JAK* and *STAT* genes have been associated with a number of malignancies and autoimmune diseases. For instance, acute lymphoblastic leukemia (53), T-cell prolymphocytic leukemia (54), and some solid organ carcinomas (55) are associated with gain of function (GOF) mutations in *JAK1*. Since JAK2 plays a crucial role in signal transduction of erythropoietin and thrombopoetin in the expansion of erythrocytes and megakaryocytes, activating mutations in *JAK2* cause a number of myeloproliferative diseases (23). V617F mutation is the most common mutation in *JAK2*, which is highly prevalent in patients with polycythemia vera, essential thrombocythemia, and myelofibrosis (56). On the other hand, mutations in *JAK3* genes have resulted in leukemia and lymphoma, including T-cell acute lymphoblastic leukemia and juvenile myelomonocytic leukemia (55, 57). Due to its selective association with the common γ chain signal transduction, *JAK3* mutations are also found in a subset of patients with X-linked severe combined immunodeficiency (SCID) (58).

GOF *STAT1* mutations contribute to chronic mucocutaneous candidiasis and several other autoimmune diseases, including cerebral aneurysms and immune dysregulation-polyendocrinopathy-enteropathy-X-linked-like syndrome (59). Higher susceptibility to fungal infection is also associated with hyperactive STAT1 due to suppressed IL-17 transcription and STAT3-driven anti-fungal response (60, 61). In contrast, loss of function (LOF) mutation of *STAT1* often leads to recurrent mycobacterial and viral infections (62). LOF mutation in *STAT2* raises susceptibility to viral infection (62). Furthermore, LOF of *STAT3* causes hyperimmunoglobulin E syndrome (Job's syndrome), which is characterized by recurrent and severe cutaneous and sinopulmonary bacterial infections, chronic dermatitis, and connective tissue abnormalities (63). Crohn's disease and psoriasis are also associated with *STAT3* SNP (64). In particular, SH2 domain is the most common site for mutation, such as in the context

of large grandular leukemia (40%) (65), chronic natural killer cell lymphoproliferative disorders (30%) (66), and aplastic anemia and myelodysplastic syndromes (67, 68). SNP of *STAT4* contributes to rheumatoid arthritis and systemic lupus erythematosus (67). Constitutive activation of *STAT5* are associated with chronic myeloid leukemia (CML), as mice with bone marrow deficient in *STAT5* are resistant to CML development (69). In contrast, *STAT5B* deficiency causes defects in regulatory T cells and NK cells, resulting in diseases such as early onset juvenile idiopathic arthritis, severe eczema, and immune thrombocytopenic purpura (70). *STAT5B* deficiency is also correlated with dwarfism (71). Lastly, asthma and allergy pathogenesis are associated with *STAT6* SNP (72).

1.3.1. Asthma

Asthma is a prevalent chronic inflammatory disorder of the airways, with symptoms of airway hyperresponsiveness (AHR), inflammation, and intermittent airflow obstruction (6). It affects around 339 million people worldwide in 2018 (73). Although asthma can be controlled using standard inhalant therapy, about 20% of the patients are unresponsive to the conventional treatments (74). To this date, over 100 genes have been identified to be associated with asthma pathogenesis, including genes encoding IL-4Rα, IL-13Rα, and STAT6 (75).

IL-4 plays a critical role in allergic asthma. Studies have shown that atopic patients have higher frequency of IL-4 producing T cells than normal controls (76). One of the main functions of IL-4 is to drive the differentiation of naïve T helper type 0 lymphocytes into Th2 lymphocytes (6). IL-4, IL-5, and IL-13 cytokines secreted by Th2 cells further promote allergic and eosinophilic inflammatory responses (77). Th2 inflammation elevates many biomarkers of asthma, including eosinophil count in sputum and blood, total serum IgE, IL-13 and IL-5 bronchial expression, fraction of exhaled nitric oxide, and bronchial epithelial

proteins including periostin and osteopontin (78). Through the induction of mucin genes, IL-4 contributes to airway obstruction via mucus hyper-secretion and goblet cell metaplasia (79). Upregulated expression of eotaxin by IL-4 triggers inflammation, eosinophil chemotaxis, and lung remodeling in chronic asthma (80, 81). IL-4 also downregulates Fas expression on T lymphocytes and eosinophils, which prolongs cell survival and leads to persistent inflammatory infiltration (75, 81). IgE production and VCAM-1 expressions on vascular endothelium are two other biomarkers induced by IL-4 (75). IgE is responsible for mast cell activation to trigger immediate allergic reactions (79). VCAM-1 on the other hand mediates migration of T cells, monocytes, basophils, and eosinophils to the site of inflammation (82).

STAT6, the downstream effector protein, also has a pivotal role in the pathogenesis of asthma. *STAT6* knockout mice have shown to have significantly reduced lung eosinophilia, AHR, peribronchial inflammation, Th2 cell and chemokine production, and mucus production in allergen-induced asthma models (83, 84). Many functions of Th2 response requires STAT6 activation, including Th2 cell differentiation, survival, trafficking, and chemokine production (85). Furthermore, IL-4 target genes that encode CD23, major histocompatibility complex (MHC) class II, IL-4Rα, V-CAM1, E-selectin, and immunoglobulin ε are STAT6-dependent (86, 87). STAT6 also stimulates the expression of eotaxin (88), smooth muscle contractility genes (e.g. *RHO*) (89), mucin genes in airway epithelium (e.g. *MUC5AC* and *GOB5*) (90), and STAT6-dependent "alternative activation" genes for macrophage polarization following IL-4/IL-13 induction (91).

In order to study the pathophysiology of allergic asthma, allergen-challenged murine models have been developed to reproduce reminiscent clinical features of human asthma. Ovalbumin (OVA), a protein derived from chicken egg, is one of the most frequently used allergen for

the induction of robust, allergic pulmonary inflammation in murine models (92). OVA is often used in combination with an adjuvant to favor Th2 immune response (92). Mice were first sensitized with OVA and adjuvant, preferentially through intranasal instillation to simulate inhalation of allergens in human (93). Subsequent OVA challenge is then performed to elicit asthma pathologies, including AHR, eosinophilia, and epithelial mucus production (92). The OVA-induced allergic asthma murine model is employed in this study to investigate the therapeutic effect of BX795 against asthma.

1.4. Synthetic JAK and STAT inhibitors

Since JAKs and STATs have demonstrated great importance in the immune homeostasis, inhibitors of JAKs and STATs became an emerging target of interest for cancer and autoimmune disease treatments. Jakinibs are small-molecule inhibitors of JAKs. Most Jakinibs developed to this date target the JH1 domain by competing with ATP at the catalytic site through non-covalent interactions (94). However, due to the high degree of JH1 homology between the four members of JAKs and several other tyrosine kinases, the development of selective JAK inhibitors face great challenges. Some of the first generation Jakinibs include: tofacitinib, ruxolitinib, baricitinib, and oclatinib (95). Tofacitinib inhibits JAK1 and JAK3 with some inhibitory activity against JAK2 (96, 97). Ruxolitinib is a JAK1/JAK2 inhibitor with moderate activity against Tyk2 (94, 98). Baricitinib is another JAK1/JAK2 inhibitor that blocks pro-inflammatory cytokine signaling, including IL-6 and IFNγ (99). Oclatinib is a non-selective pan-Jakinib used in canine eczema and atopic dermatitis treatment (15, 100). Many JAK inhibitors are currently being tested in phase 2 and phase 3 clinical trials, but only tofacitinib and ruxolitinib have been approved by U.S. Food and Drug Administration (FDA) for treatments of rheumatoid arthritis and myeloproliferative neoplasm, respectively (101-103). However, both drugs cause a number

of adverse effects, including higher susceptibility to infection and cytopenia (104, 105). Nasopharyngitis, bronchitis, septic shock, and cellulitis are some common side effects associated with tofacitinib treatment (106). Many hematopoietic growth factors, including erythropoietin and granulocyte macrophage-colony stimulating factor, activate and signal through JAK2, thus neutropenia and anemia are also recognized side effects of Jakinib (107).

In order to enhance specificity and reduce adverse off-target effects, low conservation sequences have been targeted for the development of next-generation Jakinibs (99). Mapping of FERM domain has revealed significant differences between JAK1 and Tyk2 structures, making it a potential target for JAK inhibitors (94, 96). For example, ABT-494 is a next-generation Jakinib currently tested in phase 2b trials for rheumatoid arthritis treatment (95). It is 74-fold more selective to JAK1 than JAK2 (108). High sensitivity is conferred by binding to additional sites on JAK1 apart from JH1 (108). However, ABT-494 can cause cytopenia due to off-target effects (99). Therefore, more Jakinibs should be designed to maximize efficacy and selectivity, while minimizing side effects.

In comparison to JAKs, more challenges are faced during the development of STAT inhibitors. Homology between STAT3 and other STATs, particularly STAT1, can lead to severe adverse effects due to the lack of specificity (95). STAT1 is involved in cell death, apoptosis, and antimicrobial defense. STAT3 inhibitors may non-selectively block STAT1 and cause increased survival of tumor cells from head and neck carcinoma (109). Functional redundancy between different STATs is another factor that limits the efficacy of STAT inhibitors. For instance, IL-6 primarily activates STAT3 for downstream signaling (110). However, STAT3-deficient cells are still capable of responding to IL-6 stimulation via

STAT1 (110). Hence, selective blockade of JAKs may be preferential than inhibition of STATs for drug development.

Nevertheless, several types of STAT inhibitors have been developed and tested in clinical trials. Disruption of the SH2 domain is one mechanism used to inhibit STAT dimerization and binding to receptors. Small-molecule inhibitors, such as OPB-31121 and OPB-51602, have been tested in phase I trials for hepatocellular carcinoma (111) and refractory solid malignancies treatment (112), respectively. However, these inhibitors exhibited high risk of peripheral neuropathy, with poor bioavailability and limited efficacy (111, 112). Interference with DNA binding is another strategy used to target STATs. STAT3 decoy oligonucleotides are designed to target the DNA-binding domain of STATs by sequestering STATs away from the gene (113). In a phase 0 clinical trial, it has successfully reduced cell viability and suppressed STAT3 target gene expression in head and neck cancer cells (114). Phase 0 clinical trials are developed by FDA to accelerate the clinical evaluation of new molecular agents within a small sample population (115). However, rapid degradation poses limitations on its bioavailability (114). Intrabodies against phosphorylated STAT3 is another type of STAT inhibitor that have shown to be effective in *in vitro* models (116).

1.5. TBK1 signaling pathway

TANK-binding kinase 1 (TBK1) is a serine/threonine (Ser/Thr) kinase that regulates the innate antiviral response (117). TBK1 is a member of the IκB kinase (IKK) family (117). Along with IKKε, they play an essential role in the interferon regulatory factor (IRF) 3 signaling pathway (117). TBK1 contains a N-terminal kinase domain (KD), ubiquitin-like domain, and C-terminal scaffold and dimerization domain (118). Its activity is regulated by autophosphorylation on residue Ser172 (119).

TBK1 can be activated via toll-like receptors (TLRs), retinoic acid-inducible gene I (RIG-I)-like receptors (RLRs), or cyclic GMP-AMP synthase (cGAS)- stimulator of interferon genes protein (STING) pathways (Figure 4) (120, 121). Upon viral infection, viral nucleic acids can be recognized by three categories of innate immune sensors: cytosolic DNA sensors, cytosolic RNA sensors, and endosomally localized TLRs (122). Cytosolic DNA is mainly detected by cGAS (123). cGAS produces cGAMP to bind and activate STING (124). STING subsequently recruits TBK1 to phosphorylates IRF3 (124, 125). Activated IRF3 then dimerizes, translocates to the nucleus, and binds to CREB-binding protein /P300 to stimulate the transcription of type I interferon-encoding genes, such as interferon-β (IFNβ) (126-128).

In contrast, most cytosolic viral RNAs are recognized by RLRs, which include RIG-I and melanoma differentiation-associated protein 5 (MDA5) (129, 130). RIG-I preferentially recognizes RNA containing either 5' triphosphate or 5' diphosphate (131, 132), whereas MDA5 senses double-stranded RNA (131, 133, 134). Activated RIG-I and MDA5 directly bind to mitochondrial antiviral-signaling protein (MAVS), and induce the downstream TBK1 to phosphorylate IRF3 and IRF7. IRF3 and IRF7 homo- or heterodimers then initiate type I interferon response gene transcriptions (125).

TLR is also involved in sensing nucleic acid in endolysosome (135). Out of all the receptors in the TLR family, TLR3 recognizes double-stranded RNA and binds to TRIF to activate TBK1 and the downstream IRF3 (136). TLR4 detects lipopolysaccharides or lipid A component of gram-negative bacteria, and some viral proteins, including the fusion protein of respiratory syncytial virus (137). TLR4 signaling activates both the TRIF pathway and myeloid differentiation factor 88 (MyD88) pathway (138). However, IFNβ gene transcription is predominantly induced via TRIF and TBK1-IRF3-mediated pathway (138). In contrast,

TLR7 and TLR8 recognize single-stranded RNA and recruit MyD88 to activate IRF7, either through TBK1-IKKε (139) or interleukin-1 receptor-associated kinase (IRAK) 4-IRAK1-IKKα kinase cascade (140). In comparison, CpG DNA recognized by TLR9 signals exclusively through MyD88 pathway (141). Type I IFNs produced from these signaling cascades subsequently activate the downstream pathways, including the JAK/STAT pathway.

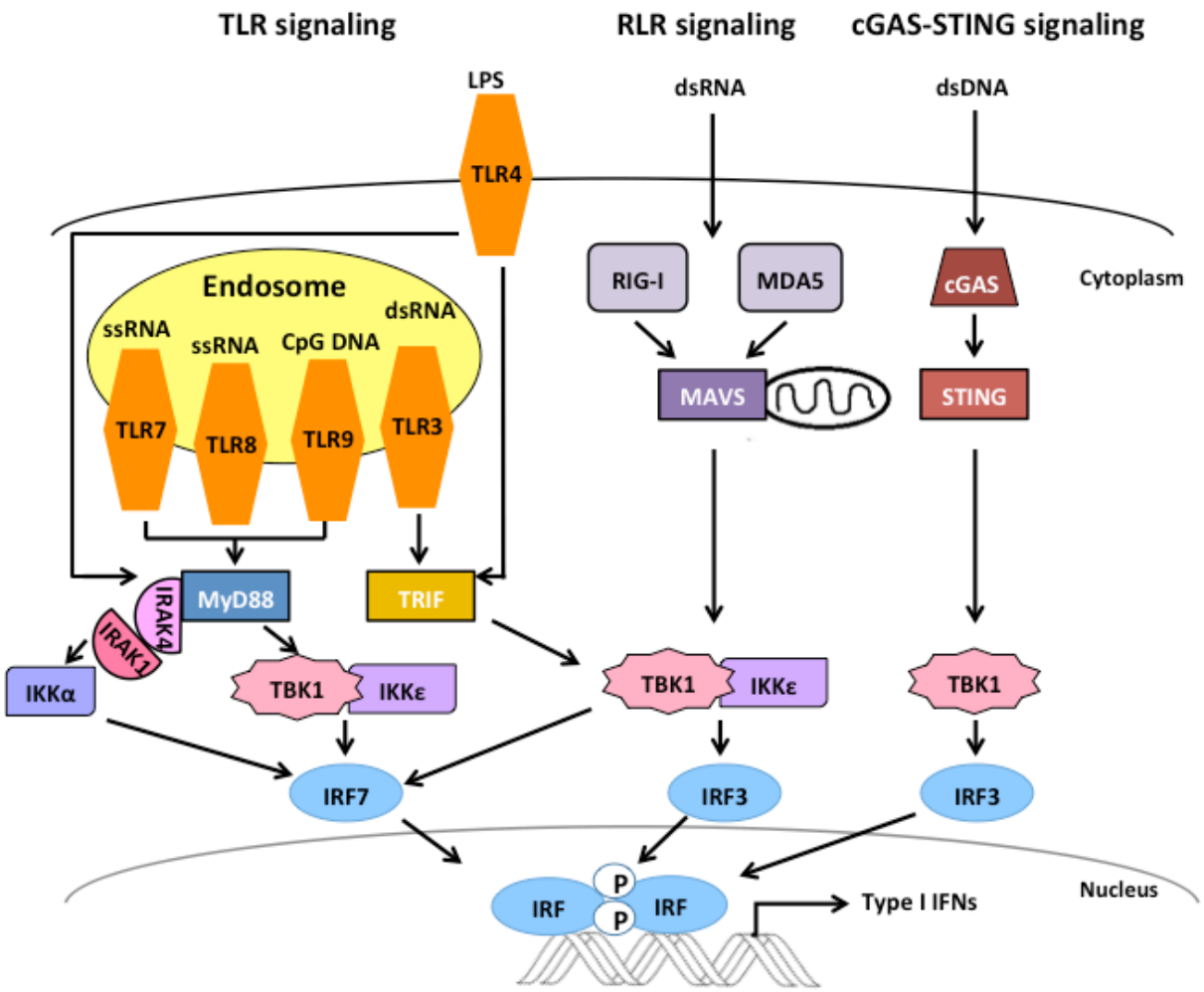

Figure 4. Schematics of TBK1 signaling pathway.

TBK1 is involved in the signaling cascade of TLR, RLR, and cGAS-STING pathways. These three signaling pathways are activated by different pathogen-associated molecular patterns, but all activate TBK1 to phosphorylate IRF3 and/or IRF7. IRF7 can also be phosphorylated by IKKα. IRF3 and IRF7 homo- or heterodimers then translocate to the nucleus to induce the production of type I IFNs.

1.6. Therapeutic potential of BX795

BX795 is a synthetic compound known to inhibit TBK1/ IKKε by binding to the kinase domain (119, 142). Recent studies have shown that BX795 inhibits a number of kinases, including PDK1 (3-phosphoinositide-dependent kinase-1) (143), JNK (c-Jun N-terminal kinase) (144), p38 MAPK (mitogen-activated protein kinase) (144), ERK8 (extracellular signal-regulated kinase 8) (142, 144), and protein kinase B (Akt) (145). In particular, one study has shown that by blocking Akt phosphorylation, BX795 elicited antiviral activity against infection of multiple strains of herpes simplex virus (HSV)-1 in cultured human and animal corneas (145). However, another study suggested that disruptions in JNK and p38 MAP kinase activation also lead to inhibition of HSV-1 and HSV-2 replication by BX795 (144). Nevertheless, both Akt and JNK are involved in the regulation of cell survival and proliferation (146, 147). Hyperactivation of Akt has been reported in a number of human solid tumors and hematological malignancies (147). Constitutive activation of JNK has also been observed in squamous cell carcinoma and T-cell acute lymphoblastic leukemia (146). BX795 thus possess the therapeutic potential for cancer treatments.

1.7. Oncolytic virotherapy

Oncolytic virotherapy is an emerging therapeutic approach for cancer treatment. It uses oncolytic viruses (OVs) to selectively replicate and kill infected tumor cells (148). Tumor cell death can be triggered by direct virus-mediated cytotoxicity or indirect immune effector mechanisms, such as tumor blood vessel destruction and upregulation of anticancer response (148). To enhance the safety, selectivity, and oncolytic activity of oncolytic virotherapy, OV can be genetically modified to encode toxic compounds or immune-stimulatory proteins (148). OVs encompass a broad spectrum of DNA and RNA viruses. Herpes simplex virus, Vaccinia virus, Adenovirus, and Parvovirus are examples of oncolytic DNA viruses (148).

RNA viruses, including Reovirus, Measles virus, Newcastle disease virus, Seneca valley virus, and Vesicular stomatitis virus (VSV), have also displayed oncolytic activity with varying degrees of preclinical successes (148).

Even though a significant number of clinical trials have been conducted on OVs, to this date, only two strains of OVs have been approved. The recombinant human type-5 adenovirus, H101, was the first oncolytic virus approved for head and neck malignancy treatment in China (149). E1B-55kDs gene responsible for p53-binding and inactivation was deleted in the recombinant virus (150). Tumor specificity is conferred through this gene deletion as the virus is only capable of replicating in tumor cells lacking functional p53 (150). In the United States and the European Union, Talimogene Laherparepvec (T-VEC), a genetically engineered HSV, was the first OV approved for locally advanced or non-resectable melanoma treatment (151). T-VEC is engineered with mutations in infectious cell proteins (ICP) 34.5 and additional expression of granulocyte macrophage-colony stimulating factor (GM-CSF) (152). Mutations in ICP34.5 protein impair viral replication, viral exit, and neurovirulence (153). In contrast, GM-CSF potentiates viral oncolysis (152).

Similar to other therapies, oncolytic virotherapy also possesses several limitations. Accurate delivery of OV to the target site is one of the main limitations. For OV delivered intravenously via systemic circulation, the liver may sequester a part of the administered OV and reduces its bioavailability (154). Previous exposure to the viruses can also lead to the production of neutralizing antibodies, which bind to viruses in the circulation and restrict target delivery (155). Due to tumor heterogeneity, it is unlikely that OV monotherapy is sufficient for cancer treatment. Combined therapy with other anticancer treatments is therefore exploited to achieve better therapeutic outcomes.

1.8. VSV virology

VSV is a prototypic enveloped, negative-sense, single-stranded RNA virus in the genus *Vesiculovirus* of the *Rhabdoviridae* family. VSV New Jersey (VSV-NJ) and VSV Indiana (VSV-IN) are the two serotypes that cause most endemics in Central and South America (156). VSV naturally infects horse, cattle, swine, and their insect vectors, resulting in fever and vesicular lesions (157, 158). VSV infection is not prevalent in the human population and is generally asymptomatic (156). However, severe pathologies such as encephalitis has been reported to be associated with wild type VSV-IN infection (159).

VSV has a 11kb genome that encodes five proteins: nucleocapsid (N) protein, phosphoprotein (P), matrix (M) protein, glycoprotein (G) protein, and large viral polymerase (L) (156). The five virus-encoded proteins, along with a number of host proteins, form the VSV virion (160). N protein encapsidates viral genome and forms a ribonucleoprotein (RNP) complex (161). G protein is a viral fusion protein that facilitates the attachment and fusion between virus envelop and host cell membrane via the ubiquitously expressed low density lipoprotein receptor, followed by clathrin-dependent endocytosis (162, 163). Endosomal acidification causes conformational changes in G protein, which facilitates viral envelope fusion with the endosomal membrane and release of RNP into the cytoplasm (164). RNP acts as the template for RNA-dependent-RNA-polymerase (RdRp) to initiate transcription and replication of viral genes (165). RdRp consists of L proteins and P proteins (165). L protein catalyzes nucleotide polymerization, whereas P protein serves as an essential subunit for L protein from proteolytic degradation and interacting with terminal sequences for viral RNA synthesis (166, 167). P protein, in complex with N protein, is also involved in the encapsidation of nascent RNA (168, 169). Viral proteins are subsequently translated by host

cell machinery, followed by packaging into bullet-shaped virion using M protein (170). In particular, M protein is responsible for majority of the cytopathic effect of VSV, including inhibition of cellular mRNA synthesis and export, cytoskeleton disorganization, and apoptosis induction (171-174). Inhibition of cellular gene expression allows VSV to replicate rapidly and reach high titre before substantial antiviral response is mounted by infected host cells (175).

1.8.1. Immune stimulation by VSV

VSV infection induces host antiviral response predominantly through the activation of RIG-I and MDA5 type I IFN signaling pathway (176). Type I IFNs then signals through the JAK/STAT pathway to upregulate ISG transcriptions and enhance antiviral activities (177). These processes lead to VSV clearance within 72h after treatment (178). In addition to antiviral responses, local inflammation induced by virus can also trigger antitumor effects through MyD88 signaling (179). Oncolysis is primarily driven by the proinflammatory response rather than ongoing virus replication (180). For example, virus lysed tumor cells release tumor-associated antigens, danger-associated molecular patterns, and pathogen-associated molecular patterns to trigger the activation, maturation, and infiltration of multiple immune cells, including tumor-specific $CD8^+$ T cells, DCs, neutrophils, and NK cells (178, 181, 182). Type III IFNs secreted by viral infected cells can stimulate the expression of NK cell ligands on tumor cells, inducing NK cell recognition and cytotoxicity (183). In addition, VSV can activate and lead to the maturation of plasmacytoid dendritic cells (pDCs), which primes $CD8^+$ T cells with tumor antigens and induces IFNα production (181, 184). Surface receptors involved in antigen presentation, such as MHC class II, CD80, CD86, and CD40, are also upregulated (185). Overall, VSV triggers both antiviral and antitumor responses in infected cells to facilitate tumor cell death.

1.8.2. VSV as an oncolytic virus

VSV bears several characteristics of an ideal OV. VSV infects a wide range of cells, allowing it to be employed in the treatments of a broad spectrum of cancers (186). The efficacy and adverse effects of VSV treatments can also easily be evaluated in multiple laboratory cell lines (187). Despite its ability to infect various cells, VSV confers its inherent tumor specificity by selectively replicating in cells with defective antiviral IFN response (186). In the human population, there is a lack of pre-existing antibodies against VSV (186). Thus the delivery of VSV is less impacted by the neutralizing antibodies in the circulation compared to other OVs. VSV has rapid replication and oncolysis kinetics, capable of producing very high virus titre. It has a small genome, which makes it easy to manipulate and engineer for recombination. For example, VSV genome can be modified to express human IFNβ (188). The resulting recombinant VSV has enhanced oncolysis and upregulated antitumor response via interferon induction (188, 189). In order to prevent neurotoxicity without compromising its oncolytic activity, VSV has also been pseudotyped with surface glycoprotein from a non-neurotropic lymphocytic choriomeningitis virus or retargeted measles virus (190, 191). Other modifications that enhance the safety profile of VSV include a methionine deletion at position 51 in the matrix protein (VSVΔ51) (192, 193). Mutation in the matrix protein inhibits the virus' ability to block host transcription of IFN-β genes (171, 194) and nuclear export of mRNA (173, 195) in infected cells, hence inducing a more rapid and robust interferon response (187). Furthermore, the entire replication cycle of VSV occurs within the cytoplasm, which eliminates the risk of integration into host genome (196). After vaccination, it activates the adaptive immunity against tumor antigen and disrupts immune tolerance in tumor microenvironment. VSV can also selectively infect tumor blood vessel endothelium and cause thrombosis in CT26 colorectal tumors (197). In addition, VSV inhibits the Akt

phosphorylation at Thr308 and Ser473 residues (198). Since Akt activation is frequently found in cancer cells, the ability of VSV to block Akt enhances its therapeutic benefit in cancer treatment (199). Currently, VSV is being tested in several phase I clinical trials against solid tumors and hematologic malignancies (trial NCT02923466, NCT03120624 and NCT03017820 on ClinicalTrials.gov) (200).

1.8.3. VSV combination therapy

Some cancer cells have conferred resistance to VSV and other OVs due to their ability to maintain intact or upregulated type I IFN antiviral responses (201-203). Tumor-infiltrating lymphocytes may inhibit and eradicate viral infection (176). Pre-existing antibodies against OVs in the circulation may also bind and block viral penetration (176). Therefore, combination therapy of OV with other therapeutic agents is employed to overcome these challenges.

Synergy between oncolytic VSV and immune checkpoint inhibition has demonstrated enhanced antitumor activity in preclinical studies (204, 205). Vesicular stomatitis virus-interferon β-sodium iodide symporter (VSV-IFNβ-NIS) is a VSV that encodes IFNβ and NIS. Its oncolytic activity was increased by anti-PD1 (programmed cell death protein 1) antibody in acute myeloid leukemia mice model (205). The combination treatment also resulted in reduced tumor burden and enhanced survival, without significant toxicity (205). Furthermore, our previous studies have illustrated a novel role of nuclear factor erythroid 2-related factor (Nrf2) in the regulation of STING antiviral pathway (206, 207). Nrf2 suppresses STING expression and disrupts the downstream type I IFN production (207). Combination therapy of VSVΔ51 and sulforaphane, an antioxidant compound that induces Nrf2, has augmented viral replication in OV-resistant cancer cells with improved therapeutic

outcomes in murine syngeneic and xenograft tumor models (206). Histone deacetylase inhibitors (HDIs) in combination with VSV have also lead to an increase in viral oncolysis by dampening IFN responses and enhancing virus-mediated apoptosis (208). HDIs are epigenetic modulators, capable of influencing the expression of antiviral genes (209). Vorinostat, a HDI, has remarkably stimulated autophagy and augmented VSV replication and oncolysis through NF-κB pathway in multiple cancer cells lines and animal models (210). Furthermore, the kinase mammalian target of rapamycin (mTOR) is also capable of inducing type I IFN response through phosphorylating 4E-BPs and S6Ks effector proteins (211). Combinatorial treatment with VSVΔM51 and rapamycin, an mTOR inhibitor, showed elevated viral oncolytic activity via suppression of mTOR complex 1-depednent type I IFN production, resulting in higher survival of immunocompetent rats with gliomas (212).

Apart from intact type I IFN signaling, defective apoptosis pathway is another mechanism to confer VSV resistance. In B cell chronic lymphocytic leukemia (CLL), overexpression of anti-apoptotic B cell leukemia/lymphoma 2 (Bcl-2) proteins disrupts the apoptotic pathway and impairs VSV oncolysis (213, 214). Combination treatment of VSV and obatoclax, a Bcl-2 inhibitor, synergistically induced the intrinsic mitochondrial apoptotic pathway via caspase-9 and caspase-3 activation, Bcl-2-associated X protein translocation, and cytochrome c release (214). Increased cell death, autophagy, improved susceptibility to VSV oncolysis, and reduced tumor growth were observed in CLL cells and SCID mice with A20 lymphoma tumors (213, 214). Overall, improved efficacy and oncolytic activity are achieved by combined therapy of VSV with immunomodulators. These studies highlight the therapeutic potential of VSV combination therapy in cancer treatments.

Ultimately, this study aims to characterize the effect and mechanism of action of BX795 on the JAK/STAT signaling pathway stimulated by different cytokines. Based on our results, BX795 inhibits STATs phosphorylation in IFNα, IFNγ, IFNλ, and IL-4-induced JAK/STAT pathways, likely through blockade of phosphorylated JAK and STAT interaction. BX795 also enhances VSV oncolytic activity in different cells lines, but fails to provide protection against OVA-induced allergic asthma.

CHAPTER 2. MATERIAL AND METHODS

2.1. Cell cultures

Jurkat cell line, U87 human primary glioblastoma cell line, and human embryonic kidney cell line (HEK293) were purchased from the American Type Culture Collection (ATCC, Manassas, VA, USA). Immortalized human hepatocytes cell line (IHH) was kindly provided by Dr. Ranjit Ray (Saint Louis University, St. Louis, MO, USA) (215). Murine bone marrow derived macrophages (BMDM) were extracted from mixed background mice. Cellosaurus cell line (OCI-Ly8) was obtained from Koren Mann (McGill, University, Canada). TBK1 -/- MEF cells were kindly provided by Dr. Wen-Chen Yeh (Toronto, ON, Canada). IHH cells, HEK293 cells, and TBK1 -/- MEF cells were grown in Dulbecco's modified Eagle's medium (DMEM; Wisent, St. Bruno, QC, Canada), supplemented with 10% fetal bovine serum (FBS); Wisent) and 1% penicillin-streptomycin (P/S; Wisent). U87 cells were grown in Eagle's Minimum Essential Medium (EMEM; Wisent), supplemented with 10% FBS and 1% P/S. BMDM cells were grown in Roswell Park Memorial Institute medium (RPMI; Wisent), supplemented with 20% FBS, 30% L929, and 1% P/S for differentiation. After differentiation, BMDM cells were grown in RPMI with 20% FBS and 1% P/S. OCI-Ly8 cells were grown in RPMI supplemented with 10% FBS and 1% P/S. All the cells were maintained at 37°C and 5% CO_2.

2.2. Plasmids and reagents

IFN-stimulated response element-luciferase reporter plasmid (ISRE-Luc) and Renilla luciferase control reporter plasmid (pRLTK) have been previously constructed (216).

2.3. Transfection and luciferase assay

HEK293 cells were transfected with 50ng of pRLTK reporter and 100ng of ISRE-Luc luciferase reporter using calcium phosphate co-precipitation method (216). At 8 hours post-transfection, cells were left untreated, infected with 40 hemagglutination units (HAU) per mL of Sendai virus (Charles River Laboratories, Pointe Claire, QC, Canada), or treated with 1000units/mL of IFN alpha-2b (Intron A, Schering Plough, Kenilworth, NJ, USA). At 24 hours after transfection, the reporter gene activities were measured by Dual-Luciferase Reporter Assay based on manufacturer's instructions (Promega, Madison, WI, USA).

2.4. Cytokine and BX795 treatment *in vitro* assay

The cytokines used for treatment include: INTRON® A interferon alfa-2b (Merck Canada Inc., Kirkland, QC, Canada), mouse IFN Alpha A (PBL Assay Science, Piscataway, NK, USA), human IFNγ (Sigma-Aldrich, Toronto, ON, Canada), human IFNλ (Sigma-Aldrich), human IL-4 (Sigma-Aldrich), and murine IL-4 (STEMCELL Technologies, Vancouver, BC, Canada). BX795 was purchased from Sigma-Aldrich (St. Louis, Missouri, USA) and dissolved in DMSO. All cells were treated with BX795 or dimethyl sulfoxide (DMSO; Thermo Fisher Scientific, Waltham, MA, USA). Dose response assay of BX795 (125nM, 250nM, 500nM, and 1000nM) was performed for cells treated with human IFNα, human IFNλ, and murine IL-4.

2.4.1. Human IFNα and IFNλ treatment *in vitro*

IHH cells were treated with 1000 units/mL of IFNα or 10ng/mL of IFNλ, along with varying concentrations of BX795 (125nM, 250nM, 500nM, and 1000nM) or 1μM DMSO for 2h and 4h.

2.4.2. Human IFNγ treatment *in vitro*

IHH cells were treated with 1μM BX795 or 1μM DMSO, along with 50ng/mL of IFNγ for 2h and 4h.

2.4.3. Human and murine IL-4 treatment *in vitro*

IHH cells were pre-treated with 1μM BX795 or 1μM DMSO for 2 hours, followed by stimulation with 20ng/mL of human IL-4 for 15min, 30min, 60min, 2h, and 4h. For BX795 dose response assay, BMDM cells were treated with 20ng/mL of murine IL-4, along with 1μM DMSO or 125nM, 250nM, 500nM, and 1000nM of BX795 for 1h and 4h. Jurkat cells were also treated with 20ng/mL of human IL-4, with 1μM DMSO or 250nM BX795 for 1h and 4h. OCI-Ly8 cells were pre-treated with BX795 (0nM, 250nM, 500nM, and 1000nM) for 1h, followed by stimulation with 5ng/mL of IL-4 for 1h and 3h.

2.5. Protein extraction and immunoblot analysis

Cells were washed once with ice-cold phosphate buffered saline (PBS), and proteins were extracted as follows. Cell pellets were lysed in ice-cold lysis buffer containing 20mM Tris-HCl (pH 7.5), 150mM NaCl, 1% Triton, 10% glycerol, distilled H_2O, 40mM beta-glycerophosphate, 1mM PMSF, 1mM Na_3VO_4, 5mM NaF, 1mM DTT, 10mM NEM, and protease inhibitor cocktail (Sigma-Aldrich) in 1:1000 dilution. The extracts were kept on ice for 30 minutes and centrifuged at 13,200 rpm for 15 minutes (4℃). The supernatants containing protein were collected and stored at -80℃.

Protein concentration was determined using Bio-Rad protein assay reagent (BioRad, Hercules, CA). Whole-cell lysates (35-40μg) were resolved using 10% sodium dodecyl sulfate-polyacrylamide gel electrophoresis (SDS-PAGE) and transferred to 0.45 μm

nitrocellulose membranes (Bio-Rad, Mississauga, ON) by semi-dry blotting (Bio-Rad). Membranes were blocked for 1 hour in 5% nonfat dried milk in PBST (phosphate-buffered saline + 0.1% Tween-20) and then incubated with any of the following primary antibodies: anti-Sendai Virus antibody (Cedarlane, Burlington, ON). Anti-phospho-JAK1 (Tyr1022/1023; #3331), anti-phospho-JAK2 (Tyr1007/1008; #3776), anti-phospho-Tyk2 (Tyr1054/1055; #9321), anti-phospho-STAT1 (Tyr701; #9171), anti-phospho-STAT2 (Tyr690; #88410), anti-phospho-STAT6 (Tyr641; #9361), anti-STAT6 (#9362S) anti-ISG15 (#2758), anti-ISG56 (#14769), and anti-cleaved Lamin A (#2035) were purchased from Cell Signaling Technology, Boston, MA. Anti-STAT1 (sc-417) and anti-STAT2 (sc-1668) were purchased from Santa Cruz Biotechnology, Mississauga, ON. Anti-RIG-I (MABF297) and anti-β-actin (ABT264) were purchased from EMD Millipore, Bedford, MA. After three 5-minute washes with PBST, membranes were incubated for 1 hour with horseradish peroxidase-conjugated goat anti-rabbit (1:5000 dilution in 5% nonfat dried milk in PBST) or anti-mouse antibodies (1:3000 dilution in 5% nonfat dried milk in PBST) (Amersham, Piscataway, NJ). After three 10- minute washes with PBST, western-blotting substrates were visualized using enhanced chemiluminescent substrate (ECL) reagents (BioRad).

2.6. Cytokine treatment and quantitative real-time PCR

DNase-treated total RNA from the samples were prepared using the Aurum™ Total RNA Mini Kit (Bio-rad). RNA concentration was determined by absorption at 260nm, and RNA quality was ensured by a 260/280 ratio $\geq$ 2.0. Total RNA was reverse transcribed using High Capacity Reverse Transcription Kit (Appliedbiosystems). qPCR assays were performed using iTaq™ Universal SYBR Green Supermix (Bio-Rad).

2.6.1. Human IFNα *in vitro* treatment

IHH cells were treated with BX795 (125nM, 250nM, 500nM, 1000nM) or 1μM DMSO, with or without IFNα (1000 units/mL) for 24h. Human primer sequences used are as follows: *IFIT Forward:* 5'-CAACAAAGCAAATGTGAGGA-3'; *IFIT Reverse:* 5'-AGGAGCAAAGAAAATGG-3'; *DDX58 Forward:* 5'-GCAGAGGCCGGCATGAC-3'; *DDX58 Reverse:* 5'-TGTAGGTAGGGTCCAGGGTCTTC-3'. *Beta actin Forward:* 5'-ACTGGACGACATGGAGAAAA-3'; *Beta actin Reverse:* 5'-GCCACACGCAGCTCATTGA-3'. All data are presented as a relative quantification, based on the relative expression of target genes versus *beta actin* as reference gene and analyzed using GraphPad Prism 5 software (GraphPad Software, La Jolla, CA, USA).

2.6.2. Human IL-4 *in vitro* treatment

OCI-Ly8 cells were pre-treated with BX795 (250nM, 500nM, and 1000nM) or 1μM DMSO for 1h, followed by induction with 5ng/mL of IL-4 for 3h. Human primer sequences used are as follows: *SOCS1 Forward:* 5'-CCCCTGGTTGTTGTAGCAG-3'; *SOCS1 Reverse:* 5'-GTAGGAGGTGCGAGTTCAGG-3'; *GAPDH Forward:* 5'-GGGAAGCCCATCACCATC-3'; *GAPDH Reverse:* 5'-CGGCCTCACCCCATTTG-3'. All data are presented as a relative quantification, based on the relative expression of target genes versus *GAPDH* as reference gene and analyzed using GraphPad Prism 5 software.

2.7. Co-immunoprecipitation

Anti-STAT1 antibody was crosslinked to protein A/G PLUS-Agarose beads (#sc-2003; Santa Cruz Biotechnology) with 0.2M triethanolamine pH 9.0 for 1h at room temperature. IHH cells were plated in 10cm dishes and treated with 1μM BX795 with or without IFNα stimulation (1000 units/mL) for 3h. Cells were then lysed with TNT lysis buffer (1% Triton

X-100, 200mM NaCl, and 20mM Tris pH 7.2) and the total protein was incubated with crosslinked antibody overnight at 4℃ on a rotator. Immunoprecipitates were collected by centrifugation and the pellets were washed three times with TNT lysis buffer. Beads with loading buffer were boiled for 5 min, and the endogenous protein level of p-JAK1, JAK1, and STAT1 proteins were analyzed by immunoblot. Protein inputs (35 μg) For p-JAK1, JAK1, and STAT1 were run in 10% SDS-PAGE and transferred to nitrocellulose membrane. The same procedure described previously in section 2.5 was used for primary and secondary antibody incubation, Bradford assay, and exposure.

2.8. VSVΔ51 production, quantification, and infection

Recombinant green fluorescent protein- tagged VSV with methionine 51 deletion in the matrix protein-coding sequence (VSVΔ51) was provided by Dr. John Bell (Ottawa Health Research Institute, Canada). Virus was propagated in Vero cells and titrated using standard plaque assay (217). Cells were infected with VSVΔ51 at a multiplicity of infection (MOI) of 0.1 for 1h at 37℃ in serum-free medium, then incubated with complete medium (combined with IFNα and/or BX795) at the indicated time points. Viral titre was imaged and measured using the Zoe Fluorescent Cell Imager (Bio-Rad) and BD FACSAria Fusion flow cytometer (Becton, Dickinson, New Jersey, USA). Calculation and population analysis were done using FACSDiva and FlowJo softwares.

2.9. Mice

Seven-week-old female BALB/c mice were obtained from Charles River Laboratories. All procedures were performed according to the guidelines of the Canadian Council on Animal Care Committee and were approved by the McGill University Animal Care Committee.

2.10. IL-4 and BX795 administration for *in vivo* murine model

Female BALB/c mice (7 weeks) were divided into three groups (5 mice per group) as follows: (1) NT, (2) IL-4, (3) IL-4 + BX795. Mice were injected intraperitoneally (IP) with sterile PBS or 2mg/kg of BX795 (in 2% DMSO, 30% polyethylene glycol (PEG), 2% Tween 80, and PBS; #S1274; Selleckchem, Houston, TX, USA) on day 0. On day 1, mice were then injected with PBS or 200ng of IL-4 in 100μL PBS, immediately followed by injections with 2% DMSO, 30% PEG, and 2% Tween 80 in PBS or 2mg/kg of BX795, both intraperitoneally. 2 mice per group were sacrificed 3h after IL-4 administration using CO_2. Spleen was collected and homogenized (20%, weight/volume in PBS) for immunoblot analysis. 3 mice per group were sacrificed 24h after IL-4 administration using CO_2. Spleen and mesenteric lymph node (MLN) were collected for flow cytometry analysis.

2.11. Ovalbumin (OVA) sensitization and BX795 administration

Asthma was induced based on the methods described by Kishta *et al*. (218). Female BALB/c mice (7-9 weeks) were sensitized with 150μL of sterile PBS or 40μg OVA (#A5503-1G; Sigma-Aldrich) and 2mg Imject™ Alum adjuvant (#77161; Thermo Fisher Scientific) dissolved in 150μL PBS via intraperitoneal injection on day 0 and 7. OVA-sensitized mice were then challenged with 100μg of OVA in 45μL PBS intranasally under isoflurane anesthesia on days 14, 15, and 16. In total, mice were divided into four groups (4 mice per group) as follows: (1) NT, (2) OVA, (3) OVA + BX795 IP, (4) OVA + BX795 IV. Mice were injected with PBS or BX795 (2.5mg/kg intraperitoneally or 1.25mg/kg intravenously (IV) via tail vein injection) on days 13, 14, 15, and 16 one hour prior to OVA sensitization. Mice were sacrificed 24h after last sensitization using CO_2. Serum, lung, and spleen were collected for further analyses. Weight loss was also evaluated to determine drug toxicity.

2.12. Cell harvest and flow cytometry analysis

Spleen and MLN were meshed and passed through 70μm nylon cell strainer (#352350; Corning Inc., Corning, NY, USA) and washed once with RPMI supplemented with 5% FBS. Red blood cells were lysed with 0.2% sodium chloride for 1 minute. 1.5-2 million cells from each mouse were then incubated with anti-CD16/CD32 (#553141; BD Biosciences, San Jose, CA, USA) for 10 minutes at room temperature.

For mice stimulated with IL-4 administration, spleen and MLN cells were stained with the following surface staining antibodies (BD Biosciences) in staining buffer (PBS containing 1% FBS) for 15 minutes at room temperature: anti-CD45 (APC), anti-CD3 (PE-Cy7), anti-CD4 (Alexa 488), anti-CD8 (BV650), and anti-CD69 (PE).

Cells were analyzed using BD Fortessa flow cytometer (Becton, Dickinson). Compensation calculations and cell population analysis were done using FACSDiva software and FlowJo software.

2.13. ELISAs

The levels of IL-4 release in serum and lung homogenates were measured using commercial enzyme-linked immunosorbent assays (ELISAs; Invitrogen, Waltham, MA, USA) based on manufacturer's instructions. The levels of OVA-specific IgE were also measured in serum samples using ELISA (BioLegend, San Diego, CA, USA) according to the manufacturer's instructions.

2.14. Statistical analysis

Graphical plotting of data and statistical analysis were performed using GraphPad Prism 5 software. The results are expressed as mean ± standard error of the mean (SEM). Differences among the treatment groups were analyzed by unpaired Student's *t* test, and were considered statistically significant with *p* values < 0.05. *, $p < 0.05$; **, $p < 0.01$; and ***, $p < 0.001$.

CHAPTER 3. RESULTS

3.1. BX795 blocks IFNα signaling pathway independent of TBK1

Since BX795 is known to block TBK1 upstream of the JAK/STAT signaling pathway, excess amount of IFNα was added to the cells to bypass this inhibition. In order to explore whether BX795 has a direct effect on the IFNα signaling pathway, a dual-luciferase reporter assay in HEK293 cells was performed. The murine paramyxovirus Sendai virus (SeV) is a potent type I IFN inducer commonly used in type I IFN signaling studies (219), and thus is used in this study as a positive control. Results showed that BX795 inhibited SeV- and IFNα-mediated induction of ISRE reporter luciferase activity in a dose-dependent manner (Figure 1A and 1B). SeV-mediated ISRE activation was reduced by <50% in the presence of 1μM BX795 (Figure 1A). In comparison, IFNα- mediated ISRE activation was reduced by >90% in the presence of 1μM BX795 (Figure 1B). These results suggest BX795 directly inhibits IFNα-stimulated JAK/STAT pathway with high potency.

To further verify the suppression on ISGs, the endogenous levels of proteins encoded by ISGs (RIG-I, ISG56, ISG15) were examined. BX795 significantly reduced SeV- and IFNα-stimulated RIG-I, ISG15, and ISG56 protein expression, with higher stronger inhibition against IFNα induction than SeV (Figure 1C). This finding confirms that BX795 blocks IFNα-induced JAK/STAT signaling pathway independent of TBK1.

A

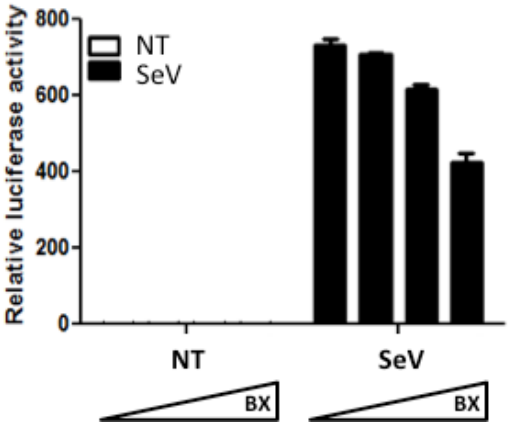
Relative luciferase activity
800
600
400
200
0
NT
SeV
NT
SeV
BX
BX

B

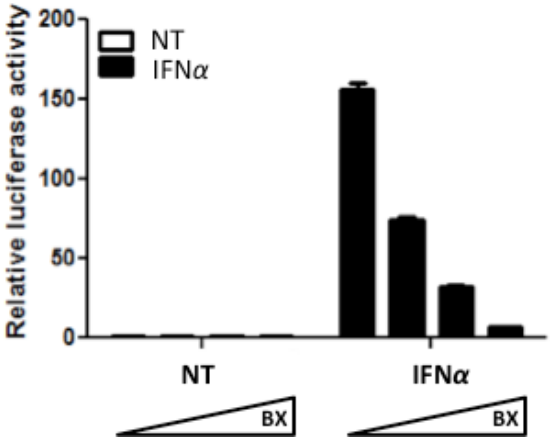
Relative luciferase activity
200
150
100
50
0
NT
IFNα
NT
IFNα
BX
BX

C

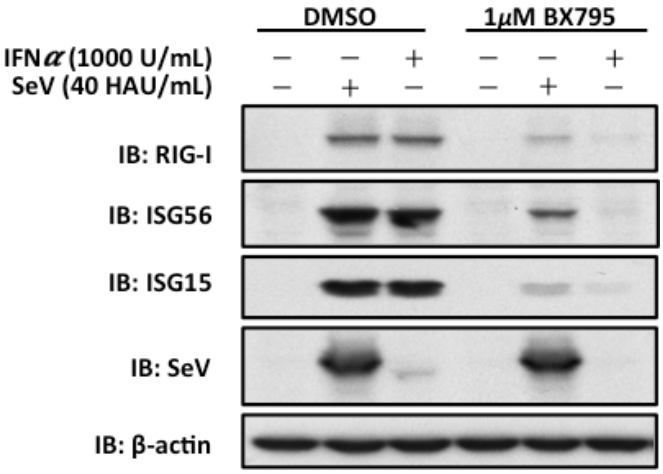
DMSO
1μM BX795
IFNα (1000 U/mL)
SeV (40 HAU/mL)
IB: RIG-I
IB: ISG56
IB: ISG15
IB: SeV
IB: β-actin

Figure 1. BX795 inhibits the ISRE activities and expressions of proteins in the IFNα – mediated type I IFN signaling pathway.

HEK293 cells were transfected with 50ng pRLTK luciferase reporter and 100ng ISRE-Luc luciferase reporter. The cells were untreated (NT), (A) infected with 40 HAU/mL of Sendai virus (SeV), or (B) stimulated with 1000 units/mL of IFNα. The cells were then treated with BX795 (60nM, 250nM, 1000nM). Luciferase activity was measured 24 hours post-transfection. (C) The cells were treated with either 1μM DMSO or 1μM of BX795 for 24 hours. Immunoblot was performed to assess expression of RIG-I, ISG56, ISG15, SeV, and β-actin proteins in whole-cell extracts.

3.2. BX795 suppresses STAT phosphorylation but enhances JAK phosphorylation

To determine the target of BX795 in IFNα- stimulated JAK/STAT signaling pathway, expression of proteins in the pathway were analyzed. We found that BX795 suppressed the phosphorylation of STAT1 and STAT2, but increased the phosphorylation of JAK1 and Tyk2 in a dose dependent manner following BX795 treatment for 2 and 4 hours (Figure 2A). BX795 did not have a significant effect on the total STAT1 and STAT2 level (Figure 2A). The level of downstream protein, ISG56, was also reduced by BX795 (Figure 2A). Similarly, the mRNA levels of ISGs, *IFIT1* (gene encoding ISG56) and *DDX58* (gene encoding RIG-I), decreased dose-dependently after 24hr of BX795 and IFNα treatment (Figure 2B and 2C). The strongest inhibition was exerted by 1μM BX795, with ~70% reduction in *IFIT1* expression and ~50% reduction in *DDX58* (Figure 2B and 2C). BX795 alone did not significantly change the basal expressions of *DDX58* and *IFIT1* (Figure 2B and 2C). Overall, BX795 dose-dependently inhibits IFNα-mediated JAK/STAT pathway both translationally and transcriptionally.

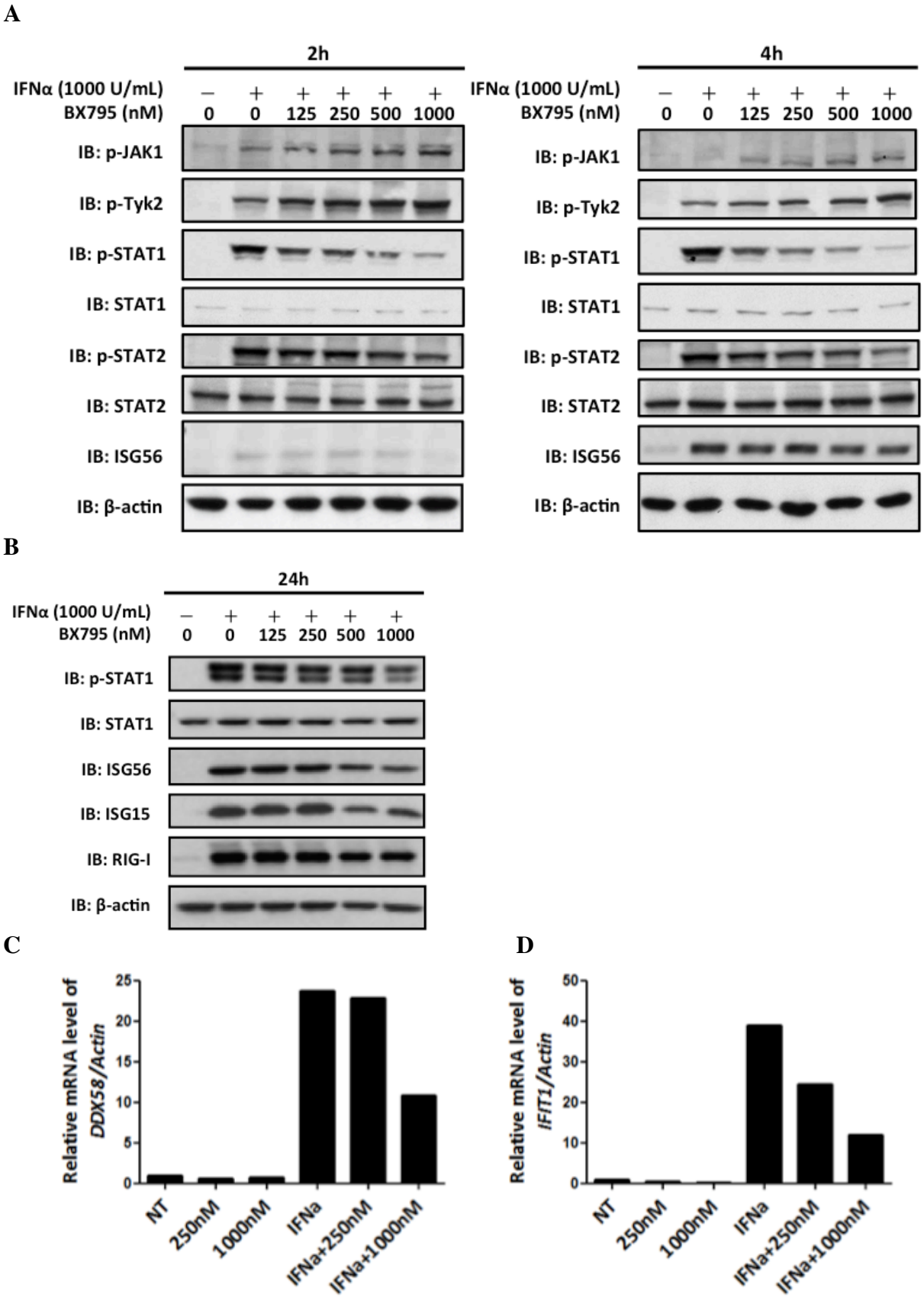
A
2h
4h
IFNα (1000 U/mL)
BX795 (nM)
0 0 125 250 500 1000
IB: p-JAK1
IB: p-Tyk2
IB: p-STAT1
IB: STAT1
IB: p-STAT2
IB: STAT2
IB: ISG56
IB: β-actin
B
24h
IB: RIG-I
IB: ISG15
C
Relative mRNA level of DDX58/Actin
D
Relative mRNA level of IFIT1/Actin
NT
250nM
1000nM
IFNa
IFNa+250nM
IFNa+1000nM

Figure 2. BX795 suppresses IFNα signaling pathway on transcriptional and translational levels.

IHH cells were treated with 1000U/mL of IFNα and BX795 at indicated concentrations for designated durations. (A) Whole-cell extracts were analyzed using immunoblotting to assess expression of p-JAK1, p-Tyk2, p-STAT1, STAT1, p-STAT2, STAT2, ISG56, and β-actin proteins after 2h and 4h of treatments and (B) the expression of p-STAT1, STAT1, ISG56, ISG15, and RIG-I after 24h of treatment. Data are representative of two or more independent experiments. mRNA levels of (C) RIG-I and (D) ISG56 were quantified using qPCR.

3.3. BX795 interferes with the interaction between p-JAK1 and STAT1

Based on the previous findings, since inhibition was first observed at the level of JAK and STAT, it is hypothesized that BX795 may block the kinase function of JAK or compete with JAK for the same binding site on STAT. Since BX795 exhibited the highest inhibitory effect at a concentration of 1μM, cells were pretreated with 1μM BX795 for 1h, followed by 3h of IFNα stimulation. Co-immunoprecipitation and immunoblot analysis revealed a slight decrease in p-JAK1 protein level after being pulled down by anti-STAT1 antibodies, whereas the total level of p-JAK1 was higher in whole-cell extracts with BX795 and IFNα combinatorial treatment compared to IFNα treatment alone (Figure 3). This finding illustrates the effect of BX795 to interfere with p-JAK1 and STAT1 protein interaction.

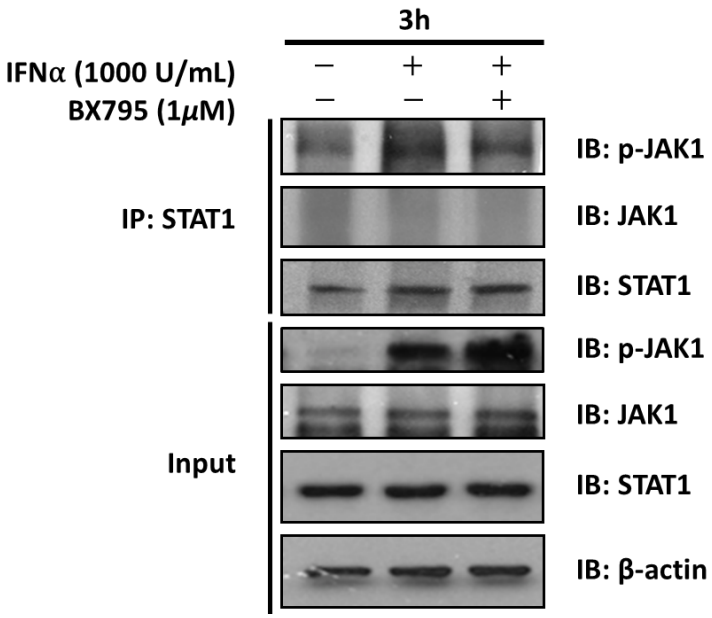

Figure 3. BX796 interferes with the interaction between p-JAK1 and STAT1.

IHH cells were treated with 1μM of BX795 and stimulated with 1000U/mL of IFNα for 3h. Whole-cell extracts were immunoprecipitated with anti-STAT1 antibody and analyzed by immunoblotting using anti-p-JAK1, anti-JAK1, and anti-STAT1 antibodies.

3.4. BX795 augments VSVΔ51 replication under IFNα stimulation

The capacity of BX795 to potentiate VSVΔ51 replication was evaluated in TBK1-/- MEFs and human glioblastoma U87 cells. The cells were infected with GFP-tagged VSVΔ51 (MOI 0.1) for 24h. Based on GFP expression, BX795 enhanced VSVΔ51 infectivity under IFNα stimulation. BX795 treatment alone did not have a significant effect on viral replication in U87 cells (Figure 4C), but slightly increased the percentage of VSVΔ51-infected TBK1-/- cells by an average of 7.37% (Figure 4B). Under IFNα stimulation, BX795 significantly increased the percentage of VSVΔ51-infected cells approximately by 4 folds for both TBK1-/- cells (2.46% VSVΔ51+IFNα versus 8.79% VSVΔ51+IFNα+BX795; $*p<0.05$) (Figure 4B) and U87 cells (18.52% VSVΔ51+IFNα versus 69.21% VSVΔ51+IFNα+BX795; $*p<0.05$) (Figure 4C).

To validate the effect of BX795 on JAK/STAT signaling pathway under viral infection, whole-cell extracts were analyzed using immunoblotting. BX795 treatment alone did not suppress VSV Δ 51-induced STAT1 phosphorylation, whereas BX795 and IFN α combinatorial treatment potently reduced STAT1 phosphorylation in comparison to IFNα treatment alone (Figure 4D and 4E).

In addition, to assess the cytotoxic effect of BX795, apoptosis were examined based on the expression of cleaved lamin A from whole-cell extracts. The combination of BX795 and IFNα enhanced VSVΔ51-mediated cell apoptosis in TBK1-/- and U87 cell lines (Figure 4D and 4E). In contrast, BX795 treatment alone only increased cleaved lamin A expression in TBK1-/- cells (Figure 4D), which corresponds to the higher viral infectivity observed from GFP expression (Figure 4B). Other proteins involved in the apoptosis pathway, such as cleaved caspase-3 and caspase-7, were also assessed. However, BX795 treatment most

significantly affected cleaved lamin A expression compared to the other apoptotic proteins, hence cleaved lamin A expression was chosen to be presented in the figure.

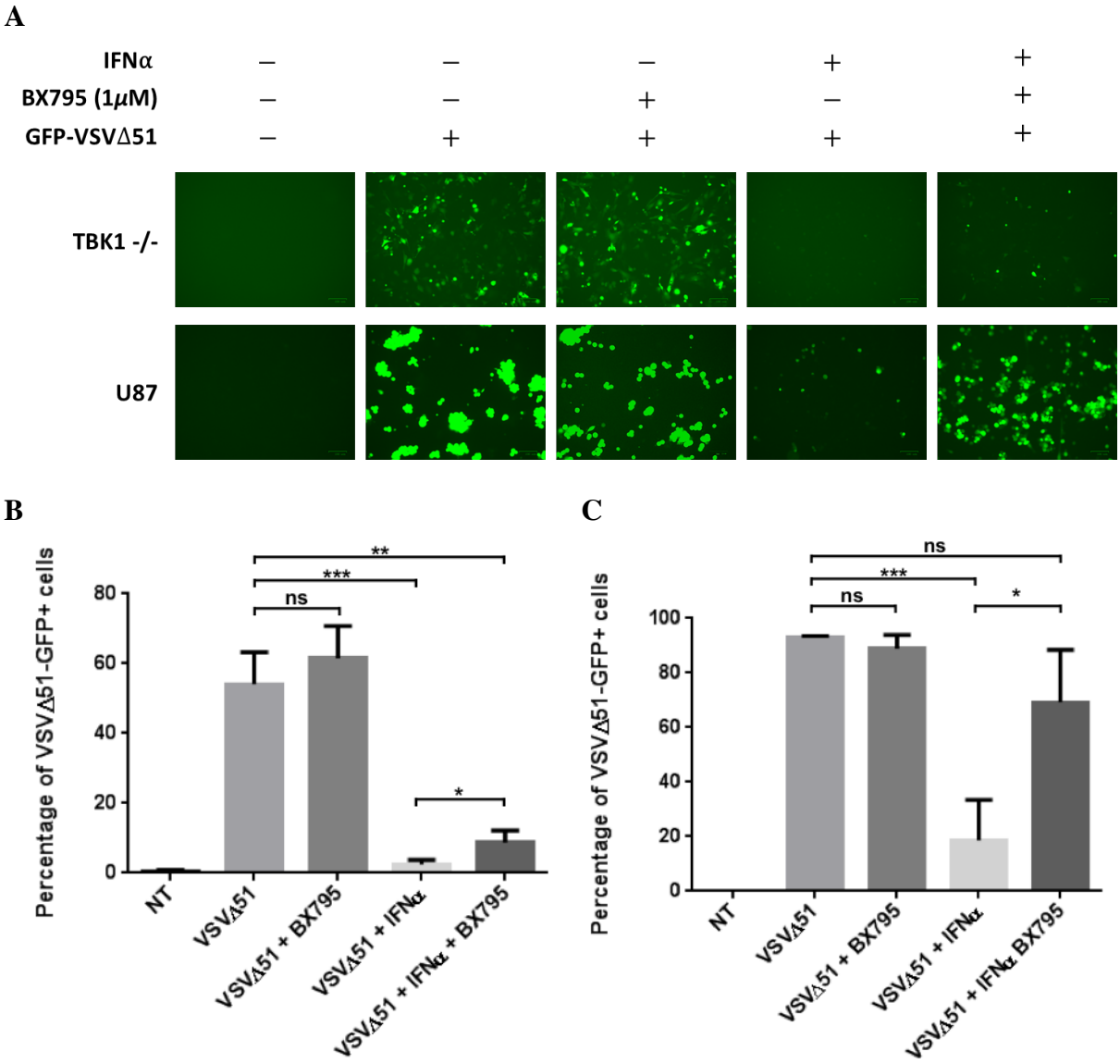
A
IFNα
BX795 (1μM)
GFP-VSVΔ51
TBK1 -/-
U87
B
Percentage of VSVΔ51-GFP+ cells
NT
VSVΔ51
VSVΔ51 + BX795
VSVΔ51 + IFNα
VSVΔ51 + IFNα + BX795
C
Percentage of VSVΔ51-GFP+ cells
NT
VSVΔ51
VSVΔ51 + BX795
VSVΔ51 + IFNα
VSVΔ51 + IFNα BX795
D
IFNα
BX795
GFP-VSVΔ51
IB: p-STAT1
IB: STAT1
IB: Cleaved lamin A
IB: β-actin
E
IFNα
BX795
GFP-VSVΔ51
IB: p-STAT1
IB: STAT1
IB: Cleaved lamin A
IB: β-actin

Figure 4. BX795 enhances VSVΔ51 replication and oncolytic activity in combination with IFNα.

Cells were pretreated with 1μM BX795 and/or 1000 units/mL human IFNα for 1h. Cells were then infected with VSVΔ51 at a multiplicity of infection (MOI) of 0.1 for 24h. (A) Infectivity was imaged using the ZOE Fluorescent Cell Imager in TBK1-/- cell and U87 cells. Viral count was also measured using flow cytometry based on GFP expression in (B) TBK1-/- cells and (C) U87 cells. Data are the means $\pm$ SEM from three experiments. Statistical analysis was performed by unpaired Student's *t* test (*, $p < 0.05$; **, $p < 0.01$; ***, $p < 0.001$). Whole-cell extracts were analyzed using immunoblot for p-STAT1, STAT1, cleaved lamin A, and β-actin in (D) TBK1-/- cells and (E) U87 cells.

3.5. BX795 suppresses IFNγ- and IFNλ- induced JAK/STAT signaling pathways

IFNγ and IFNλ are two other cytokines known to activate the JAK/STAT signaling pathway (220, 221). To determine whether BX795 acts as a broad spectrum JAK/STAT or IFNAR inhibitor, IHH cells were stimulated with IFNγ and IFNλ with BX795. Under IFNγ induction (50ng/mL), BX795 enhanced the phosphorylation of JAK1 and JAK2 proteins after 2h and 4h of treatment (Figure 5A). In contrast, BX795 reduced STAT1 phosphorylation after 4h (Figure 5A). The total STAT1 level was unaffected by BX795 (Figure 5A). Overall, BX795 blocks IFN*γ*- mediated JAK/STAT pathway.

Since IFNλ-mediated JAK/STAT signaling pathway activates the same JAK (JAK1 and Tyk2) and STAT proteins (STAT1 and STAT2) as IFNα- mediated JAK/STAT pathway, a dose response assay was performed to assess the specificity of BX795 as a JAK/STAT inhibitor. Under IFNλ stimulation (10ng/mL), BX795 elicited a stronger inhibition on p-STAT1 compared to p-STAT2 proteins. Increasing concentrations of BX795 suppressed STAT 1 phosphorylation dose-dependently after 2h and 4h treatment, but did not significantly affect STAT2 phosphorylation and the total protein levels of STAT1 and STAT2 (Figure 5B). The results suggest that BX795 has a higher potency against STAT1 protein. Overall, BX795 acts as a broad-spectrum inhibitor of JAK/STAT pathway stimulated by all three types of IFNs.

A

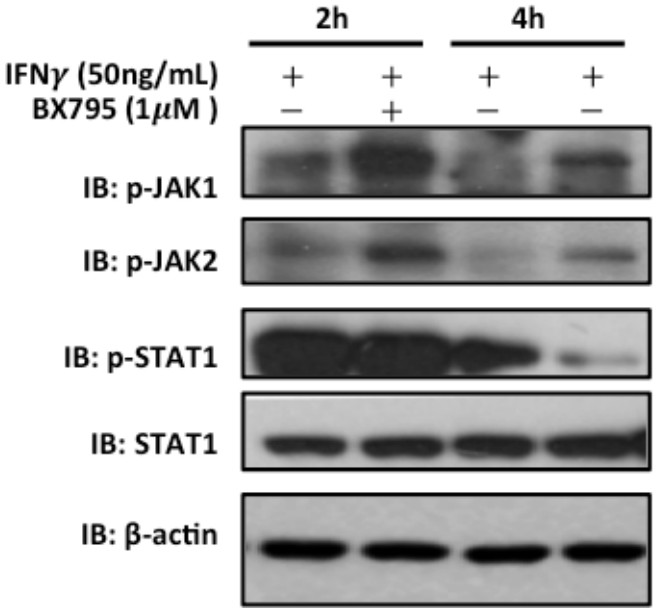
2h
4h
IFNγ (50ng/mL) + + + +
BX795 (1μM) − + − −
IB: p-JAK1
IB: p-JAK2
IB: p-STAT1
IB: STAT1
IB: β-actin

B

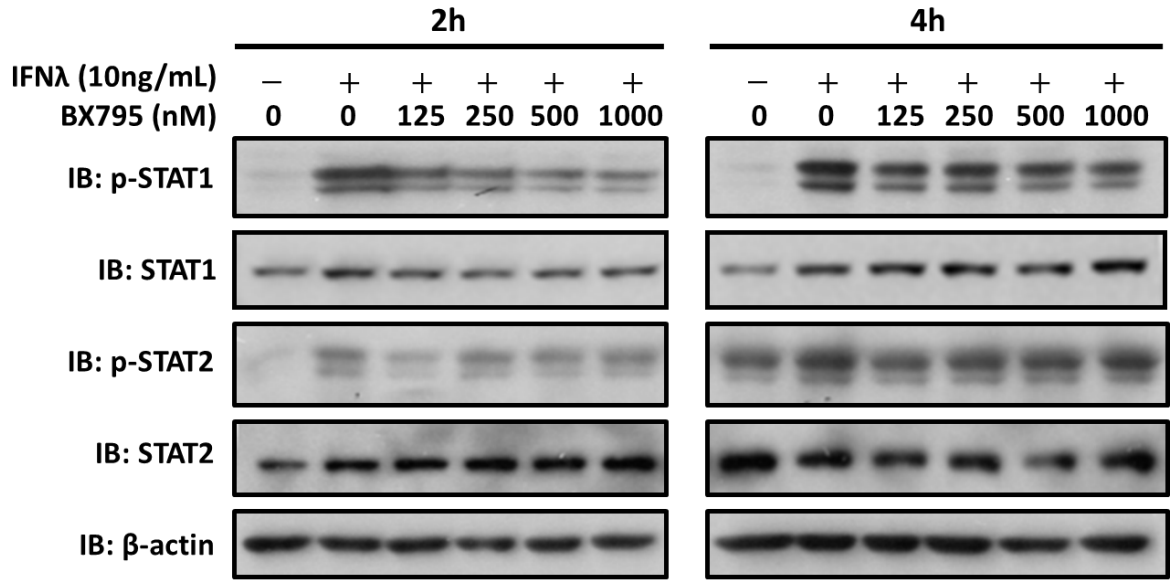
2h
4h
IFNλ (10ng/mL) − + + + + + − + + + + +
BX795 (nM) 0 0 125 250 500 1000 0 0 125 250 500 1000
IB: p-STAT1
IB: STAT1
IB: p-STAT2
IB: STAT2
IB: β-actin

Figure 5. BX795 inhibits STAT phosphorylation in IFNγ- and IFNλ- mediated JAK/STAT signaling pathways.

(A) IHH cells were treated with 1μM of BX795 or 1μM of DMSO along with 50ng/mL of IFNγ or DMEM medium for 2h and 4h. Whole-cell extracts were analyzed using immunoblot to assess expression of p-JAK1, p-JAK2, p-STAT1, STAT1, and β-actin proteins. (B) IHH cells were treated with 10ng/mL IFNλ and increasing concentrations of BX795 as indicated. Immunoblot was performed on whole-cell extracts to measure the level of p-STAT1, STAT1, p-STAT2, STAT2, and β-actin proteins. Data are representative of two or more independent experiments.

3.6. BX795 blocks IL-4- mediated JAK/STAT signaling pathway *in vitro* and *in vivo*

Apart from interferons, interleukins, such as IL-4, have also been shown to activate the JAK/STAT signaling pathway (222, 223). Whole-cell extracts collected at five time points (15min, 30min, 60min, 2h, and 4h) from IHH cells were analyzed using immunoblot. The results showed that under IL-4 induction, STAT6 phosphorylation was significantly suppressed by BX795 within 1h of treatment (Figure 6A). Inhibition was still detectable after 4h of treatment, but the strengths weakened overtime (Figure 6A). Since IL-4 plays a pivotal role in modulating immune response, immune cells including T cells (Jurkat cells), macrophages (murine BMDM), and B cells (OCI-Ly8 cells) were also tested to examine the effect of BX795. BX795 reduced p-STAT6 level in all three cell lines after 1h of treatment (Figure 5B-D). Significant suppression on p-STAT6 proteins were observed with 250nM BX795 in human cells (Figure 6C and D), whereas 1000nM BX795 was required to elicit similar responses in murine BDMD (Figure 6B). This result suggests that BX795 has a higher potency in human cells, however this is not conclusive as variations in human and murine IL-4 and receptor structures may account for the difference. Similarly, the mRNA levels of *SOCS1*, a downstream gene activated by p-STAT6, were also assessed using qPCR. At a concentration of 250nM, BX795 decreased *SOCS1* level by approximately 10 folds after 24h of treatment and IL-4 induction (Figure 6E). BX795 alone did not alter the basal *SOCS1* levels at all concentrations (Figure 6E). Overall, BX795 blocks IL-4-mediated JAK/STAT signaling pathway on both translational and transcriptional levels.

After validating the effect of BX795 using *in vitro* cell models, *in vivo* mice models were also employed to evaluate the clinical therapeutic potential of BX795. Mice were injected with 200ng IL-4 and 2mg/kg BX795 (Figure 7A). STAT6 phosphorylation in spleen cells was then assessed using immunoblot 3h after treatment. Wild type cells had low basal p-STAT6

levels that were undetectable in immunoblot (Figure 7B). IL-4 stimulation increased STAT6 phosphorylation (Figure 7B). In contrast, BX795 potently suppressed STAT6 phosphorylation after IL-4 induction when compared to IL-4 treatment alone, but had no effect on the total STAT6 level (Figure 7B). BX795 is therefore validated as a JAK/STAT6 inhibitor based on *in vitro* and *in vivo* results.

Apart from activating the JAK/STAT pathway, IL-4 also triggers the activation of T cells. Based on the expression of CD69, an early activation marker of T cell, the percentages of activated $CD4^+$ cells in mesenteric lymph node and spleen were slightly reduced under 24h of BX795 treatment, although the difference was not significant (Figure 8A and C). BX795 had no effect on the activation of $CD8^+$ cells in mesenteric lymph node and spleen (Figure B and D).

A

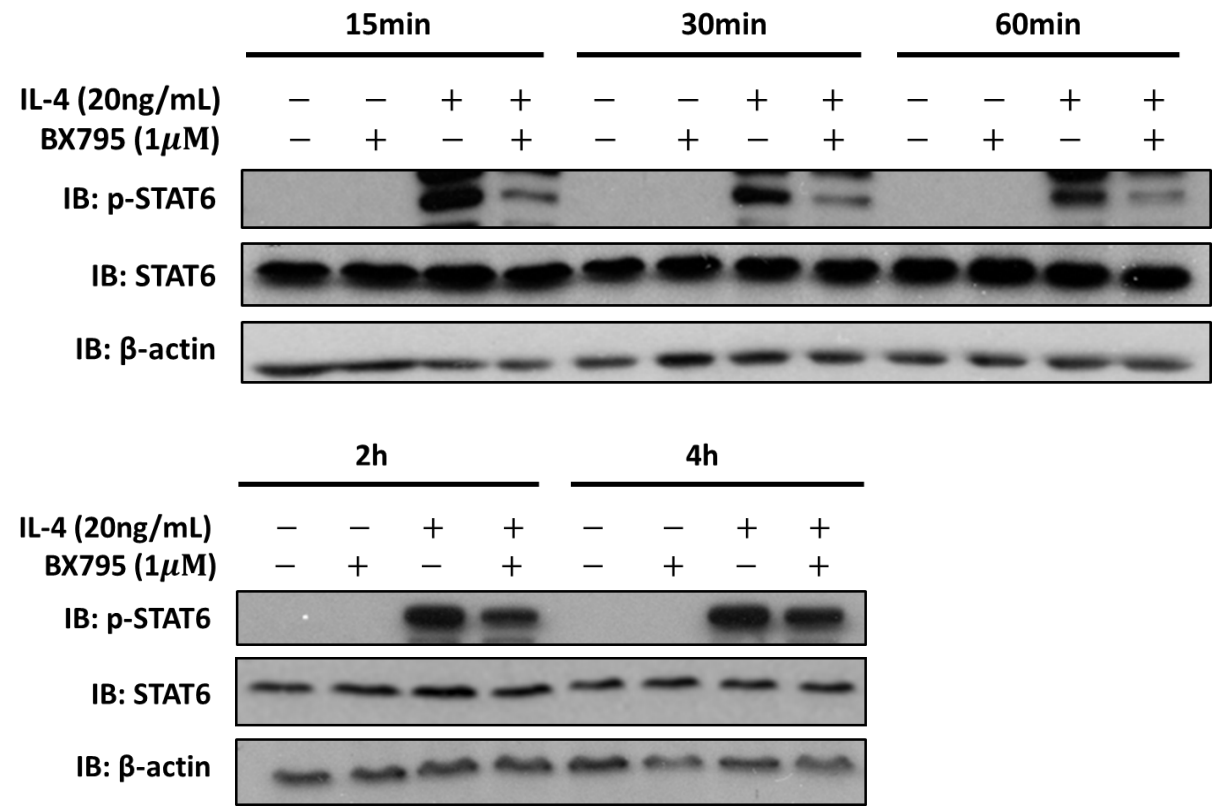
15min
30min
60min
IL-4 (20ng/mL)
BX795 (1μM)
IB: p-STAT6
IB: STAT6
IB: β-actin
2h
4h
IL-4 (20ng/mL)
BX795 (1μM)
IB: p-STAT6
IB: STAT6
IB: β-actin

B

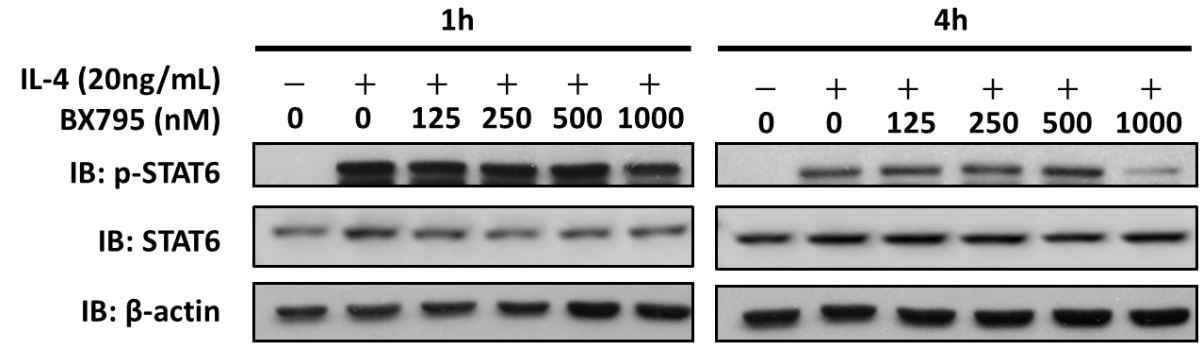
1h
4h
IL-4 (20ng/mL)
BX795 (nM)
0 0 125 250 500 1000
0 0 125 250 500 1000
IB: p-STAT6
IB: STAT6
IB: β-actin

C

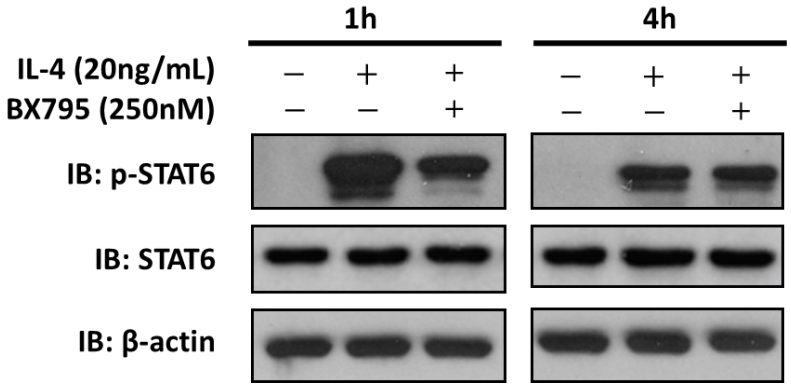
1h
4h
IL-4 (20ng/mL)
BX795 (250nM)
IB: p-STAT6
IB: STAT6
IB: β-actin

D

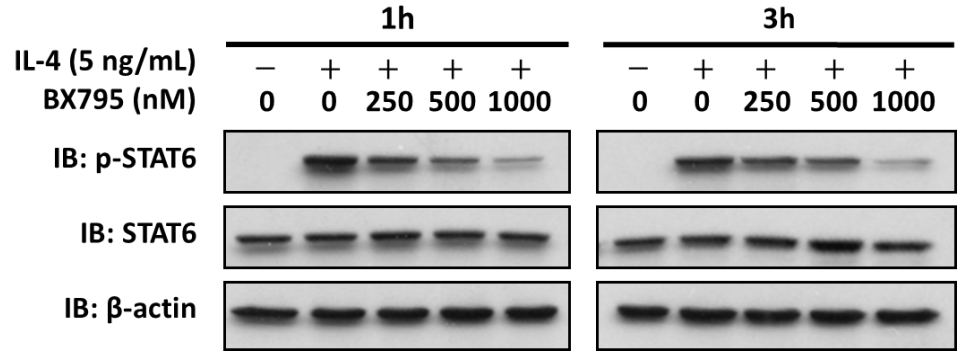
1h
3h
IL-4 (5 ng/mL)
BX795 (nM)
0 0 250 500 1000
0 0 250 500 1000
IB: p-STAT6
IB: STAT6
IB: β-actin

E

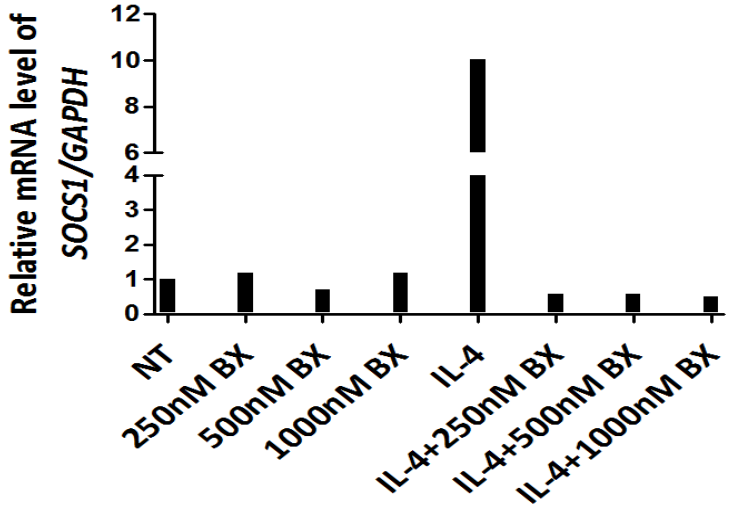
Relative mRNA level of SOCS1/GAPDH
12
10
8
6
4
3
2
1
0
NT
250nM BX
500nM BX
1000nM BX
IL-4
IL-4+250nM BX
IL-4+500nM BX
IL-4+1000nM BX

Figure 6. BX795 suppresses the phosphorylation of STAT6 proteins in IL-4-mediated JAK/STAT signaling pathway.

(A) IHH cells were pre-treated with 1μM BX795 or 1μM DMSO for 2 hours, followed by stimulation with 20ng/mL of human IL-4 for 15min, 30min, 60min, 2h, and 4h. (B) Murine bone marrow derived macrophages (BMDM) were treated with 20ng/mL of mouse IL-4 and different concentrations of BX795 (0nM, 125nM, 250nM, 500nM, 1000nM) for 1h and 4h. (C) Jurkat cells were treated with 20ng/mL of human IL-4 and 250nM BX795 for 1h and 4h. (D) OCI-Ly8 cells were pre-treated with BX795 (0nM, 250nM, 500nM, and 1000nM) for 1h, followed by stimulation with 5ng/mL of human IL-4 for 1h and 3h. Immunoblot was performed on whole-cell extracts to assess expression of p-STAT6, STAT6, and β-actin proteins. (E) Relative mRNA level of *SOCS1* after 1h of BX795 pretreatment and 3h of IL-4 induction was quantified using qPCR. Data are representative of two or more independent experiments.

A

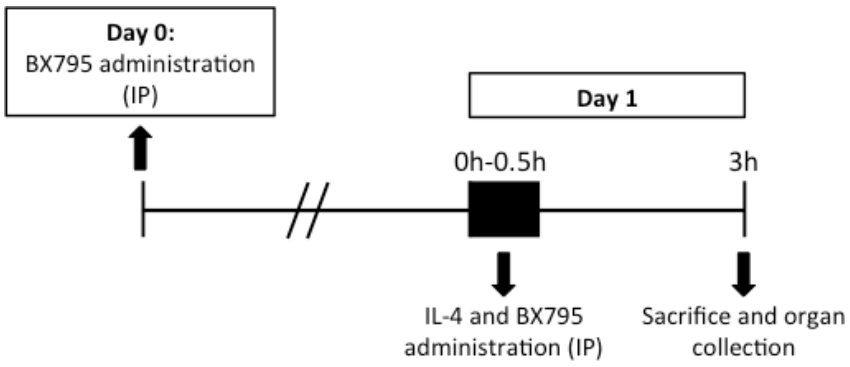
Day 0:
BX795 administration
(IP)
Day 1
0h-0.5h
3h
IL-4 and BX795
administration (IP)
Sacrifice and organ
collection

B

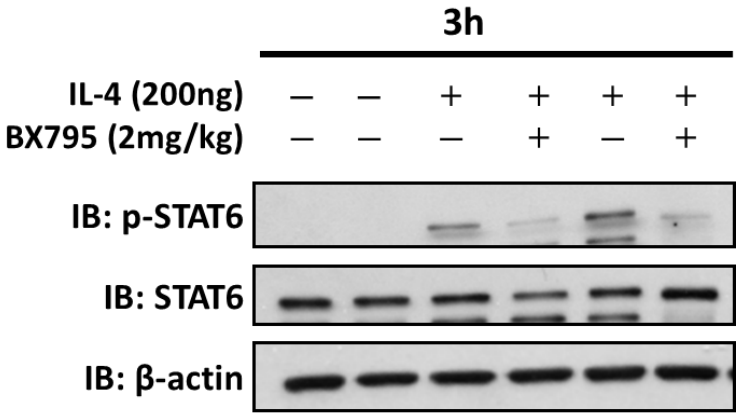
3h
IL-4 (200ng) – – + + + +
BX795 (2mg/kg) – – – + – +
IB: p-STAT6
IB: STAT6
IB: β-actin

Figure 7. BX795 suppresses p-STAT6 protein level *in vivo*.

(A) Schematics for IL-4 administration and BX795 treatment *in vivo*. Six 7-week Balb/c mice were treated with either 100μLPBS or 200ng IL-4 in 100μL PBS, along with 2% DMSO in PBS or 2mg/kg of BX795 for 3h. (B) Immunoblot was performed on extracted spleen cells to assess expression of p-STAT6, STAT6, and β-actin proteins.

A

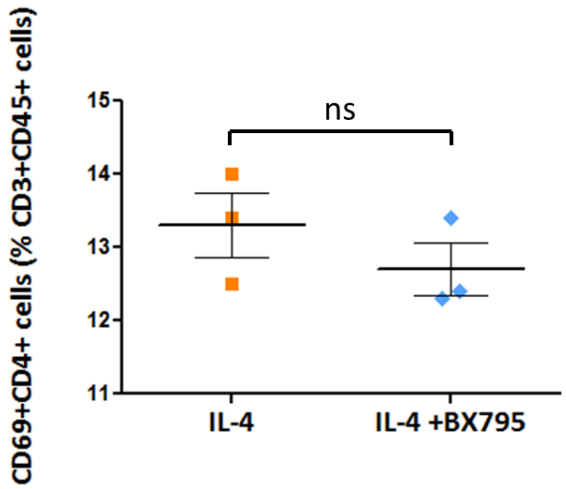
CD69+CD4+ cells (% CD3+CD45+ cells)
15
14
13
12
11
ns
IL-4
IL-4 +BX795

B

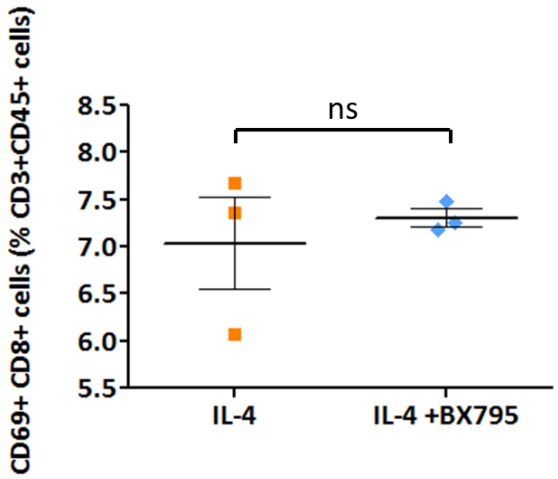
CD69+ CD8+ cells (% CD3+CD45+ cells)
8.5
8.0
7.5
7.0
6.5
6.0
5.5
ns
IL-4
IL-4 +BX795

C

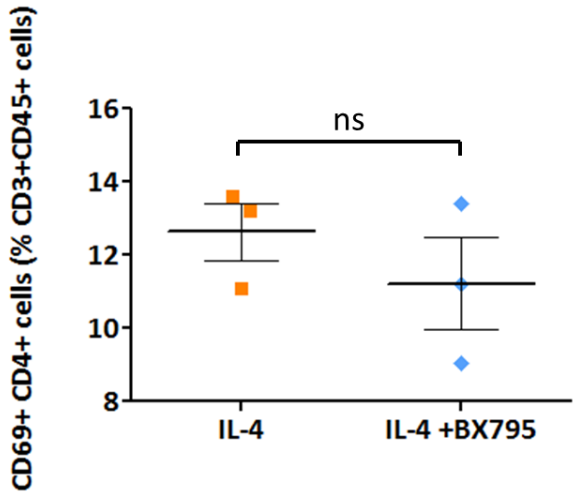
CD69+ CD4+ cells (% CD3+CD45+ cells)
16
14
12
10
8
ns
IL-4
IL-4 +BX795

D

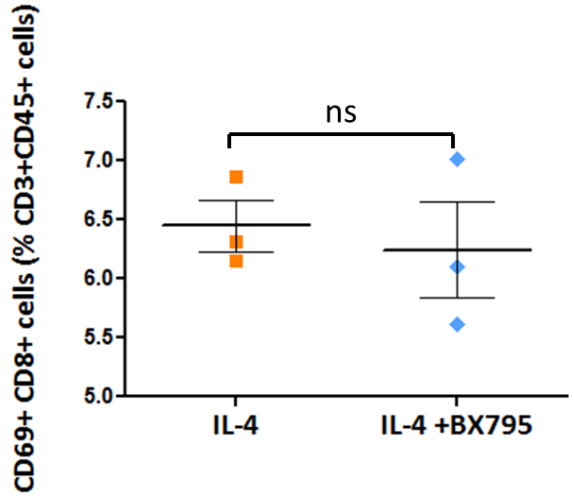
CD69+ CD8+ cells (% CD3+CD45+ cells)
7.5
7.0
6.5
6.0
5.5
5.0
ns
IL-4
IL-4 +BX795

Figure 8. BX795 has no effect on the activation of T cell subpopulations upon IL-4 induction.

Six 7-week Balb/c mice were treated with either 100µLPBS or 200ng IL-4 in 100µL PBS, along with 2% DMSO in PBS or 2mg/kg of BX795 for 24h. All data are normalized and expressed as percentage of $CD3^+CD45^+$ lymphocytes. In mesenteric lymph node, the percentage of (A) $CD69^+CD4^+$ cells and (B) $CD69^+CD8^+$ cells were measured using flow cytometry. The percentage of (C) $CD69^+CD4^+$ cells and (D) $CD69^+CD8^+$ cells in spleen were also evaluated. The results are expressed as the mean with SEM; n=3. * $p < 0.05$, ** $p < 0.01$, *** $p < 0.001$; ns denotes no statistical significance.

3.7. BX795 augments production of IL-4 and p-STAT6 in lung homogenate and serum IgE in OVA-induced allergic asthma model.

In order to evaluate the effect of BX795 in a disease-relevant setting, ovalbumin-induced allergic asthma mice model was used to test the capacity of BX795 in suppressing chronic p-STAT6 activation. Mice were sensitized with OVA for two weeks, followed by OVA challenge (100μg for 3 days) and BX795 administration via intraperitoneal (IP) injection (2.5mg/kg) or intravenous (IV) injection (1.25mg/kg) for 4 days (Figure 9A). Weight was monitored to assess the cytotoxicity of BX795 and OVA treatments (Figure 9B). There were no significant weight losses between mice receiving no treatment, OVA treatment, and BX795 treatments (Figure 9C). OVA challenge alone induced IL-4 production in lung homogenate by approximately 20 fold (Figure 9D). With the addition of 2.5mg/kg of BX795 through IP injection, IL-4 concentration increased by 2 fold compared to OVA treatment alone (29pg/mL for OVA versus 58pg/mL for OVA and BX795 IP treatment), although the increase was not considered statistically significant (Figure 9D). However, after changing the administration route to IV and reducing BX795 dose by half, IL-4 concentration did not increase significantly (29pg/mL for OVA versus 35 pg/mL for OVA and BX795 IV treatment). On the other hand, neither OVA treatment nor BX795 treatment affected the IL-4 level significantly in serum (Figure 9E). High level of circulating IgE is another biomarker for asthma. The result showed that the level of OVA-specific IgE in serum augmented by approximately 5 fold under OVA challenge (Figure 9F). Similar to changes in IL-4 production in lung homogenate, BX795 treatment also increased serum OVA-specific IgE at a concentration of 2.5mg/kg via IP route (154ng/mL for OVA and BX795 IP treatment versus 98ng/mL for OVA alone) and 1.25mg/kg via IV route (135ng/mL), although both changes are not statistically significant (Figure 9F). Furthermore, immunoblot analysis also revealed an increase in p-STAT6 proteins in lung homogenate of mice receiving BX795 and OVA

combinatorial treatment, compared to OVA challenge alone (Figure 9G). Lower dose of BX795 was associated with lower STAT6 phosphorylation, however the influence of administration route still needs to be investigated.

A

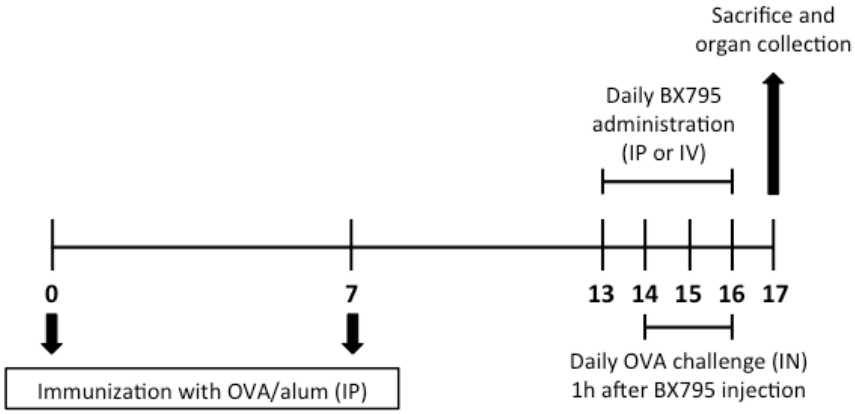
Sacrifice and
organ collection
Daily BX795
administration
(IP or IV)
0
7
13
14
15
16
17
Immunization with OVA/alum (IP)
Daily OVA challenge (IN)
1h after BX795 injection

B

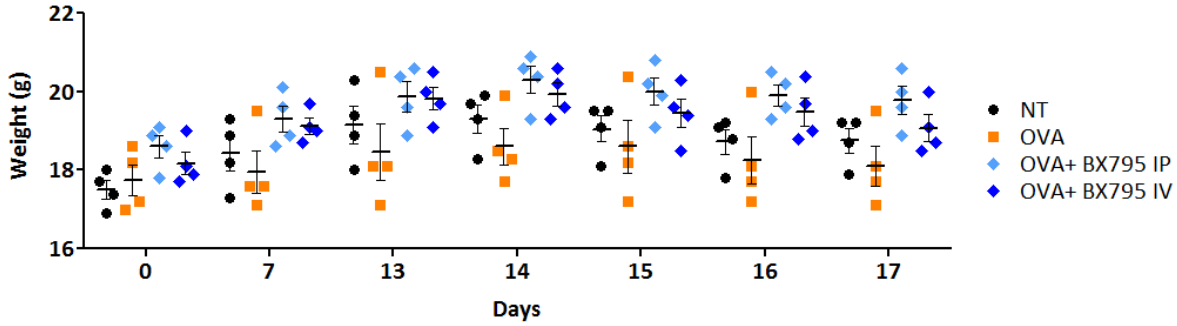
Weight (g)
22
20
18
16
0
7
13
14
15
16
17
Days
NT
OVA
OVA+ BX795 IP
OVA+ BX795 IV

C

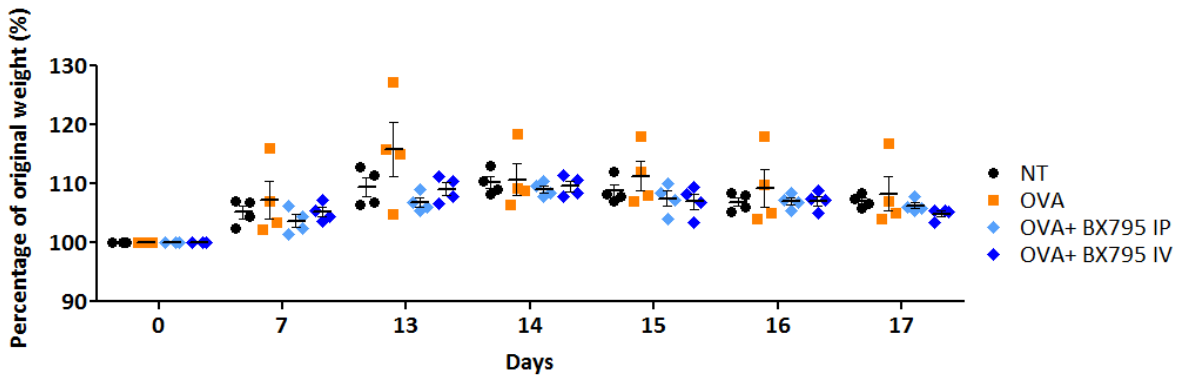
Percentage of original weight (%)
130
120
110
100
90
0
7
13
14
15
16
17
Days
NT
OVA
OVA+ BX795 IP
OVA+ BX795 IV

D

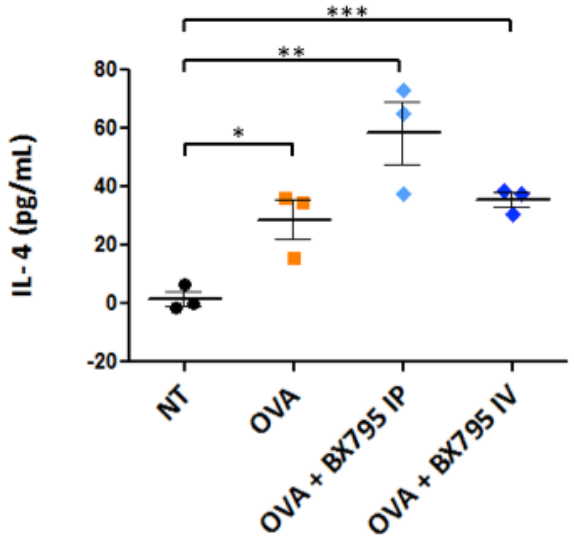
***
**
*
80
60
40
20
0
-20
IL-4 (pg/mL)
NT
OVA
OVA + BX795 IP
OVA + BX795 IV

E

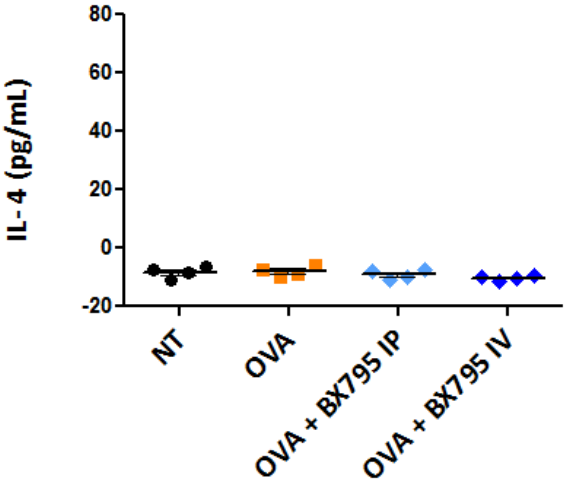
80
60
40
20
0
-20
IL-4 (pg/mL)
NT
OVA
OVA + BX795 IP
OVA + BX795 IV

F

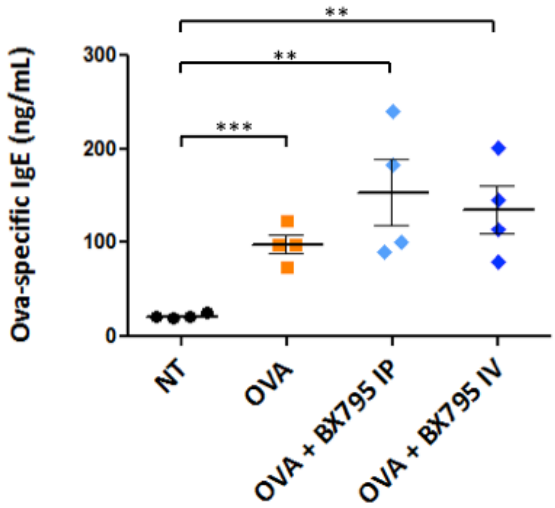
**
**
***
300
200
100
0
Ova-specific IgE (ng/mL)
NT
OVA
OVA + BX795 IP
OVA + BX795 IV

G

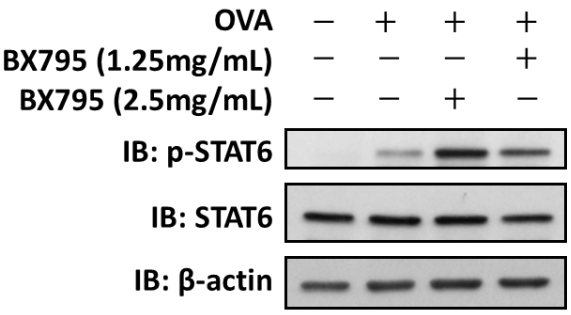
OVA – + + +
BX795 (1.25mg/mL) – – – +
BX795 (2.5mg/mL) – – + –
IB: p-STAT6
IB: STAT6
IB: β-actin

Figure 9. BX795 upregulates serum IgE, and lung homogenate IL-4 and p-STAT6 level in OVA-induced allergic model.

(A) Schematics of OVA/alum, OVA, and BX795 administration. 6-8 week BALB/c mice were injected intraperitoneally with either PBS or 40μg OVA in 2mg Alum in 150μL PBS on day 0 and 7. Selected mice were injected with either 2.5mg/kg of BX795 intraperitoneally or with 1.25mg/kg of BX795 intravenously from day 13-16. Designated mice were challenged with 100μg OVA in 45μL PBS intranasally from day 14-16. (B) The cytotoxicity of each treatment was evaluated by monitoring mouse body weight and (C) weight loss. The level of IL-4 production was measured in (D) lung homogenate and (E) serum 24h after last OVA challenge. (F) OVA-specific IgE was measured from the serum of mice in each group 24h after last OVA challenge. The results are presented as mean with SEM; n= 3 for lung homogenate and n=4 for serum. *p < 0.05, **p < 0.01, and ***p < 0.001 indicates statistically significant differences. (G) Extracted spleen cells were analyzed using immunoblot to assess expression of p-STAT6, STAT6, and β-actin proteins. Data are representative of four independent experiments.

CHAPTER 4. DISCUSSION

4.1. BX795 directly inhibits JAK/STAT pathway mediated by IFNα, IFNγ, IFNλ, and IL-4

JAK/STAT signaling pathway and the upstream TBK1 signaling pathway plays a critical role in mounting immune response against bacterial and viral infections. BX795, a synthetic TBK1 inhibitor, has been reported to display off-target inhibition on a number of kinases, including PDK1, JNK, and Akt (142, 144). Our study also demonstrated its capacity to inhibit the JAK/STAT signaling pathway. The results showed that BX795 suppressed JAK/STAT pathways mediated by four types of cytokines: IFNα, IFNγ, IFNλ, and IL-4 (Figure 2, 5, and 6). Since BX795 blocked the phosphorylation of different JAKs (p-JAK1, p-Tyk2, P-JAK2) and STATs (p-STAT1, p-STAT2, p-STAT6), this suggests that BX795 acts as a broad-spectrum JAK and/or STAT protein inhibitor. However, BX795 may have higher selectivity towards certain STAT proteins, such as STAT1 in the IFNλ signaling pathway. The selectivity requires further verification through co-immunoprecipitation.

Moreover, in a study done by Xiao et al., TBK1 deficiency results in an increase in STAT1 phosphorylation at residue Tyr701 (224). Our results revealed a decrease in the STAT1 phosphorylation at Tyr701, despite the known inhibition on TBK1 exerted by BX795. This further validates that BX795 directly inhibits JAK/STAT proteins with high potency.

Furthermore, one study has measured the IC50 (half maximal inhibitory concentration) of BX795 against a number of kinases (142). Out of the 70 protein kinases tested, BX795 inhibited TBK1 with the highest potency (IC50 6 ± 1nM) (142). However, in this study, 125nM is the lowest concentration of BX795 evaluated. In order to better compare the

potency and selectivity of BX795 on the different protein kinases, a titration assay should be performed to identify the IC50 of BX795 against JAKs.

4.2. BX795 acts as a potential JAK inhibitor

Since many cytokines signal through JAK/STAT pathway to exert their function, JAK and STAT proteins have became an important target for the treatments against a number of autoimmune and skin diseases, including rheumatoid arthritis, psoriatic arthritis, atopic dermatitis, and alopecia areata. JAK inhibitors, which block one or more JAKs, have been developed over recent years for clinical uses. Our present study revealed that BX795 displays characteristics of a JAK inhibitor. A previous study has shown that JAK inhibitors binding to JAK resulted in an increase in JAK activation loop phosphorylation, despite inhibition of its kinase function and STAT phosphorylation (120). A similar phosphorylation pattern was also observed in our study, with increased JAK1 and Tyk2 phosphorylation but reduced STAT1 and STAT2 phosphorylation. This suggests that BX795 may behave as a JAK inhibitor. The reduction in interaction between p-JAK1 and STAT1 also implies BX795 may block the binding of JAK to STATs. In addition, previous studies have demonstrated that the combination of VSVΔ51 with JAK inhibitor I or ruxolitinib (JAK1/JAK2 inhibitor) drastically improves viral replication and oncolysis in VSV-resistant PDAC cell lines (202, 225). In our study, we also observed an increase in VSVΔ51 replication when treated with a combination of BX795 and IFNα, in comparison to cells under IFNα induction alone. Altogether, it is highly likely that BX795 acts as a JAK inhibitor.

Since most JAK inhibitors target the JH1 domain (94) and most STAT inhibitors target the SH2 domain (13), the interaction between BX795 and these domains should be evaluated to unfold the exact mechanism of action of BX795. Furthermore, studies have shown that

BX795 acts as ATP competitive inhibitors in the case of TBK1 and PDK1 (142, 143). Protein kinase assays should thus be performed to verify the capacity of BX795 to compete with ATP.

4.3. BX795 and VSVΔ51 combinatorial treatment enhances viral oncolysis under IFNα induction

Oncolytic virotherapy, an emerging anti-cancer treatment approach, has achieved numerous clinical successes with the approval of three OVs for clinical uses (200, 226). However, intact antiviral immunity confers resistance against OV infections in numerous tumor cell lines and specimens (226). Combinations of OVs and small molecules have been explored to potentiate viral oncolysis in resistant cancer cells (206, 209, 227). In the present study, we demonstrated that under IFNα treatment, which simulates persistent antiviral response, BX795 potently enhanced viral replication and facilitated cell killing in TBK1-/- and tumor cell line (U87) at a concentration of 1μM. Without IFNα induction, BX795 slightly augmented virus-mediated apoptosis and infectivity in TBK1-/- cells, although the difference was determined to be not statistically significant. The multiplicity of infection should be lowered in future experiments for better evaluation of virus-induced apoptosis. Nevertheless, the results portray the potentiality of using BX795 and VSVΔ51 combinatorial treatment to target OV-resistant cancer cells with intact type I IFN signaling. The safety of BX795 has been proven in other studies, in which low cytotoxicity was displayed even at a concentration of 100μM (144, 145). Previous study has already reported the tumor clearing and cell death inducing capacity of oncolytic VSV (M51R, with mutation in M protein) in U87 cells and *in vivo* (228). However, the efficacy of this combinatorial virotherapy should be further investigated using *in vivo* model.

4.4. BX795 suppresses STAT6 phosphorylation under direct IL-4 induction *in vivo*

Since BX795 exhibited promising inhibitory effect on STAT6 phosphorylation in three immune cell lines, the therapeutic effect of BX795 were then evaluated in mice models. As expected, BX795 blocked STAT6 phosphorylation in mice injected with IL-4. However, the proportion of activated T cells did not differ markedly under BX795 treatment, potentially due to time restraint. Studies have shown that T cell response peaks around 7-15 days after initial stimulation (229). However, T cell activation in this study was evaluated 1 day after initial exposure. Therefore, in order to better assess the effect of BX795 on T cell activation, the expression of activation markers on T cells should be analyzed 7 days after the initial exposure using flow cytometry. Furthermore, since IL-4 drives the differentiation of Th2 cells, the expression of Th2 markers can also be evaluated.

4.5. BX795 enhances Th2 response biomarkers in OVA allergen-induced acute asthma model

STAT6 activation and Th2 response are critically involved in the pathogenesis of asthma. Since BX795 strongly inhibited STAT6 phosphorylation in both *in vivo* and *in vitro* models, similar suppression was expected in the OVA-induced acute asthma murine model. However, surprisingly we observed an increase in almost all Th2 response biomarkers, including IL-4 concentration and STAT6 phosphorylation in lung homogenates and OVA-specific IgE level in serum. Several studies have reported an increase in serum IL-4 level in asthmatic human patients (230, 231). However, our results showed no significant changes in the serum IL-4 level in mice sensitized with OVA. On the other hand, compounds that displayed therapeutic benefit in OVA-induced asthma models are often associated with reduced production of IL-4,

IL-5, and IL-13 (232, 233). Therefore, the response observed in our study suggests that BX795 exerts a stronger effect on targets beyond the inhibition of STAT6 phosphorylation.

One possible mechanism for enhanced Th2 response is a stronger inhibition on Th1 response exerted by BX795. The induction of Th1 response and Th1 cytokines (IFNγ) production has shown to provide protection against asthma and allergy through Th2 response inhibition (234-236). For example, patients with severe asthma have significantly lower IFNγ production than healthy individuals (237, 238). One study also suggested that allergy resolution is more closely related with the normalization of IFNγ level rather than reduced Th2 cytokine production (239). Since our *in vitro* studies illustrated the potent inhibition on STAT1 phosphorylation by BX795, it is possible that BX795 inhibits STAT1 with higher selectivity and suppresses Th1 response, which relieves the suppression on Th2 response and leads to further enhancement.

However, upregulated IFNγ was also observed in some severe asthmatics (240). The potential of IFNγ to induce IL-4 production suggests that IFNγ quantity may greatly influence the enhancement or suppression of Th2 priming (241). Since BX795 used in our study is administered systemically and transported through circulation, its off-target effects need to be taken into consideration during the evaluation of its therapeutic efficacy. BX795 is a known TBK1 inhibitor. A higher frequency of IFNγ- producing $CD4^+$ and $CD8^+$ T cells has been observed in TBK1 knockout mice (224). Therefore, upregulated IFNγ secretion may induce IL-4 production and contribute to elevated Th2 response. The effect of BX795 on Th1 responses and IFNγ production should be assessed in the future using OVA-induced asthma murine models.

In order to understand the unexpected Th2 response stimulation shown in this study, more analyses need to be performed. Since elevated serum levels of IL-5 and IL-13 are key clinical features observed in patients with acute asthma, the concentration of IL-5 and IL-13 in serum and bronchoalveolar lavage fluid (BALF) of OVA-induced mice should be quantified (231). Other structural and physiological asthma biomarkers should also be evaluated. For example, histological analysis of the lung can be performed to examine changes in the inflammatory cell infiltration and the thickness of bronchiole epithelium and alveolar septa in response to BX795 treatment. Recruitment of eosinophil, neutrophil, and alveolar macrophages in BALF should be assessed to characterize the type of inflammation. Mice should also be challenged with methacholine to determine if BX795 reduces airway resistance. The expression of VCAM-1, eotaxin, Th2 chemokines, and mucin genes (e.g. *MUC5AC)* are other biomarkers that require further investigations. In a study done by Dengler et al., they successfully demonstrated the therapeutic benefit of iJak-381 (JAK1 inhibitor) in suppressing lung inflammation and improving airway hyperresponsiveness based on a wide range of asthma biomarkers (232). For example, the transcription of IL-13 dependent genes (*NOS2, CCL11,* and *MUC5AC*) and STAT6-regulated genes (*CCL26* and POSTN) have shown to be reduced by iJak-381 (232). Decreased eosinophils and neutrophils recruitment, along with reduced airway resistance were also observed. Therefore, if BX795 exhibits therapeutic benefit in asthma treatment, similar outcomes should be reproduced.

Due to the heterogeneous nature of asthma, cytokines other than the ones involved in Th2 response, such as IL-6 and type I IFN, should also be examined. Studies have shown that increased IL-6 concentration in plasma is associated with elevated neutrophilic inflammation, worsened lung function, and increased exacerbation frequency in patients with severe asthma (242). In the absence of viral infection, some asthmatic patients is still able to exhibit type I

IFN-responsive gene signaling metric in their lung tissue and peripheral blood (243). This can result in increased exacerbation frequency and pathogenic burden in the airways (243). Therefore, the cytokine concentration of IL-6 and IFNα/β in BALF and serum should be measured in the future.

Overall, all the above-mentioned procedures will contribute to a better understanding of the role of BX795 in Th2-mediated asthma pathogenesis. Additional assessments regarding the systemic and pulmonary toxicity and adverse effects of BX795 should be performed apart from weight observation. A dose response test should also be performed to determine the optimal dosage for treatment.

4.5. Limitations in the OVA-induced acute allergic asthma model

Even though the acute asthma challenge model used in our study has shown to manifest the key features of clinical asthma in other studies, including airway inflammation, AHR, and elevated IgE levels, some features still deviate from the pathologies observed in asthmatic human patients. For example, studies have shown that there are discrepancies in the distribution and pattern of pulmonary inflammation between asthmatic patient and the acute asthma model (244). OVA challenge was only able to trigger modest pulmonary inflammation and mild AHR (245). Some studies have also reported resolution of AHR and airway inflammation within a few weeks after the final antigen challenge in acute models (246). In contrast, asthmatic patients often have persistent airway inflammation. Furthermore, many pathologies developed in chronic human asthma, including chronic inflammation and remodeling of airway wall, are absent in the acute asthma model due to time restraint (245). Therefore, the compatibility of using acute induction models for the assessment of novel treatments against chronic asthma is questionable. Chronic challenge murine models should

be used in the future to better evaluate the effectiveness of BX795 on lung function and inflammation.

Despite of the shortcomings of acute asthma model, there are also some limitations to the OVA-induced allergic asthma model. First, the physiological differences between human and mice impedes the full reproduction of asthma phenotypes in mice (247). For example, mice have simpler lung anatomy and lack the coughing behavior, which may substantially influence the retention and efficacy of the drug in lung (247). Therefore, other animals with similar lung architecture as human, such as guinea pig, should be tested in the future to evaluate the therapeutic effect of BX795 (248). Second, repeated exposure to OVA may result in desensitization and tolerance of the airway (249, 250). In studies that failed to detect bronchial hyperresponsiveness, decreased levels of IL-5, IL-10, and lower eosinophilia were also observed, indicating the progression towards tolerance (251). Therefore, other allergens that manifests more relevant and specific clinical asthma outcomes should be used for intervention evaluation.

Recent studies have shown that house dust mite (HDM) sensitization exhibited clinical features more relevant to asthma than OVA. Therefore, HDM has gained increasing interest as the allergen to induce allergic respiratory diseases in murine models. HDM possesses cysteine protease activity to promote inflammatory cytokine release, epithelial desquamation, and allergen transport facilitation (252). It induces Th2 and IgE responses while triggering pulmonary inflammation (253, 254). Pro-fibrotic lung tissue remodeling, an asthma biomarker, was also developed under HDM sensitization (255). Furthermore, studies have demonstrated that HDM sensitization triggers a more specific airway inflammation than OVA, evident from the elevated eosinophils and imbalance in Th1/Th2 response (251). HDM

also leads to augmented lung peripheral response to a non-specific cholinergic constrictor stimulus, which is not observed in OVA-induced models (251). Therefore for future investigation, BX795 should be tested in HDM-sensitized asthma models to assess its clinical efficacy.

In particular, HDM can be induced with Respiratory syncytial virus (RSV) to further enhance airway inflammation. Studies have shown that most asthma exacerbations are triggered by respiratory viral infections, such as RSV (256, 257). In the study done by Mori et al., RSV markedly augmented cell infiltrations in BALF, including macrophages, lymphocytes, neutrophils, and eosinophils, compared to HDM-sensitization alone (258). Recurrent RSV infections after HDM treatment also increased total serum IgE and Th2 cytokine productions (e.g. IL-13), along with AHR, mucus hyperproduction, and persistent airway inflammation (259-261). However, there are some debates between whether the AHR and eosinophilic inflammation is predominately caused by Th1 or Th2 response upon primary RSV infection. Schwarze et al. demonstrated that Th1 cytokine productions from the peribronchial lymph node cells are associated with AHR and inflammation in acute RSV infection (262). In addition, F glycoprotein of RSV has also been reported to induce Th1 response (263). Nevertheless, a large number of studies showed that RSV reinfection induces a Th2-biased response. Increased production of Th2 cytokines and elevated proportion of Th2 cytokine-producing T lymphocytes were observed in mice with prior exposure to allergen followed by RSV infection (264-267). Barends et al. further demonstrated that RSV inoculation only enhanced allergic diseases when the immune system has been primed with Th2 response (265). Therefore, RSV-induced HDM-sensitization with recurrent RSV infections after allergen challenge should be a better asthmatic model for drug testing, as it elicits stronger Th2-driven allergic responses.

4.6. Concluding remarks

Since currently no other studies have demonstrated a direct correlation between BX795 and JAK/STAT signaling pathway, our study for the first time revealed the capacity of BX795 to inhibit IFNα, IFNγ, IFNλ, and IL-4-mediated JAK/STAT pathways. BX795 can provide insights on the development of therapeutic agents against a wide range of JAK/STAT related autoimmune diseases and cancers. Since BX795 is commonly used as a TBK1 inhibitor in antiviral response researches, researchers now need to take into consideration of its additional inhibitory role in the JAK/STAT signaling pathway before making conclusions from their studies. Even though BX795 was not able to elicit therapeutic benefit against asthma, it indeed showed promising enhancement in the oncolysis of VSVΔ51 combined therapy under IFNα induction. Further investigation on the efficacy and toxicity of BX795 are still required using *in vivo* models.

REFERENCE

1. Rawlings JS, Rosler KM, Harrison DA. The JAK/STAT signaling pathway. Journal of cell science. 2004;117(8):1281-3.
2. Banerjee S, Biehl A, Gadina M, Hasni S, Schwartz DM. JAK–STAT signaling as a target for inflammatory and autoimmune diseases: current and future prospects. Drugs. 2017:1-26.
3. Seif F, Khoshmirsafa M, Aazami H, Mohsenzadegan M, Sedighi G, Bahar M. The role of JAK-STAT signaling pathway and its regulators in the fate of T helper cells. Cell Communication and Signaling. 2017;15(1):23.
4. Tepass U. FERM proteins in animal morphogenesis. Current opinion in genetics & development. 2009;19(4):357-67.
5. Endo TA, Masuhara M, Yokouchi M, Suzuki R, Sakamoto H, Mitsui K, et al. A new protein containing an SH2 domain that inhibits JAK kinases. Nature. 1997;387(6636):921.
6. Starr R, Willson TA, Viney EM, Murray LJ, Rayner JR, Jenkins BJ, et al. A family of cytokine-inducible inhibitors of signalling. Nature. 1997;387(6636):917.
7. Hammarén HM, Ungureanu D, Grisouard J, Skoda RC, Hubbard SR, Silvennoinen O. ATP binding to the pseudokinase domain of JAK2 is critical for pathogenic activation. Proceedings of the National Academy of Sciences. 2015;112(15):4642-7.
8. Wilks A, Harpur A, Kurban R, Ralph S, Zürcher G, Ziemiecki A. Two novel protein-tyrosine kinases, each with a second phosphotransferase-related catalytic domain, define a new class of protein kinase. Molecular and cellular biology. 1991;11(4):2057-65.
9. Lim WA, Pawson T. Phosphotyrosine signaling: evolving a new cellular communication system. Cell. 2010;142(5):661-7.
10. Babon JJ, Lucet IS, Murphy JM, Nicola NA, Varghese LN. The molecular regulation of Janus kinase (JAK) activation. Biochemical Journal. 2014;462(1):1-13.
11. Mitchell TJ, John S. Signal transducer and activator of transcription (STAT) signalling and T‐cell lymphomas. Immunology. 2005;114(3):301-12.
12. Ota N, Brett TJ, Murphy TL, Fremont DH, Murphy KM. N-domain–dependent nonphosphorylated STAT4 dimers required for cytokine-driven activation. Nature immunology. 2004;5(2):208.
13. Lai P-S, Rosa DA, Magdy Ali A, Gómez-Biagi RF, Ball DP, Shouksmith AE, et al. A STAT inhibitor patent review: progress since 2011. Expert opinion on therapeutic patents. 2015;25(12):1397-421.
14. Mavers M, Ruderman EM, Perlman H. Intracellular signal pathways: potential for therapies. Current rheumatology reports. 2009;11(5):378-85.
15. Schwartz DM, Bonelli M, Gadina M, O'shea JJ. Type I/II cytokines, JAKs, and new strategies for treating autoimmune diseases. Nature Reviews Rheumatology. 2016;12(1):25-36.
16. Hervas-Stubbs S, Perez-Gracia JL, Rouzaut A, Sanmamed MF, Le Bon A, Melero I. Direct effects of type I interferons on cells of the immune system. Clinical Cancer Research. 2011;17(9):2619-27.
17. Nguyen KB, Salazar-Mather TP, Dalod MY, Van Deusen JB, Wei X-q, Liew FY, et al. Coordinated and distinct roles for IFN-α β, IL-12, and IL-15 regulation of NK cell responses to viral infection. The Journal of Immunology. 2002;169(8):4279-87.

18. Bogdan C, Mattner J, Schleicher U. The role of type I interferons in non‐viral infections. Immunological reviews. 2004;202(1):33-48.
19. Le Bon A, Schiavoni G, D'Agostino G, Gresser I, Belardelli F, Tough DF. Type I interferons potently enhance humoral immunity and can promote isotype switching by stimulating dendritic cells in vivo. Immunity. 2001;14(4):461-70.
20. Kolumam GA, Thomas S, Thompson LJ, Sprent J, Murali-Krishna K. Type I interferons act directly on CD8 T cells to allow clonal expansion and memory formation in response to viral infection. Journal of Experimental Medicine. 2005;202(5):637-50.
21. Chen K, Liu J, Cao X. Regulation of type I interferon signaling in immunity and inflammation: a comprehensive review. Journal of autoimmunity. 2017;83:1-11.
22. McComb S, Cessford E, Alturki NA, Joseph J, Shutinoski B, Startek JB, et al. Type-I interferon signaling through ISGF3 complex is required for sustained Rip3 activation and necroptosis in macrophages. Proceedings of the National Academy of Sciences. 2014;111(31):E3206-E13.
23. Platanias LC. Mechanisms of type-I-and type-II-interferon-mediated signalling. Nature Reviews Immunology. 2005;5(5):375-86.
24. Ivashkiv LB, Donlin LT. Regulation of type I interferon responses. Nature reviews Immunology. 2014;14(1):36.
25. Schroder K, Hertzog PJ, Ravasi T, Hume DA. Interferon‐γ: an overview of signals, mechanisms and functions. Journal of leukocyte biology. 2004;75(2):163-89.
26. Fukao T, Matsuda S, Koyasu S. Synergistic effects of IL-4 and IL-18 on IL-12-dependent IFN-γ production by dendritic cells. The Journal of Immunology. 2000;164(1):64-71.
27. Schindler H, Lutz MB, Röllinghoff M, Bogdan C. The production of IFN-γ by IL-12/IL-18-activated macrophages requires STAT4 signaling and is inhibited by IL-4. The Journal of Immunology. 2001;166(5):3075-82.
28. Carnaud C, Lee D, Donnars O, Park S-H, Beavis A, Koezuka Y, et al. Cutting edge: cross-talk between cells of the innate immune system: NKT cells rapidly activate NK cells. The Journal of Immunology. 1999;163(9):4647-50.
29. Boehm U, Klamp T, Groot M, Howard J. Cellular responses to interferon-γ. Annual review of immunology. 1997;15(1):749-95.
30. Stark GR. How cells respond to interferons revisited: from early history to current complexity. Cytokine & growth factor reviews. 2007;18(5-6):419-23.
31. Syedbasha M, Egli A. Interferon lambda: modulating immunity in infectious diseases. Frontiers in immunology. 2017;8:119.
32. Dai J, Megjugorac NJ, Gallagher GE, Raymond Y, Gallagher G. IFN-λ1 (IL-29) inhibits GATA3 expression and suppresses Th2 responses in human naive and memory T cells. Blood. 2009;113(23):5829-38.
33. Koltsida O, Hausding M, Stavropoulos A, Koch S, Tzelepis G, Übel C, et al. IL‐28A (IFN‐λ2) modulates lung DC function to promote Th1 immune skewing and suppress allergic airway disease. EMBO molecular medicine. 2011;3(6):348-61.
34. Ge D, Fellay J, Thompson AJ, Simon JS, Shianna KV, Urban TJ, et al. Genetic variation in IL28B predicts hepatitis C treatment-induced viral clearance. Nature. 2009;461(7262):399.
35. Eslam M, Hashem AM, Leung R, Romero-Gomez M, Berg T, Dore GJ, et al. Interferon-λ rs12979860 genotype and liver fibrosis in viral and non-viral chronic liver disease. Nature communications. 2015;6:6422.

36. Kotenko SV, Gallagher G, Baurin VV, Lewis-Antes A, Shen M, Shah NK, et al. IFN-λs mediate antiviral protection through a distinct class II cytokine receptor complex. Nature immunology. 2003;4(1):69.
37. Kotenko SV, Izotova LS, Mirochnitchenko OV, Esterova E, Dickensheets H, Donnelly RP, et al. Identification of the Functional Interleukin-22 (IL-22) Receptor Complex The Il-10r2 Chain (Il-10rβ) Is A Common Chain Of Both The Il-10 And Il-22 (Il-10-Related T Cell-Derived Inducible Factor, Il-Tif) Receptor Complexes. Journal of Biological Chemistry. 2001;276(4):2725-32.
38. Donnelly RP, Kotenko SV. Interferon-lambda: a new addition to an old family. Journal of Interferon & Cytokine Research. 2010;30(8):555-64.
39. Zamorano J, Wang HY, Wang L-M, Pierce JH, Keegan AD. IL-4 protects cells from apoptosis via the insulin receptor substrate pathway and a second independent signaling pathway. The Journal of Immunology. 1996;157(11):4926-34.
40. Yanagida M, Fukamachi H, Ohgami K, Kuwaki T, Ishii H, Uzumaki H, et al. Effects of T-helper 2-type cytokines, interleukin-3 (IL-3), IL-4, IL-5, and IL-6 on the survival of cultured human mast cells. Blood. 1995;86(10):3705-14.
41. Seder RA, Paul WE, Davis MM, de St Groth BF. The presence of interleukin 4 during in vitro priming determines the lymphokine-producing potential of CD4+ T cells from T cell receptor transgenic mice. Journal of Experimental Medicine. 1992;176(4):1091-8.
42. Geha RS, Jabara HH, Brodeur SR. The regulation of immunoglobulin E class-switch recombination. Nature Reviews Immunology. 2003;3(9):721.
43. Gordon S. Alternative activation of macrophages. Nature reviews immunology. 2003;3(1):23.
44. Finkelman FD, Shea-Donohue T, Goldhill J, Sullivan CA, Morris SC, Madden KB, et al. Cytokine regulation of host defense against parasitic gastrointestinal nematodes: lessons from studies with rodent models. Annual review of immunology. 1997;15(1):505-33.
45. Schleimer RP, Sterbinsky SA, Kaiser J, Bickel CA, Klunk DA, Tomioka K, et al. IL-4 induces adherence of human eosinophils and basophils but not neutrophils to endothelium. Association with expression of VCAM-1. The Journal of Immunology. 1992;148(4):1086-92.
46. Maggi E. The TH1/TH2 paradigm in allergy. Immunotechnology. 1998;3(4):233-44.
47. Yeganeh B, Wiechec E, Ande SR, Sharma P, Moghadam AR, Post M, et al. Targeting the mevalonate cascade as a new therapeutic approach in heart disease, cancer and pulmonary disease. Pharmacology & therapeutics. 2014;143(1):87-110.
48. Nelms K, Keegan AD, Zamorano J, Ryan JJ, Paul WE. The IL-4 receptor: signaling mechanisms and biologic functions. Annual review of immunology. 1999;17(1):701-38.
49. Ramalingam TR, Pesce JT, Sheikh F, Cheever AW, Mentink-Kane MM, Wilson MS, et al. Unique functions of the type II interleukin 4 receptor identified in mice lacking the interleukin 13 receptor α1 chain. Nature immunology. 2008;9(1):25.
50. Grunewald SM, Werthmann A, Schnarr B, Klein CE, Bröcker EB, Mohrs M, et al. An antagonistic IL-4 mutant prevents type I allergy in the mouse: inhibition of the IL-4/IL-13 receptor system completely abrogates humoral immune response to allergen and development of allergic symptoms in vivo. The Journal of Immunology. 1998;160(8):4004-9.

51. Miyazaki T, Kawahara A, Fujii H, Nakagawa Y, Minami Y, Liu Z-J, et al. Functional activation of Jak1 and Jak3 by selective association with IL-2 receptor subunits. Science. 1994;266(5187):1045-7.
52. Russell SM, Johnston JA, Noguchi M, Kawamura M, Bacon CM, Friedmann M, et al. Interaction of IL-2R beta and gamma c chains with Jak1 and Jak3: implications for XSCID and XCID. Science. 1994;266(5187):1042-5.
53. Mullighan CG, Zhang J, Harvey RC, Collins-Underwood JR, Schulman BA, Phillips LA, et al. JAK mutations in high-risk childhood acute lymphoblastic leukemia. Proceedings of the National Academy of Sciences. 2009;106(23):9414-8.
54. Bellanger D, Jacquemin V, Chopin M, Pierron G, Bernard O, Ghysdael J, et al. Recurrent JAK1 and JAK3 somatic mutations in T-cell prolymphocytic leukemia. Leukemia. 2014;28(2):417.
55. Jeong EG, Kim MS, Nam HK, Min CK, Lee S, Chung YJ, et al. Somatic mutations of JAK1 and JAK3 in acute leukemias and solid cancers. Clinical cancer research. 2008;14(12):3716-21.
56. Spivak JL. Narrative review: Thrombocytosis, polycythemia vera, and JAK2 mutations: The phenotypic mimicry of chronic myeloproliferation. Annals of internal medicine. 2010;152(5):300-6.
57. Sakaguchi H, Okuno Y, Muramatsu H, Yoshida K, Shiraishi Y, Takahashi M, et al. Exome sequencing identifies secondary mutations of SETBP1 and JAK3 in juvenile myelomonocytic leukemia. Nature genetics. 2013;45(8):937.
58. Macchi P, Villa A, Giliani S, Sacco MG, Frattini A, Porta F, et al. Mutations of Jak-3 gene in patients with autosomal severe combined immune deficiency (SCID). Nature. 1995;377(6544):65.
59. Uzel G, Sampaio EP, Lawrence MG, Hsu AP, Hackett M, Dorsey MJ, et al. Dominant gain-of-function STAT1 mutations in FOXP3 wild-type immune dysregulation–polyendocrinopathy–enteropathy–X-linked–like syndrome. Journal of Allergy and Clinical Immunology. 2013;131(6):1611-23. e3.
60. Miossec P, Kolls JK. Targeting IL-17 and T H 17 cells in chronic inflammation. Nature reviews Drug discovery. 2012;11(10):763.
61. Casanova J-L, Holland SM, Notarangelo LD. Inborn errors of human JAKs and STATs. Immunity. 2012;36(4):515-28.
62. O'Shea JJ, Schwartz DM, Villarino AV, Gadina M, McInnes IB, Laurence A. The JAK-STAT pathway: impact on human disease and therapeutic intervention. Annual review of medicine. 2015;66:311-28.
63. Minegishi Y, Saito M, Tsuchiya S, Tsuge I, Takada H, Hara T, et al. Dominant-negative mutations in the DNA-binding domain of STAT3 cause hyper-IgE syndrome. Nature. 2007;448(7157):1058.
64. Ellinghaus D, Ellinghaus E, Nair RP, Stuart PE, Esko T, Metspalu A, et al. Combined analysis of genome-wide association studies for Crohn disease and psoriasis identifies seven shared susceptibility loci. The American Journal of Human Genetics. 2012;90(4):636-47.
65. Koskela HL, Eldfors S, Ellonen P, van Adrichem AJ, Kuusanmäki H, Andersson EI, et al. Somatic STAT3 mutations in large granular lymphocytic leukemia. New England Journal of Medicine. 2012;366(20):1905-13.
66. Jerez A, Clemente MJ, Makishima H, Koskela H, LeBlanc F, Ng KP, et al. STAT3 mutations unify the pathogenesis of chronic lymphoproliferative disorders of NK cells and T-cell large granular lymphocyte leukemia. Blood. 2012;120(15):3048-57.

67. Jerez A, Clemente MJ, Makishima H, Rajala H, Gómez-Seguí I, Olson T, et al. STAT3 mutations indicate the presence of subclinical T-cell clones in a subset of aplastic anemia and myelodysplastic syndrome patients. Blood. 2013;122(14):2453-9.
68. Ishida F, Matsuda K, Sekiguchi N, Makishima H, Taira C, Momose K, et al. STAT3 gene mutations and their association with pure red cell aplasia in large granular lymphocyte leukemia. Cancer science. 2014;105(3):342-6.
69. Nelson EA, Walker SR, Weisberg E, Bar-Natan M, Barrett R, Gashin LB, et al. The STAT5 inhibitor pimozide decreases survival of chronic myelogenous leukemia cells resistant to kinase inhibitors. Blood. 2011;117(12):3421-9.
70. Cohen AC, Nadeau KC, Tu W, Hwa V, Dionis K, Bezrodnik L, et al. Cutting edge: decreased accumulation and regulatory function of CD4+ CD25high T cells in human STAT5b deficiency. The Journal of Immunology. 2006;177(5):2770-4.
71. Kofoed EM, Hwa V, Little B, Woods KA, Buckway CK, Tsubaki J, et al. Growth hormone insensitivity associated with a STAT5b mutation. New England Journal of Medicine. 2003;349(12):1139-47.
72. Duetsch G, Illig T, Loesgen S, Rohde K, Klopp N, Herbon N, et al. STAT6 as an asthma candidate gene: polymorphism-screening, association and haplotype analysis in a Caucasian sib-pair study. Human molecular genetics. 2002;11(6):613-21.
73. Network GA. The global asthma report 2018. 2018.
74. Bateman E. GOAL Investigators Group. Can guideline defined asthma control be achieved? The Gaining Optimal Asthma ControL study. Am J Respir Crit Care Med. 2004;170:836-44.
75. Steinke JW, Borish L. Th2 cytokines and asthma—Interleukin-4: its role in the pathogenesis of asthma, and targeting it for asthma treatment with interleukin-4 receptor antagonists. Respiratory research. 2001;2(2):66.
76. Chan SC, Brown MA, Willcox TM, Li SH, Stevens SR, Tara D, et al. Abnormal IL-4 gene expression by atopic dermatitis T lymphocytes is reflected in altered nuclear protein interactions with IL-4 transcriptional regulatory element. Journal of investigative dermatology. 1996;106(5):1131-6.
77. Chung KF. Targeting the interleukin pathway in the treatment of asthma. The Lancet. 2015;386(9998):1086-96.
78. Bagnasco D, Ferrando M, Varricchi G, Passalacqua G, Canonica GW. A critical evaluation of anti-IL-13 and anti-IL-4 strategies in severe asthma. International archives of allergy and immunology. 2016;170(2):122-31.
79. Dabbagh K, Takeyama K, Lee H-M, Ueki IF, Lausier JA, Nadel JA. IL-4 induces mucin gene expression and goblet cell metaplasia in vitro and in vivo. The Journal of Immunology. 1999;162(10):6233-7.
80. Doucet C, Brouty-Boyé D, Pottin-Clemenceau C, Jasmin C, Canonica GW, Azzarone B. IL-4 and IL-13 specifically increase adhesion molecule and inflammatory cytokine expression in human lung fibroblasts. International immunology. 1998;10(10):1421-33.
81. Hoontrakoon R, Kailey J, Bratton D. IL-4 and TNF α Synergize to Enhance Eosinophil Survival. The Journal of Allergy & Clinical Immunology. 1999;103(1).
82. Moser R, Fehr J, Bruijnzeel P. IL-4 controls the selective endothelium-driven transmigration of eosinophils from allergic individuals. The Journal of Immunology. 1992;149(4):1432-8.
83. Akimoto T, Numata F, Tamura M, Takata Y, Higashida N, Takashi T, et al. Abrogation of bronchial eosinophilic inflammation and airway hyperreactivity in signal transducers and activators of transcription (STAT) 6-deficient mice. Journal of Experimental Medicine. 1998;187(9):1537-42.

84. Kuperman D, Schofield B, Wills-Karp M, Grusby MJ. Signal transducer and activator of transcription factor 6 (Stat6)-deficient mice are protected from antigen-induced airway hyperresponsiveness and mucus production. Journal of Experimental Medicine. 1998;187(6):939-48.
85. Mathew A, MacLean JA, DeHaan E, Tager AM, Green FH, Luster AD. Signal transducer and activator of transcription 6 controls chemokine production and T helper cell type 2 cell trafficking in allergic pulmonary inflammation. Journal of Experimental Medicine. 2001;193(9):1087-96.
86. Mikita T, Campbell D, Wu P, Williamson K, Schindler U. Requirements for interleukin-4-induced gene expression and functional characterization of Stat6. Molecular and Cellular Biology. 1996;16(10):5811-20.
87. Bennett BL, Cruz R, Lacson RG, Manning AM. Interleukin-4 suppression of tumor necrosis factor α-stimulated E-selectin gene transcription is mediated by STAT6 antagonism of NF-κB. Journal of Biological Chemistry. 1997;272(15):10212-9.
88. Hirst SJ, Hallsworth MP, Peng Q, Lee TH. Selective induction of eotaxin release by interleukin-13 or interleukin-4 in human airway smooth muscle cells is synergistic with interleukin-1 β and is mediated by the interleukin-4 receptor α-chain. American journal of respiratory and critical care medicine. 2002;165(8):1161-71.
89. Goto K, Chiba Y, Matsusue K, Hattori Y, Maitani Y, Sakai H, et al. The proximal STAT6 and NF-κB sites are responsible for IL-13-and TNF-α-induced RhoA transcriptions in human bronchial smooth muscle cells. Pharmacological research. 2010;61(5):466-72.
90. Thai P, Chen Y, Dolganov G, Wu R. Differential regulation of MUC5AC/Muc5ac and hCLCA-1/mGob-5 expression in airway epithelium. American journal of respiratory cell and molecular biology. 2005;33(6):523-30.
91. Lawrence T, Natoli G. Transcriptional regulation of macrophage polarization: enabling diversity with identity. Nature reviews immunology. 2011;11(11):750.
92. Kumar RK, Herbert C, Foster PS. The "classical" ovalbumin challenge model of asthma in mice. Current drug targets. 2008;9(6):485-94.
93. Aun MV, Bonamichi-Santos R, Arantes-Costa FM, Kalil J, Giavina-Bianchi P. Animal models of asthma: utility and limitations. Journal of asthma and allergy. 2017;10:293.
94. Clark JD, Flanagan ME, Telliez J-B. Discovery and Development of Janus Kinase (JAK) Inhibitors for Inflammatory Diseases: Miniperspective. Journal of medicinal chemistry. 2014;57(12):5023-38.
95. Banerjee S, Biehl A, Gadina M, Hasni S, Schwartz DM. JAK–STAT signaling as a target for inflammatory and autoimmune diseases: current and future prospects. Drugs. 2017;77(5):521-46.
96. Vijayakrishnan L, Venkataramanan R, Gulati P. Treating inflammation with the Janus kinase inhibitor CP-690,550. Trends in pharmacological sciences. 2011;32(1):25-34.
97. Changelian PS, Flanagan ME, Ball DJ, Kent CR, Magnuson KS, Martin WH, et al. Prevention of organ allograft rejection by a specific Janus kinase 3 inhibitor. Science. 2003;302(5646):875-8.
98. Quintás-Cardama A, Kantarjian H, Cortes J, Verstovsek S. Janus kinase inhibitors for the treatment of myeloproliferative neoplasias and beyond. Nature reviews Drug discovery. 2011;10(2):127.
99. Norman P. Selective JAK inhibitors in development for rheumatoid arthritis. Expert opinion on investigational drugs. 2014;23(8):1067-77.

100. Saridomichelakis MN, Olivry T. An update on the treatment of canine atopic dermatitis. The Veterinary Journal. 2016;207:29-37.
101. Nakayamada S, Kubo S, Iwata S, Tanaka Y. Chemical JAK inhibitors for the treatment of rheumatoid arthritis. Expert opinion on pharmacotherapy. 2016;17(16):2215-25.
102. Fragoulis GE, McInnes IB, Siebert S. JAK-inhibitors. New players in the field of immune-mediated diseases, beyond rheumatoid arthritis. Rheumatology. 2019;58(Supplement_1):i43-i54.
103. Punwani N, Burn T, Scherle P, Flores R, Shi J, Collier P, et al. Downmodulation of key inflammatory cell markers with a topical Janus kinase 1/2 inhibitor. British Journal of Dermatology. 2015;173(4):989-97.
104. Tefferi A, Pardanani A, editors. Serious adverse events during ruxolitinib treatment discontinuation in patients with myelofibrosis. Mayo Clinic Proceedings; 2011: Elsevier.
105. Cohen S, Radominski SC, Gomez‐Reino JJ, Wang L, Krishnaswami S, Wood SP, et al. Analysis of Infections and All‐Cause Mortality in Phase II, Phase III, and Long‐Term Extension Studies of Tofacitinib in Patients With Rheumatoid Arthritis. Arthritis & Rheumatology. 2014;66(11):2924-37.
106. Strand V, Ahadieh S, French J, Geier J, Krishnaswami S, Menon S, et al. Systematic review and meta-analysis of serious infections with tofacitinib and biologic disease-modifying antirheumatic drug treatment in rheumatoid arthritis clinical trials. Arthritis research & therapy. 2015;17(1):362.
107. Kremer JM, Bloom BJ, Breedveld FC, Coombs JH, Fletcher MP, Gruben D, et al. The safety and efficacy of a JAK inhibitor in patients with active rheumatoid arthritis: results of a double‐blind, placebo‐controlled phase IIa trial of three dosage levels of CP‐690,550 versus placebo. Arthritis & Rheumatism: Official Journal of the American College of Rheumatology. 2009;60(7):1895-905.
108. Voss J, Graff C, Schwartz A, Hyland D, Argiriadi M, Camp H, et al. THU0127 Pharmacodynamics of a novel JAK1 selective inhibitor in rat arthritis and anemia models and in healthy human subjects. Annals of the Rheumatic Diseases. 2014;73(Suppl 2):222-.
109. Shim S-H, Sung M-W, Park S-W, Heo DS. Absence of STAT1 disturbs the anticancer effect induced by STAT3 inhibition in head and neck carcinoma cell lines. International journal of molecular medicine. 2009;23(6):805-10.
110. Costa-Pereira AP, Tininini S, Strobl B, Alonzi T, Schlaak JF, Is' harc H, et al. Mutational switch of an IL-6 response to an interferon-γ-like response. Proceedings of the National Academy of Sciences. 2002;99(12):8043-7.
111. Okusaka T, Ueno H, Ikeda M, Mitsunaga S, Ozaka M, Ishii H, et al. Phase 1 and pharmacological trial of OPB‐31121, a signal transducer and activator of transcription‐3 inhibitor, in patients with advanced hepatocellular carcinoma. Hepatology Research. 2015;45(13):1283-91.
112. Wong A, Soo RA, Tan D, Lee SC, Lim J, Marban P, et al. Phase I and biomarker study of OPB-51602, a novel signal transducer and activator of transcription (STAT) 3 inhibitor, in patients with refractory solid malignancies. Annals of Oncology. 2015;26(5):998-1005.
113. Sen M, Grandis JR. Nucleic acid-based approaches to STAT inhibition. Jak-Stat. 2012;1(4):285-91.

114. Sen M, Thomas SM, Kim S, Yeh JI, Ferris RL, Johnson JT, et al. First-in-human trial of a STAT3 decoy oligonucleotide in head and neck tumors: implications for cancer therapy. Cancer discovery. 2012;2(8):694-705.
115. Kummar S, Rubinstein L, Kinders R, Parchment RE, Gutierrez ME, Murgo AJ, et al. Phase 0 clinical trials: conceptions and misconceptions. The Cancer Journal. 2008;14(3):133-7.
116. Koo MY, Park J, Lim JM, Joo SY, Shin S-P, Shim HB, et al. Selective inhibition of the function of tyrosine-phosphorylated STAT3 with a phosphorylation site-specific intrabody. Proceedings of the National Academy of Sciences. 2014;111(17):6269-74.
117. Fitzgerald KA, McWhirter SM, Faia KL, Rowe DC, Latz E, Golenbock DT, et al. IKK ε and TBK1 are essential components of the IRF3 signaling pathway. Nature immunology. 2003;4(5):491.
118. Xu G, Lo Y-C, Li Q, Napolitano G, Wu X, Jiang X, et al. Crystal structure of inhibitor of κ B kinase β. Nature. 2011;472(7343):325.
119. Ma X, Helgason E, Phung QT, Quan CL, Iyer RS, Lee MW, et al. Molecular basis of Tank-binding kinase 1 activation by transautophosphorylation. Proceedings of the National Academy of Sciences. 2012;109(24):9378-83.
120. Andraos R, Qian Z, Bonenfant D, Rubert J, Vangrevelinghe E, Scheufler C, et al. Modulation of activation-loop phosphorylation by JAK inhibitors is binding mode dependent. Cancer discovery. 2012;2(6):512-23.
121. Everts B, Amiel E, Huang SC-C, Smith AM, Chang C-H, Lam WY, et al. TLR-driven early glycolytic reprogramming via the kinases TBK1-IKKε supports the anabolic demands of dendritic cell activation. Nature immunology. 2014;15(4):323.
122. Tan X, Sun L, Chen J, Chen ZJ. Detection of microbial infections through innate immune sensing of nucleic acids. Annual review of microbiology. 2018;72:447-78.
123. Sun L, Wu J, Du F, Chen X, Chen ZJ. Cyclic GMP-AMP synthase is a cytosolic DNA sensor that activates the type I interferon pathway. Science. 2013;339(6121):786-91.
124. Ishikawa H, Barber GN. STING is an endoplasmic reticulum adaptor that facilitates innate immune signalling. Nature. 2008;455(7213):674.
125. Liu S, Cai X, Wu J, Cong Q, Chen X, Li T, et al. Phosphorylation of innate immune adaptor proteins MAVS, STING, and TRIF induces IRF3 activation. Science. 2015;347(6227):aaa2630.
126. Agalioti T, Lomvardas S, Parekh B, Yie J, Maniatis T, Thanos D. Ordered recruitment of chromatin modifying and general transcription factors to the IFN-β promoter. Cell. 2000;103(4):667-78.
127. Lin R, Heylbroeck C, Pitha PM, Hiscott J. Virus-dependent phosphorylation of the IRF-3 transcription factor regulates nuclear translocation, transactivation potential, and proteasome-mediated degradation. Molecular and cellular biology. 1998;18(5):2986-96.
128. Yoneyama M, Suhara W, Fukuhara Y, Fukuda M, Nishida E, Fujita T. Direct triggering of the type I interferon system by virus infection: activation of a transcription factor complex containing IRF‐3 and CBP/p300. The EMBO journal. 1998;17(4):1087-95.
129. Yoneyama M, Kikuchi M, Natsukawa T, Shinobu N, Imaizumi T, Miyagishi M, et al. The RNA helicase RIG-I has an essential function in double-stranded RNA-induced innate antiviral responses. Nature immunology. 2004;5(7):730.
130. Kang D-c, Gopalkrishnan RV, Wu Q, Jankowsky E, Pyle AM, Fisher PB. mda-5: An interferon-inducible putative RNA helicase with double-stranded RNA-dependent

ATPase activity and melanoma growth-suppressive properties. Proceedings of the National Academy of Sciences. 2002;99(2):637-42.
131. Goubau D, Schlee M, Deddouche S, Pruijssers AJ, Zillinger T, Goldeck M, et al. Antiviral immunity via RIG-I-mediated recognition of RNA bearing 5′ -diphosphates. Nature. 2014;514(7522):372.
132. Pichlmair A, Schulz O, Tan CP, Näslund TI, Liljeström P, Weber F, et al. RIG-I-mediated antiviral responses to single-stranded RNA bearing 5'-phosphates. Science. 2006;314(5801):997-1001.
133. Peisley A, Lin C, Wu B, Orme-Johnson M, Liu M, Walz T, et al. Cooperative assembly and dynamic disassembly of MDA5 filaments for viral dsRNA recognition. Proceedings of the National Academy of Sciences. 2011;108(52):21010-5.
134. Wu B, Peisley A, Richards C, Yao H, Zeng X, Lin C, et al. Structural basis for dsRNA recognition, filament formation, and antiviral signal activation by MDA5. Cell. 2013;152(1-2):276-89.
135. Kawai T, Akira S. The role of pattern-recognition receptors in innate immunity: update on Toll-like receptors. Nature immunology. 2010;11(5):373.
136. Alexopoulou L, Holt AC, Medzhitov R, Flavell RA. Recognition of double-stranded RNA and activation of NF- κ B by Toll-like receptor 3. Nature. 2001;413(6857):732.
137. Haynes LM, Moore DD, Kurt-Jones EA, Finberg RW, Anderson LJ, Tripp RA. Involvement of toll-like receptor 4 in innate immunity to respiratory syncytial virus. Journal of virology. 2001;75(22):10730-7.
138. Takeda K, Akira S. Toll-like receptors in innate immunity. International immunology. 2005;17(1):1-14.
139. Honda K, Yanai H, Negishi H, Asagiri M, Sato M, Mizutani T, et al. IRF-7 is the master regulator of type-I interferon-dependent immune responses. Nature. 2005;434(7034):772.
140. Hoshino K, Sugiyama T, Matsumoto M, Tanaka T, Saito M, Hemmi H, et al. I κ B kinase- α is critical for interferon- α production induced by Toll-like receptors 7 and 9. Nature. 2006;440(7086):949.
141. Lund J, Sato A, Akira S, Medzhitov R, Iwasaki A. Toll-like receptor 9–mediated recognition of Herpes simplex virus-2 by plasmacytoid dendritic cells. Journal of Experimental Medicine. 2003;198(3):513-20.
142. Clark K, Plater L, Peggie M, Cohen P. Use of the Pharmacological Inhibitor BX795 to Study the Regulation and Physiological Roles of TBK1 and I κ B Kinase ϵ A DISTINCT UPSTREAM KINASE MEDIATES SER-172 PHOSPHORYLATION AND ACTIVATION. Journal of Biological Chemistry. 2009;284(21):14136-46.
143. Feldman RI, Wu JM, Polokoff MA, Kochanny MJ, Dinter H, Zhu D, et al. Novel small molecule inhibitors of 3-phosphoinositide-dependent kinase-1. Journal of Biological Chemistry. 2005;280(20):19867-74.
144. Su A-r, Qiu M, Li Y-l, Xu W-t, Song S-w, Wang X-h, et al. BX-795 inhibits HSV-1 and HSV-2 replication by blocking the JNK/p38 pathways without interfering with PDK1 activity in host cells. Acta Pharmacologica Sinica. 2017;38(3):402.
145. Jaishankar D, Yakoub AM, Yadavalli T, Agelidis A, Thakkar N, Hadigal S, et al. An off-target effect of BX795 blocks herpes simplex virus type 1 infection of the eye. Science translational medicine. 2018;10(428):eaan5861.
146. Bubici C, Papa S. JNK signalling in cancer: in need of new, smarter therapeutic targets. British journal of pharmacology. 2014;171(1):24-37.

147. Bellacosa A, Kumar CC, Di Cristofano A, Testa JR. Activation of AKT kinases in cancer: implications for therapeutic targeting. Advances in cancer research. 2005;94:29-86.
148. Fountzilas C, Patel S, Mahalingam D. Review: oncolytic virotherapy, updates and future directions. Oncotarget 8: 102617–102639. 2017.
149. Garber K. China approves world's first oncolytic virus therapy for cancer treatment. JOURNAL-NATIONAL CANCER INSTITUTE. 2006;98(5):298.
150. Dobner T, Horikoshi N, Rubenwolf S, Shenk T. Blockage by adenovirus E4orf6 of transcriptional activation by the p53 tumor suppressor. Science. 1996;272(5267):1470-3.
151. Food U, Administration D. FDA approves first-of-its-kind product for the treatment of melanoma. Silver Spring, MD. 2015:611-9.
152. Toda M, Martuza RL, Rabkin SD. Tumor growth inhibition by intratumoral inoculation of defective herpes simplex virus vectors expressing granulocyte–macrophage colony-stimulating factor. Molecular Therapy. 2000;2(4):324-9.
153. Bolovan CA, Sawtell NM, Thompson RL. ICP34. 5 mutants of herpes simplex virus type 1 strain 17syn+ are attenuated for neurovirulence in mice and for replication in confluent primary mouse embryo cell cultures. Journal of virology. 1994;68(1):48-55.
154. Alemany R, Suzuki K, Curiel DT. Blood clearance rates of adenovirus type 5 in mice. Journal of General Virology. 2000;81(11):2605-9.
155. Dubin G, Fishman N, Eisenberg R, Cohen G, Friedman H. The role of herpes simplex virus glycoproteins in immune evasion. Herpes Simplex Virus: Springer; 1992. p. 111-20.
156. Lyles D, Rupprecht C, Knipe D, Howley P. Fields virology. Lippincott Williams &. 2006;31:1364-94.
157. Hansen D, Thurmond M, Thorburn M. Factors associated with the spread of clinical vesicular stomatitis in California dairy cattle. American journal of veterinary research. 1985;46(4):789-95.
158. Cornish T, Stallknecht D, Brown C, Seal B, Howerth E. Pathogenesis of experimental vesicular stomatitis virus (New Jersey serotype) infection in the deer mouse (Peromyscus maniculatus). Veterinary pathology. 2001;38(4):396-406.
159. Quiroz E, Moreno N, Peralta PH, Tesh RB. A human case of encephalitis associated with vesicular stomatitis virus (Indiana serotype) infection. The American journal of tropical medicine and hygiene. 1988;39(3):312-4.
160. Moerdyk-Schauwecker M, DeStephanis D, Hastie E, Grdzelishvili VZ. Detecting protein–protein interactions in vesicular stomatitis virus using a cytoplasmic yeast two hybrid system. Journal of virological methods. 2011;173(2):203-12.
161. Zhang X, Green TJ, Tsao J, Qiu S, Luo M. Role of intermolecular interactions of vesicular stomatitis virus nucleoprotein in RNA encapsidation. Journal of virology. 2008;82(2):674-82.
162. Finkelshtein D, Werman A, Novick D, Barak S, Rubinstein M. LDL receptor and its family members serve as the cellular receptors for vesicular stomatitis virus. Proceedings of the National Academy of Sciences. 2013;110(18):7306-11.
163. Cureton DK, Massol RH, Whelan SP, Kirchhausen T. The length of vesicular stomatitis virus particles dictates a need for actin assembly during clathrin-dependent endocytosis. PLoS pathogens. 2010;6(9):e1001127.
164. Stanifer ML, Cureton DK, Whelan SP. A recombinant vesicular stomatitis virus bearing a lethal mutation in the glycoprotein gene uncovers a second site suppressor that restores fusion. Journal of virology. 2011;85(16):8105-15.

165. Rose J, Schubert M. Rhabdovirus genomes and their products. The rhabdoviruses: Springer; 1987. p. 129-66.
166. Isaac CL, Keene JD. RNA polymerase-associated interactions near template promoter sequences of defective interfering particles of vesicular stomatitis virus. Journal of virology. 1982;43(1):241-9.
167. Canter D, Perrault J. Stabilization of vesicular stomatitis virus L polymerase protein by P protein binding: a small deletion in the C-terminal domain of L abrogates binding. Virology. 1996;219(2):376-86.
168. Masters PS, Banerjee AK. Resolution of multiple complexes of phosphoprotein NS with nucleocapsid protein N of vesicular stomatitis virus. Journal of virology. 1988;62(8):2651-7.
169. Davis N, Arnheiter H, Wertz G. Vesicular stomatitis virus N and NS proteins form multiple complexes. Journal of virology. 1986;59(3):751-4.
170. Jayakar HR, Whitt MA. Identification of two additional translation products from the matrix (M) gene that contribute to vesicular stomatitis virus cytopathology. Journal of virology. 2002;76(16):8011-8.
171. Ahmed M, McKenzie MO, Puckett S, Hojnacki M, Poliquin L, Lyles DS. Ability of the matrix protein of vesicular stomatitis virus to suppress beta interferon gene expression is genetically correlated with the inhibition of host RNA and protein synthesis. Journal of virology. 2003;77(8):4646-57.
172. Faria PA, Chakraborty P, Levay A, Barber GN, Ezelle HJ, Enninga J, et al. VSV disrupts the Rae1/mrnp41 mRNA nuclear export pathway. Molecular cell. 2005;17(1):93-102.
173. Petersen JM, Her L-S, Varvel V, Lund E, Dahlberg JE. The matrix protein of vesicular stomatitis virus inhibits nucleocytoplasmic transport when it is in the nucleus and associated with nuclear pore complexes. Molecular and cellular biology. 2000;20(22):8590-601.
174. Whitaker-Dowling PA, Youngner JS, Widnell CC. Sequential disassembly of the cytoskeleton in BHK21 cells infected with vesicular stomatitis virus. Virology. 1990;177(1):289-97.
175. Rieder M, Conzelmann K-K. Rhabdovirus evasion of the interferon system. Journal of Interferon & Cytokine Research. 2009;29(9):499-510.
176. Melzer MK, Lopez-Martinez A, Altomonte J. Oncolytic vesicular stomatitis virus as a viro-immunotherapy: defeating cancer with a “hammer” and “anvil”. Biomedicines. 2017;5(1):8.
177. Muller U, Steinhoff U, Reis L, Hemmi S, Pavlovic J, Zinkernagel RM, et al. Functional role of type I and type II interferons in antiviral defense. Science. 1994;264(5167):1918-21.
178. Altomonte J, Wu L, Chen L, Meseck M, Ebert O, García-Sastre A, et al. Exponential enhancement of oncolytic vesicular stomatitis virus potency by vector-mediated suppression of inflammatory responses in vivo. Molecular Therapy. 2008;16(1):146-53.
179. Wongthida P, Diaz RM, Galivo F, Kottke T, Thompson J, Melcher A, et al. VSV oncolytic virotherapy in the B16 model depends upon intact MyD88 signaling. Molecular Therapy. 2011;19(1):150-8.
180. Galivo F, Diaz RM, Wongthida P, Thompson J, Kottke T, Barber G, et al. Single-cycle viral gene expression, rather than progressive replication and oncolysis, is required for VSV therapy of B16 melanoma. Gene therapy. 2010;17(2):158.
181. Guo ZS, Liu Z, Bartlett DL. Oncolytic immunotherapy: dying the right way is a key to eliciting potent antitumor immunity. Frontiers in oncology. 2014;4:74.

182. Diaz RM, Galivo F, Kottke T, Wongthida P, Qiao J, Thompson J, et al. Oncolytic immunovirotherapy for melanoma using vesicular stomatitis virus. Cancer research. 2007;67(6):2840-8.
183. Wongthida P, Diaz RM, Galivo F, Kottke T, Thompson J, Pulido J, et al. Type III IFN interleukin-28 mediates the antitumor efficacy of oncolytic virus VSV in immune-competent mouse models of cancer. Cancer research. 2010;70(11):4539-49.
184. Barchet W, Cella M, Odermatt B, Asselin-Paturel C, Colonna M, Kalinke U. Virus-induced interferon α production by a dendritic cell subset in the absence of feedback signaling in vivo. Journal of Experimental Medicine. 2002;195(4):507-16.
185. Swiecki M, Colonna M. Unraveling the functions of plasmacytoid dendritic cells during viral infections, autoimmunity, and tolerance. Immunological reviews. 2010;234(1):142-62.
186. Stojdl DF, Lichty B, Knowles S, Marius R, Atkins H, Sonenberg N, et al. Exploiting tumor-specific defects in the interferon pathway with a previously unknown oncolytic virus. Nature medicine. 2000;6(7):821.
187. Stojdl DF, Lichty BD, Paterson JM, Power AT, Knowles S, Marius R, et al. VSV strains with defects in their ability to shutdown innate immunity are potent systemic anti-cancer agents. Cancer cell. 2003;4(4):263-75.
188. Jenks N, Myers R, Greiner SM, Thompson J, Mader EK, Greenslade A, et al. Safety studies on intrahepatic or intratumoral injection of oncolytic vesicular stomatitis virus expressing interferon-β in rodents and nonhuman primates. Human gene therapy. 2010;21(4):451-62.
189. Obuchi M, Fernandez M, Barber GN. Development of recombinant vesicular stomatitis viruses that exploit defects in host defense to augment specific oncolytic activity. Journal of virology. 2003;77(16):8843-56.
190. Muik A, Kneiske I, Werbizki M, Wilflingseder D, Giroglou T, Ebert O, et al. Pseudotyping vesicular stomatitis virus with lymphocytic choriomeningitis virus glycoproteins enhances infectivity for glioma cells and minimizes neurotropism. Journal of virology. 2011;85(11):5679-84.
191. Ayala-Breton C, Barber GN, Russell SJ, Peng K-W. Retargeting vesicular stomatitis virus using measles virus envelope glycoproteins. Human gene therapy. 2011;23(5):484-91.
192. Publicover J, Ramsburg E, Robek M, Rose JK. Rapid pathogenesis induced by a vesicular stomatitis virus matrix protein mutant: viral pathogenesis is linked to induction of tumor necrosis factor alpha. Journal of virology. 2006;80(14):7028-36.
193. Wu L, Huang T-g, Meseck M, Altomonte J, Ebert O, Shinozaki K, et al. rVSV (M Δ 51)-M3 is an effective and safe oncolytic virus for cancer therapy. Human gene therapy. 2008;19(6):635-47.
194. Ferran MC, Lucas-Lenard JM. The vesicular stomatitis virus matrix protein inhibits transcription from the human beta interferon promoter. Journal of virology. 1997;71(1):371-7.
195. Von Kobbe C, van Deursen JM, Rodrigues JP, Sitterlin D, Bachi A, Wu X, et al. Vesicular stomatitis virus matrix protein inhibits host cell gene expression by targeting the nucleoporin Nup98. Molecular cell. 2000;6(5):1243-52.
196. Barber GN. VSV-tumor selective replication and protein translation. Oncogene. 2005;24(52):7710.
197. Breitbach CJ, De Silva NS, Falls TJ, Aladl U, Evgin L, Paterson J, et al. Targeting tumor vasculature with an oncolytic virus. Molecular Therapy. 2011;19(5):886-94.

198. Dunn EF, Connor JH. Dominant inhibition of Akt/protein kinase B signaling by the matrix protein of a negative-strand RNA virus. Journal of virology. 2011;85(1):422-31.
199. Robey RB, Hay N, editors. Is Akt the "Warburg kinase"?—Akt-energy metabolism interactions and oncogenesis. Seminars in cancer biology; 2009: Elsevier.
200. Felt SA, Grdzelishvili VZ. Recent advances in vesicular stomatitis virus-based oncolytic virotherapy: a 5-year update. The Journal of general virology. 2017;98(12):2895.
201. Blackham AU, Northrup SA, Willingham M, Sirintrapun J, Russell GB, Lyles DS, et al. Molecular determinants of susceptibility to oncolytic vesicular stomatitis virus in pancreatic adenocarcinoma. journal of surgical research. 2014;187(2):412-26.
202. Moerdyk-Schauwecker M, Shah NR, Murphy AM, Hastie E, Mukherjee P, Grdzelishvili VZ. Resistance of pancreatic cancer cells to oncolytic vesicular stomatitis virus: role of type I interferon signaling. Virology. 2013;436(1):221-34.
203. Blackham AU, Northrup SA, Willingham M, D'Agostino Jr RB, Lyles DS, Stewart IV JH. Variation in susceptibility of human malignant melanomas to oncolytic vesicular stomatitis virus. Surgery. 2013;153(3):333-43.
204. Cockle JV, Rajani K, Zaidi S, Kottke T, Thompson J, Diaz RM, et al. Combination viroimmunotherapy with checkpoint inhibition to treat glioma, based on location-specific tumor profiling. Neuro-oncology. 2015;18(4):518-27.
205. Shen W, Patnaik MM, Ruiz A, Russell SJ, Peng K-W. Immunovirotherapy with vesicular stomatitis virus and PD-L1 blockade enhances therapeutic outcome in murine acute myeloid leukemia. Blood. 2016;127(11):1449-58.
206. Olagnier D, Lababidi RR, Hadj SB, Sze A, Liu Y, Naidu SD, et al. Activation of Nrf2 signaling augments vesicular stomatitis virus oncolysis via autophagy-driven suppression of antiviral immunity. Molecular Therapy. 2017;25(8):1900-16.
207. Olagnier D, Brandtoft AM, Gunderstofte C, Villadsen NL, Krapp C, Thielke AL, et al. Nrf2 negatively regulates STING indicating a link between antiviral sensing and metabolic reprogramming. Nature communications. 2018;9(1):3506.
208. Nguyên TL-A, Abdelbary H, Arguello M, Breitbach C, Leveille S, Diallo J-S, et al. Chemical targeting of the innate antiviral response by histone deacetylase inhibitors renders refractory cancers sensitive to viral oncolysis. Proceedings of the National Academy of Sciences. 2008;105(39):14981-6.
209. Shulak L, Beljanski V, Chiang C, Dutta SM, Van Grevenynghe J, Belgnaoui SM, et al. Histone deacetylase inhibitors potentiate vesicular stomatitis virus oncolysis in prostate cancer cells by modulating NF-κB-dependent autophagy. Journal of virology. 2014;88(5):2927-40.
210. Shulak L. Vorinostat potentiates vesicular stomatitis virus oncolysis by modulating autophagy in an NF-κB-dependent manner: Division of Experimental Medicine, Department of Medicine, McGill University ⋯; 2013.
211. Costa-Mattioli M, Sonenberg N. RAPping production of type I interferon in pDCs through mTOR. Nature immunology. 2008;9(10):1097.
212. Alain T, Lun X, Martineau Y, Sean P, Pulendran B, Petroulakis E, et al. Vesicular stomatitis virus oncolysis is potentiated by impairing mTORC1-dependent type I IFN production. Proceedings of the National Academy of Sciences. 2010;107(4):1576-81.
213. Tumilasci VF, Oliere S, Nguyên TL-A, Shamy A, Bell J, Hiscott J. Targeting the apoptotic pathway with BCL-2 inhibitors sensitizes primary chronic lymphocytic leukemia cells to vesicular stomatitis virus-induced oncolysis. Journal of virology. 2008;82(17):8487-99.

214. Samuel S, Tumilasci VF, Oliere S, Nguyên TL-A, Shamy A, Bell J, et al. VSV oncolysis in combination with the BCL-2 inhibitor obatoclax overcomes apoptosis resistance in chronic lymphocytic leukemia. Molecular Therapy. 2010;18(12):2094-103.
215. Ray RB, Meyer K, Ray R. Hepatitis C virus core protein promotes immortalization of primary human hepatocytes. Virology. 2000;271(1):197-204.
216. Zhao T, Yang L, Sun Q, Arguello M, Ballard DW, Hiscott J, et al. The NEMO adaptor bridges the nuclear factor-κB and interferon regulatory factor signaling pathways. Nature immunology. 2007;8(6):592.
217. Goulet M-L, Olagnier D, Xu Z, Paz S, Belgnaoui SM, Lafferty EI, et al. Systems analysis of a RIG-I agonist inducing broad spectrum inhibition of virus infectivity. PLoS pathogens. 2013;9(4):e1003298.
218. Kishta OA, Sabourin A, Simon L, McGovern T, Raymond M, Galbas T, et al. March1 E3 Ubiquitin Ligase Modulates Features of Allergic Asthma in an Ovalbumin-Induced Mouse Model of Lung Inflammation. Journal of immunology research. 2018;2018.
219. Bedsaul JR, Zaritsky LA, Zoon KC. Type I Interferon-Mediated Induction of Antiviral Genes and Proteins Fails to Protect Cells from the Cytopathic Effects of Sendai Virus Infection. Journal of Interferon & Cytokine Research. 2016;36(11):652-65.
220. Zhou Z, Hamming OJ, Ank N, Paludan SR, Nielsen AL, Hartmann R. Type III interferon (IFN) induces a type I IFN-like response in a restricted subset of cells through signaling pathways involving both the Jak-STAT pathway and the mitogen-activated protein kinases. Journal of virology. 2007;81(14):7749-58.
221. Horvath CM. The Jak-STAT pathway stimulated by interferon γ. Sci STKE. 2004;2004(260):tr8-tr.
222. Busch-Dienstfertig M, González-Rodríguez S. IL-4, JAK-STAT signaling, and pain. Jak-Stat. 2013;2(4):e27638.
223. Pastuschek J, Poetzsch J, Morales-Prieto DM, Schleußner E, Markert UR, Georgiev G. Stimulation of the JAK/STAT pathway by LIF and OSM in the human granulosa cell line COV434. Journal of reproductive immunology. 2015;108:48-55.
224. Xiao Y, Zou Q, Xie X, Liu T, Li HS, Jie Z, et al. The kinase TBK1 functions in dendritic cells to regulate T cell homeostasis, autoimmunity, and antitumor immunity. Journal of Experimental Medicine. 2017;214(5):1493-507.
225. Cataldi M, Shah NR, Felt SA, Grdzelishvili VZ. Breaking resistance of pancreatic cancer cells to an attenuated vesicular stomatitis virus through a novel activity of IKK inhibitor TPCA-1. Virology. 2015;485:340-54.
226. Russell SJ, Peng K-W, Bell JC. Oncolytic virotherapy. Nature biotechnology. 2012;30(7):658.
227. Yebdri FB, Van Grevenynghe J, Tang VA, Goulet M-L, Wu JH, Stojdl DF, et al. Triptolide-mediated inhibition of interferon signaling enhances vesicular stomatitis virus-based oncolysis. Molecular Therapy. 2013;21(11):2043-53.
228. Cary ZD, Willingham MC, Lyles DS. Oncolytic vesicular stomatitis virus induces apoptosis in U87 glioblastoma cells by a type II death receptor mechanism and induces cell death and tumor clearance in vivo. Journal of virology. 2011;85(12):5708-17.
229. Pennock ND, White JT, Cross EW, Cheney EE, Tamburini BA, Kedl RM. T cell responses: naive to memory and everything in between. Advances in physiology education. 2013;37(4):273-83.
230. Afshari JT, Hosseini RF, Farahabadi SH, Heydarian F, Boskabady MH, Khoshnavaz R, et al. Association of the expression of IL-4 and IL-13 genes, IL-4 and IgE serum levels with allergic asthma. Iranian Journal of Allergy, Asthma and Immunology. 2007:69-72.

231. Lee YC, Lee KH, Lee HB, Rhee YK. Serum levels of interleukins (IL)-4, IL-5, IL-13, and interferon-γ in acute asthma. Journal of Asthma. 2001;38(8):665-71.
232. Dengler HS, Wu X, Peng I, Rinderknecht CH, Kwon Y, Suto E, et al. Lung-restricted inhibition of Janus kinase 1 is effective in rodent models of asthma. Science translational medicine. 2018;10(468):eaao2151.
233. Sung Y-Y, Kim S-H, Yuk HJ, Yang W-K, Lee YM, Son E, et al. Siraitia grosvenorii residual extract attenuates ovalbumin-induced lung inflammation by down-regulating IL-4, IL-5, IL-13, IL-17, and MUC5AC expression in mice. Phytomedicine. 2019;61:152835.
234. Iwamoto I, Nakajima H, Endo H, Yoshida S. Interferon gamma regulates antigen-induced eosinophil recruitment into the mouse airways by inhibiting the infiltration of CD4+ T cells. Journal of experimental medicine. 1993;177(2):573-6.
235. Cohn L, Homer RJ, Niu N, Bottomly K. T helper 1 cells and interferon γ regulate allergic airway inflammation and mucus production. Journal of Experimental Medicine. 1999;190(9):1309-18.
236. Elser B, Lohoff M, Kock S, Giaisi M, Kirchhoff S, Krammer PH, et al. IFN-γ represses IL-4 expression via IRF-1 and IRF-2. Immunity. 2002;17(6):703-12.
237. Leonard C, Tormey V, Burke C, Poulter L. Allergen-induced cytokine production in atopic disease and its relationship to disease severity. American journal of respiratory cell and molecular biology. 1997;17(3):368-75.
238. Renzi PM, Turgeon JP, Marcotte JE, Drblik SP, Berube D, Gagnon MF, et al. Reduced interferon-γ production in infants with bronchiolitis and asthma. American journal of respiratory and critical care medicine. 1999;159(5):1417-22.
239. Smart JM, Horak E, Kemp AS, Robertson CF, Tang ML. Polyclonal and allergen-induced cytokine responses in adults with asthma: resolution of asthma is associated with normalization of IFN-γ responses. Journal of Allergy and Clinical Immunology. 2002;110(3):450-6.
240. Raundhal M, Morse C, Khare A, Oriss TB, Milosevic J, Trudeau J, et al. High IFN-γ and low SLPI mark severe asthma in mice and humans. The Journal of clinical investigation. 2015;125(8):3037-50.
241. Bocek P, Foucras G, Paul WE. Interferon γ enhances both in vitro and in vivo priming of CD4+ T cells for IL-4 production. Journal of Experimental Medicine. 2004;199(12):1619-30.
242. Peters MC, McGrath KW, Hawkins GA, Hastie AT, Levy BD, Israel E, et al. Plasma interleukin-6 concentrations, metabolic dysfunction, and asthma severity: a cross-sectional analysis of two cohorts. The lancet Respiratory medicine. 2016;4(7):574-84.
243. Bhakta NR, Christenson SA, Nerella S, Solberg OD, Nguyen CP, Choy DF, et al. IFN-stimulated gene expression, type 2 inflammation, and endoplasmic reticulum stress in asthma. American journal of respiratory and critical care medicine. 2018;197(3):313-24.
244. Foster PS, Yang M, Herbert C, Kumar RK. CD4+ T-lymphocytes regulate airway remodeling and hyper-reactivity in a mouse model of chronic asthma. Laboratory investigation. 2002;82(4):455.
245. Nials AT, Uddin S. Mouse models of allergic asthma: acute and chronic allergen challenge. Disease models & mechanisms. 2008;1(4-5):213-20.
246. McMillan S, Lloyd C. Prolonged allergen challenge in mice leads to persistent airway remodelling. Clinical & Experimental Allergy. 2004;34(3):497-507.

247. Chapman DG, Tully JE, Nolin JD, Janssen‐Heininger YM, Irvin CG. Animal models of allergic airways disease: where are we and where to next? Journal of cellular biochemistry. 2014;115(12):2055-64.
248. Ricciardolo FL, Nijkamp F, Rose VD, Folkerts G. The guinea pig as an animal model for asthma. Current drug targets. 2008;9(6):452-65.
249. DiGiovanni FA, Ellis R, Wattie J, Hirota JA, Southam DS, Inman MD. Concurrent dual allergen exposure and its effects on airway hyperresponsiveness, inflammation and remodeling in mice. Disease models & mechanisms. 2009;2(5-6):275-82.
250. Swirski FK, Sajic D, Robbins CS, Gajewska BU, Jordana M, Stämpfli MR. Chronic exposure to innocuous antigen in sensitized mice leads to suppressed airway eosinophilia that is reversed by granulocyte macrophage colony-stimulating factor. The Journal of Immunology. 2002;169(7):3499-506.
251. Doras C, Petak F, Bayat S, Baudat A, Von Garnier C, Eigenmann P, et al. Lung responses in murine models of experimental asthma: Value of house dust mite over ovalbumin sensitization. Respiratory physiology & neurobiology. 2018;247:43-51.
252. Kauffman HF, Tamm M, Timmerman JAB, Borger P. House dust mite major allergens Der p 1 and Der p 5 activate human airway-derived epithelial cells by protease-dependent and protease-independent mechanisms. Clinical and Molecular Allergy. 2006;4(1):5.
253. Comoy EE, Pestel J, Duez C, Stewart GA, Vendeville C, Fournier C, et al. The house dust mite allergen, Dermatophagoides pteronyssinus, promotes type 2 responses by modulating the balance between IL-4 and IFN-γ. The Journal of Immunology. 1998;160(5):2456-62.
254. Kikuchi Y, Takai T, Kuhara T, Ota M, Kato T, Hatanaka H, et al. Crucial commitment of proteolytic activity of a purified recombinant major house dust mite allergen Der p1 to sensitization toward IgE and IgG responses. The journal of immunology. 2006;177(3):1609-17.
255. Locke NR, Royce SG, Wainewright JS, Samuel CS, Tang ML. Comparison of airway remodeling in acute, subacute, and chronic models of allergic airways disease. American journal of respiratory cell and molecular biology. 2007;36(5):625-32.
256. Johnston SL, Pattemore PK, Sanderson G, Smith S, Lampe F, Josephs L, et al. Community study of role of viral infections in exacerbations of asthma in 9-11 year old children. Bmj. 1995;310(6989):1225-9.
257. Johnston S. The immunology of virus infection in asthma. European Respiratory Journal. 2001;18(6):1013-25.
258. Mori H, Parker NS, Rodrigues D, Hulland K, Chappell D, Hincks JS, et al. Differences in respiratory syncytial virus and influenza infection in a house-dust-mite-induced asthma mouse model: consequences for steroid sensitivity. Clinical science. 2013;125(12):565-74.
259. Matsuse H, Behera AK, Kumar M, Rabb H, Lockey RF, Mohapatra SS. Recurrent respiratory syncytial virus infections in allergen-sensitized mice lead to persistent airway inflammation and hyperresponsiveness. The Journal of Immunology. 2000;164(12):6583-92.
260. Kondo Y, Matsuse H, Machida I, Kawano T, Saeki S, Tomari S, et al. Effects of primary and secondary low‐grade respiratory syncytial virus infections in a murine model of asthma. Clinical & Experimental Allergy. 2004;34(8):1307-13.
261. Dakhama A, Park J-W, Taube C, El Gazzar M, Kodama T, Miyahara N, et al. Alteration of airway neuropeptide expression and development of airway

hyperresponsiveness following respiratory syncytial virus infection. American Journal of Physiology-Lung Cellular and Molecular Physiology. 2005;288(4):L761-L70.
262. Schwarze J, Hamelmann E, Bradley KL, Takeda K, Gelfand EW. Respiratory syncytial virus infection results in airway hyperresponsiveness and enhanced airway sensitization to allergen. The Journal of clinical investigation. 1997;100(1):226-33.
263. Becker Y. Respiratory syncytial virus (RSV) evades the human adaptive immune system by skewing the Th1/Th2 cytokine balance toward increased levels of Th2 cytokines and IgE, markers of allergy—a review. Virus genes. 2006;33(2):235-52.
264. Barends M, Boelen A, De Rond L, Kwakkel J, Bestebroer T, Dormans J, et al. Influence of respiratory syncytial virus infection on cytokine and inflammatory responses in allergic mice. Clinical & Experimental Allergy. 2002;32(3):463-71.
265. Barends M, Van Oosten M, De Rond C, Dormans J, Osterhaus A, Neijens H, et al. Timing of infection and prior immunization with respiratory syncytial virus (RSV) in RSV-enhanced allergic inflammation. Journal of Infectious Diseases. 2004;189(10):1866-72.
266. WELLIVER RC. Respiratory syncytial virus and other respiratory viruses. The Pediatric infectious disease journal. 2003;22(2):S6-S12.
267. Mäkelä MJ, Tripp R, Dakhama A, Park J-W, Ikemura T, Joetham A, et al. Prior airway exposure to allergen increases virus-induced airway hyperresponsiveness. Journal of allergy and clinical immunology. 2003;112(5):861-9.